NEANDC (E) - 192 U Vol. V
INDC (Ger) - 20 / L + Special

PROGRESS REPORT ON NUCLEAR DATA RESEARCH IN THE FEDERAL REPUBLIC OF GERMANY

for the Period April 1, 1977 to March 31, 1978

April 1978

Editor:
S.M. Qaim
Institut für Chemie (1): Nuklearchemie
Kernforschungsanlage Jülich GmbH

NEANDC (E) - 192 U Vol. V
INDC (Ger) - 20 / L + Special

PROGRESS REPORT ON NUCLEAR DATA RESEARCH IN THE FEDERAL REPUBLIC OF GERMANY

for the Period April 1, 1977 to March 31, 1978

April 1978

Editor:
S.M. Qaim
Institut für Chemie (1): Nuklearchemie
Kernforschungsanlage Jülich GmbH

F O R E W O R D

This report has been prepared for the exchange of nuclear data research information between the Federal Republic of Germany and the other member states of IAEA and NEA. It brings together progress reports from KFZ Karlsruhe, KFA Jülich, the Universities of Hamburg, Kiel, Köln, Darmstadt, Mainz, München and Tübingen, as well as from PTB Braunschweig and ZAED Karlsruhe.

Each contribution is presented under the laboratory heading where the work was done. If the work is relevant to requests in the World Request List for Nuclear Data, WRENDA 76/77 (INDC(SEC)-55/URSF), the corresponding request numbers have been listed after the title and authors' names of the respective contribution.

Acknowledgement is made to Prof. G. Stöcklin for his support in the preparation of the manuscript and to the Board of Directors of KFA Jülich for a financial grant to publish this report. The CINDA type index has been prepared by Dr. H. Behrens and Mr. G. Schusch of ZAED Karlsruhe and is issued as a supplement to this report.

Jülich, April 1978 S.M. Qaim

C O N T E N T S

Page

INSTITUT FÜR ANGEWANDTE KERNPHYSIK
KERNFORSCHUNGSZENTRUM KARLSRUHE

INSTITUT FÜR ANGEWANDTE KERNPHYSIK
KERNFORSCHUNGSZENTRUM KARLSRUHE

1. Isochronous Cyclotron

1.1 A Time-of-Flight Device for Ultra-High Resolution Transmission Measurements

S. Cierjacks, G. Schmalz, D. Erbe, B. Leugers

For studying several problems in neutron physics it is desired to carry out measurements using methods with largely improved energy resolutions of the order 10^{-4}. A typical example of this kind is the study of T=3/2 isobaric analog states in light T_z=1/2 nuclei. In particular, for this type of study the fast neutron spectrometer at the Karlsruhe isochronous cyclotron was further modified [1]. A substantial improvement of the energy resolution of the spectrometer was achieved by optimizing the phase conditions of the accelerated deuteron beam in the centre of the cyclotron and by applying modified neutron detectors with largely improved time characteristics. For achieving a long term stability of optimum cyclotron phase conditions a new computer-controlled beam diagnostic system was employed for fast measuring and readjusting the pulse width of the neutron burst. Fig. 1 shows a typical computer display of this system. The neutron burst width characterized by the width of the prompt gamma-peak was measured with a fast plastic scintillation counter. It can be seen from the corrected spectrum and from the result of the computer analysis (line 3), that the neutron pulse width is definitely smaller than 0.7 ns(FWHM), though a simultaneous deflection of about 45 micro-structure pulses extending over a radial range of more than 5 cm is involved. With the new device an ultra-high resolution transmission measurement on oxygen and carbon was carried out over a running period of four weeks. Typically, a total spectrometer resolution of <0.8 ns was achieved at an average beam intensity of 10 μA and at a pulse repetition rate of 50 kHz. Despite the severe masking of the internal cyclotron beam the above average beam current compares favourably with the previously achieved 20 μA at 100 kHz.

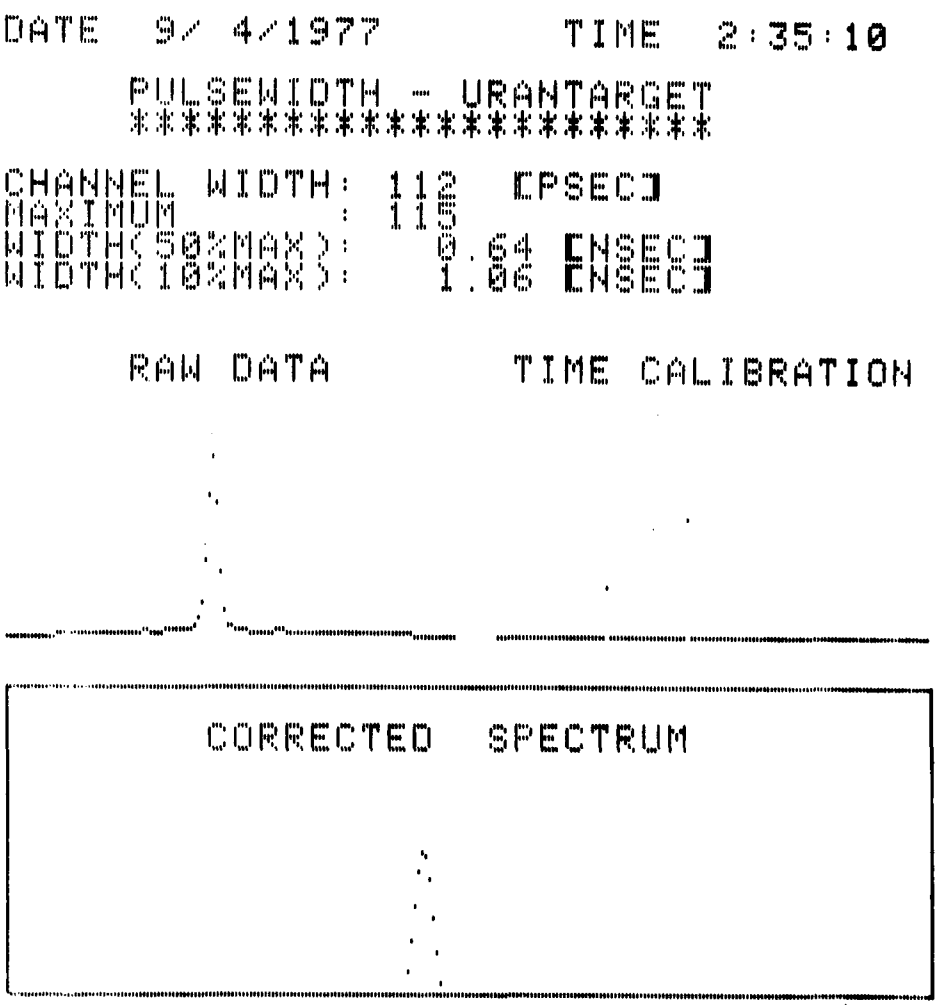

GfK IAKII/S3

Fig. 1 Neutron Pulse Width (Computerdisplay).

1.2 High Precision Measurements of Neutron Resonance Energies of Carbon and Oxygen Between 3-15 MeV

S. Cierjacks, D. Erbe, G. Schmalz, B. Leugers

In recent years neutron energy standards have been requested to remove existing discrepancies in neutron cross sections which obviously originated from discrepancies in energy for different spectrometers. In order to provide a set of carefully selected standard resonance energies, the INDC in 1975 set up a Standard Subcommittee, which presently has almost finalized its task [2]. Some representative standard resonances and their present accuracies selected by the INDC-Subcommittee are listed in Table I. Between 1 eV and 10 MeV a total of 43 standard resonance energies were proposed having typically an accuracy of $\Delta E/E_R \sim 10^{-4}$, an exception being only the MeV range where accuracies are of the order of $\Delta E/E_R \sim 10^{-3}$ which decrease to almost 10^{-2} at 10 MeV. In the present work new precision measurements of carbon and oxygen resonances were done. These represent an improvement of previous resonance energy determinations from our laboratory by more than an order of magnitude.

Transmission measurements for both elements were carried out at the 190 m flight path of the Karlsruhe fast neutron spectrometer, employing a 250 psec channel width for data accumulation. A largely decreased neutron pulse width of 0.7 nsec was employed throughout the experimental runs. The relative errors $\Delta E/E$ are dependent on $\Delta t/t$ and $\Delta \ell/\ell$, where t is the total flight-time of the neutrons to transverse the flight path of the length ℓ. The length of the 190 m flight path was measured by an electro-optical method with an accuracy of ± 1.2 mm, giving a value $\Delta \ell/\ell = 6 \times 10^{-6}$. Thus the major contribution to the energy uncertainty comes from the total time uncertainty which is $4.10^{-5} < \Delta t/t < 10^{-4}$

In Table II, ten resonances in oxygen and two resonances in carbon are listed together with their values of Γ/E_R and $\Delta E/E_R$. The value Γ/E_R has been selected by the INDC Subcommittee as a measure for its usefullness as a standard resonance. It is suggested that these resonances be used in addition to the presently recommended neutron resonances in the MeV range.

Table I. Representative standard resonances and their present accuracy. Compare ref. 2

Ref. level	Isotope	Nominal energy	ΔE/E
		eV	
1	Ir-191	0.6551±0.0014	$2.1 \cdot 10^{-3}$
8	U-238	145.617 ±0.033	$2.2 \cdot 10^{-4}$
10	U-238	314.18 ±0.24	$7.9 \cdot 10^{-4}$
12	U-238	463.18 ±0.24	$5.2 \cdot 10^{-4}$
14	U-238	708.22 ±0.20	$2.8 \cdot 10^{-4}$
		keV	
16	U-238	1.41988±0.00032	$2.2 \cdot 10^{-4}$
18	U-238	2.48947±0.0005	$2.0 \cdot 10^{-4}$
20	Pb-206	3.360 ±0.001	$3.0 \cdot 10^{-4}$
24	Al-27	5.903 ±0.008	$1.3 \cdot 10^{-3}$
25	S-32	30.378 ±0.006	$2.0 \cdot 10^{-4}$
26	Na-23	53.191 ±0.027	$5.1 \cdot 10^{-4}$
27	Si-28	67.73 ±0.02	$3.0 \cdot 10^{-4}$
28	Pb-206	71.191 ±0.018	$2.5 \cdot 10^{-4}$
29	Fe-56	90.134 ±0.016	$1.8 \cdot 10^{-4}$
30	S-32	97.512 ±0.028	$2.9 \cdot 10^{-4}$
31	S-32	112.186 ±0.033	$2.9 \cdot 10^{-4}$
32	Fe-56	122.475 ±0.022	$1.8 \cdot 10^{-4}$
33	Fe-56	266.347 ±0.053	$2.0 \cdot 10^{-4}$
35	Mg-24	498.2 ±0.2	$4.0 \cdot 10^{-4}$
		MeV	
37	O-16	1.651 ± 0.002	$1.2 \cdot 10^{-3}$
38	Mg-24	1.709 ± 0.002	$1.2 \cdot 10^{-3}$
40	C-12	2.818 ± 0.004	$1.4 \cdot 10^{-3}$
41	O-16	3.2111± 0.003	$1.0 \cdot 10^{-3}$
42	C-12	6.293 ± 0.008	$1.3 \cdot 10^{-3}$
43	C-12	12.100 ± 0.1	$8.2 \cdot 10^{-3}$

Table II. Suggested standard resonances for the MeV-range

E_n (keV)	Γ(keV)	Γ/E	ΔE/E
	Oxygen		
10729.0±1.2	20.0	$1.9 \cdot 10^{-3}$	$1.0 \cdot 10^{-4}$
9414.7±1.0	4.3	$4.6 \cdot 10^{-4}$	$1.0 \cdot 10^{-4}$
7371.6±0.7	3.0	$4.0 \cdot 10^{-4}$	$9.0 \cdot 10^{-5}$
6674.6±0.6	3.8	$5.7 \cdot 10^{-4}$	$9.0 \cdot 10^{-5}$
6075.7±0.6	5.0	$8.0 \cdot 10^{-4}$	$8.2 \cdot 10^{-5}$
5369.5±0.5	4.5	$8.4 \cdot 10^{-4}$	$8.2 \cdot 10^{-5}$
4594.4±0.4	2.5	$5.4 \cdot 10^{-4}$	$8.1 \cdot 10^{-5}$
3443.6±0.2	1.5	$3.8 \cdot 10^{-4}$	$5.8 \cdot 10^{-5}$
3441.2±0.2	0.5	$1.5 \cdot 10^{-4}$	$5.7 \cdot 10^{-5}$
3211.7±0.2	1.6	$5.0 \cdot 10^{-4}$	$5.7 \cdot 10^{-5}$
	Carbon		
6647.8±0.6	4.2	$6.4 \cdot 10^{-4}$	$8.2 \cdot 10^{-5}$
4936.8±0.4	3.2	$6.3 \cdot 10^{-4}$	$8.1 \cdot 10^{-5}$

1.3 Absolute Fast Fission Cross Sections of ^{235}U, ^{239}Pu and ^{240}Pu

K. Kari, S. Cierjacks

(Relevant to request numbers: 693765, 714020, 732112, 742086, 742136, 754019, 691439, 691467, 692426, 693070, 714024, 742006, 742099, 754009, 762211, 721088, 721089, 742008, 742002, 742105, 754003, 762213, 763005, 763006)

Absolute fission cross sections of ^{235}U, ^{239}Pu and ^{240}Pu were determined between 1-20 MeV using the H(n,p)-reaction as neutron standard. The measurements were carried out at the cyclotron placing the fission counter at the 11 m flight path and the flux detectors at the 57 m station in the same neutron beam. The simultaneous flux measurement in the irradiating neutron beam was possible since the transmission of the fission detector was higher than 99 %. Fission events were measured by gas scintillation counters filled with an Ar-N_2 mixture. The results of the present determination of the ^{239}Pu and ^{240}Pu fission cross sections are shown in Figs. 2 and 3. The accuracy of the absolute cross sections is 3.0 - 3.8 % for both nuclei depending on the incident neutron energy. The data in Figs. 2 and 3 are compared with previous results from other laboratories [3-11]. At 14 MeV the Karlsruhe results compare for ^{239}Pu favourably with new, still unpublished results from Bruyères-le-Châtel [6] and for ^{240}Pu with the data point of White [7]. Below 5 MeV our data for both the nuclei lie slightly above the bulk of measurements from other laboratories.

1.4 γ-ray Production Cross Sections from Inelastic Neutron Scattering on Cr and Ni

F. Voß, S. Cierjacks, D. Erbe, G. Schmalz

(Relevant to request numbers: 661012, 732040, 661024, 712008)

The analysis of γ-ray production measurements of inelastic scattering on Cr and Ni has been completed. In the experiments a large Ge(Li) crystal of 42 cm^3 was used to detect inelastic scattering events from metallic ring samples. Associated γ-rays were measured at a back-angle of 125°. The experimental data were corrected for multiple scattering and γ-ray absorption in the samples and the γ-ray detector. A geometry and energy dependent detector efficiency was determined using an IAEA set of standard γ-sources. Total γ-ray production cross sections were obtained by multiplying the 125° differential data with 4π.

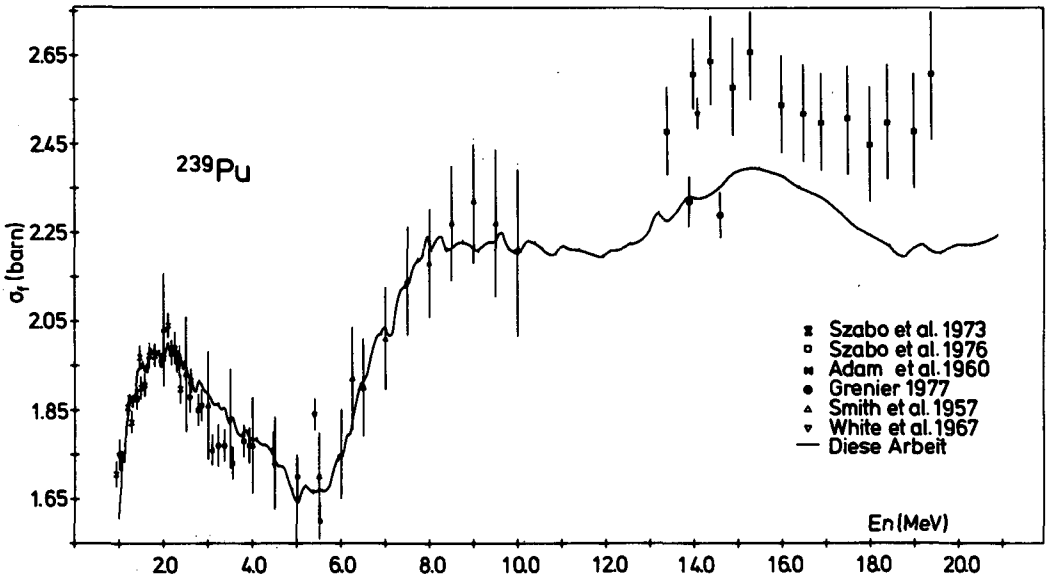

Fig. 2 Fission cross section of ^{239}Pu and comparison with previous results.

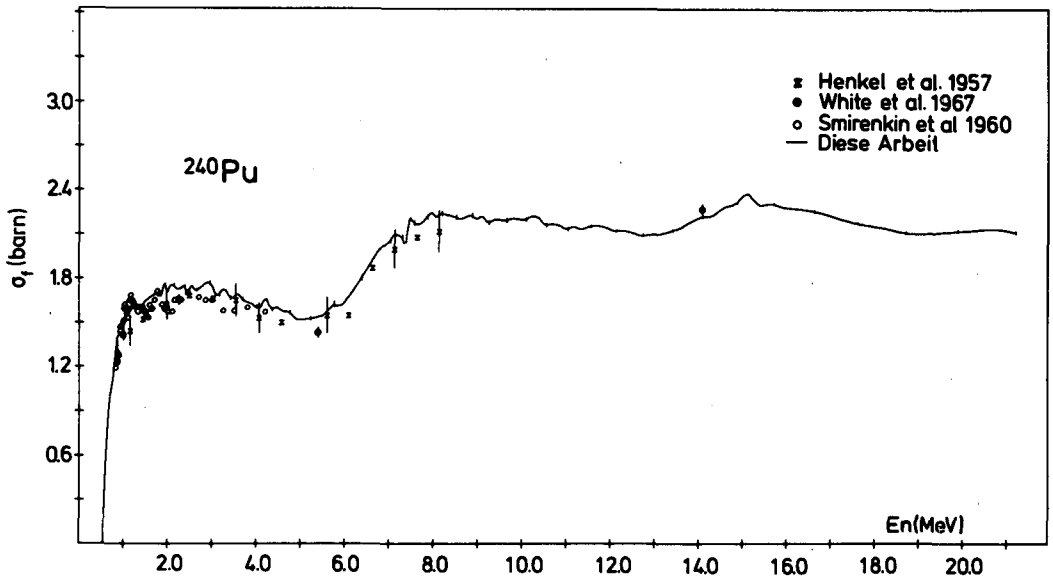

Fig. 3 Fission cross section of ^{240}Pu and comparison with previous results.

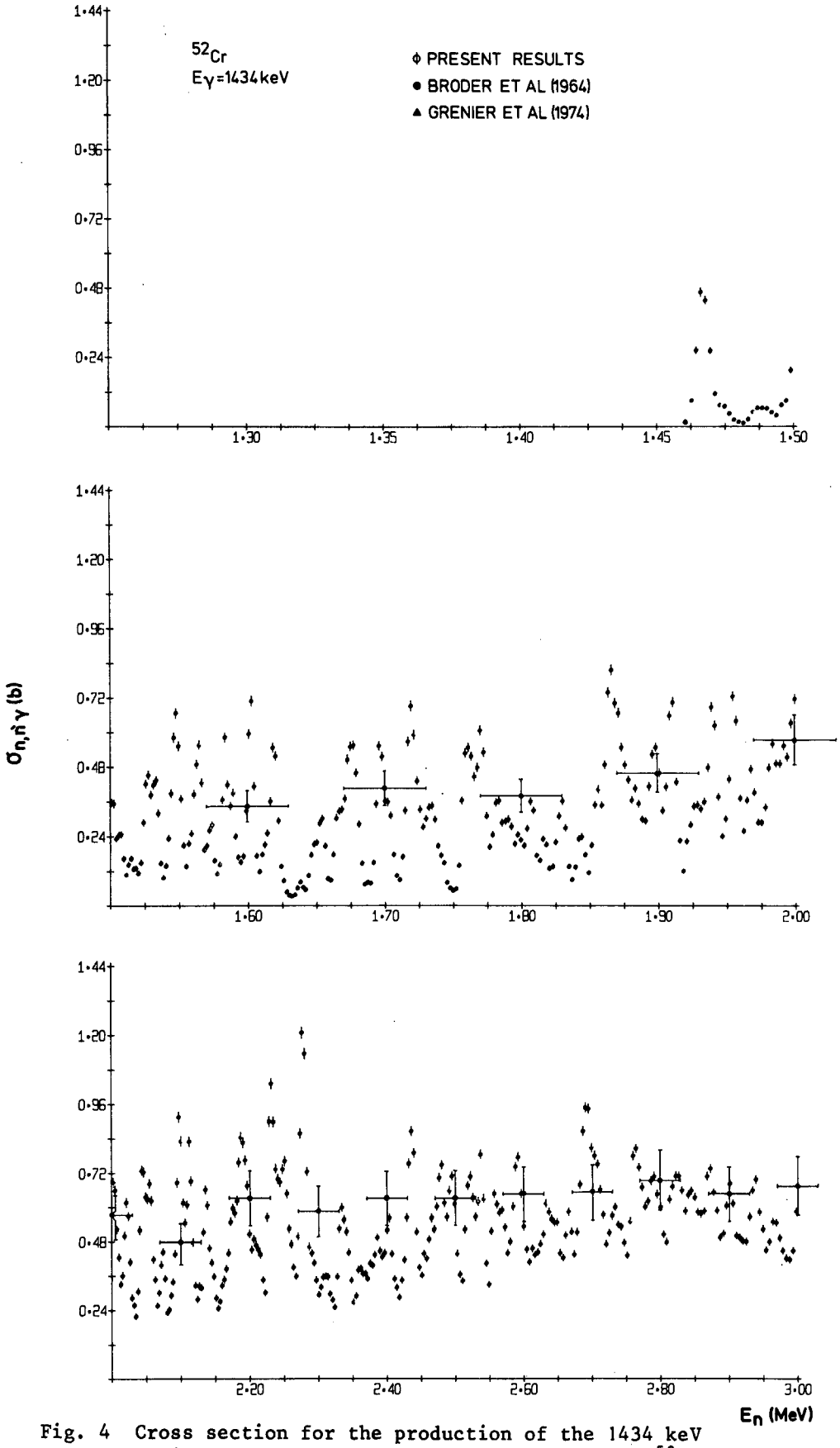

Fig. 4 Cross section for the production of the 1434 keV γ-line from inelastic neutron scattering in ^{52}Cr.

Final results of excitation functions in the energy range from thresholds up to 10 MeV are now available for the following γ-transitions: the 781 keV γ-line in ^{50}Cr, the 935, 1332, 1434, 1531 and 1728 keV γ-lines in ^{52}Cr, the 1005 and 1457 keV γ-lines in ^{58}Ni and the 467, 826, 1173 and 1333 keV γ-lines in ^{60}Ni. A typical result from this work is shown in Fig. 4. In this diagram the cross section for the production of the 1333 keV γ-line in ^{60}Ni is shown together with previous results from other laboratories. The total set of γ-ray production cross sections obtained both for the chromium and nickel isotopes has been sent to CCDN Saclay and is now available for international exchange.

1.5 Elastic Neutron Scattering on Iron Between 450 and 3000 keV and Determination of ^{56}Fe Resonance Parameters

S. Cierjacks, I. Schouky

(Relevant to request numbers: 753034, 691085, 691086, 691087, 742029, 741046)

With regard to shielding applications it was previously pointed out that for various shielding materials large deficiencies in sufficiently resolved elastic scattering cross section data existed between 1 keV and 10 MeV. In order to provide the lacking cross sections the previous program of differential scattering cross section measurements was continued. In addition to the measurements on oxygen and silicon high resolution scattering data of Fe were measured with the Karlsruhe fast neutron time-of-flight-spectrometer. The analysis of the experimental results between 0.45 and 3 MeV at ten scattering angles between 20° and 150° has been completed [12]. From the large body of results which are available on request from CCDN, Figs. 5 and 6 show a characteristic example of the iron data between 0.4 and 0.9 MeV. The high-resolution elastic scattering data were used to derive J and ℓ values of neutron resonances by means of shape analyses.

In the range from 450 to 900 keV spins and parities were assigned to 117 resonances out of a total of 138. Combining the scattering results with the previous 190 m total cross section data and using single channel, multilevel R-matrix theory, we obtained complete resonance parameters for most of the assigned compound nuclear levels. The results of this work were presented at the Specialists Meeting on Neutron Data of Structural Materials for Fast Reactors at Geel in December 1977. These are listed in Table III.

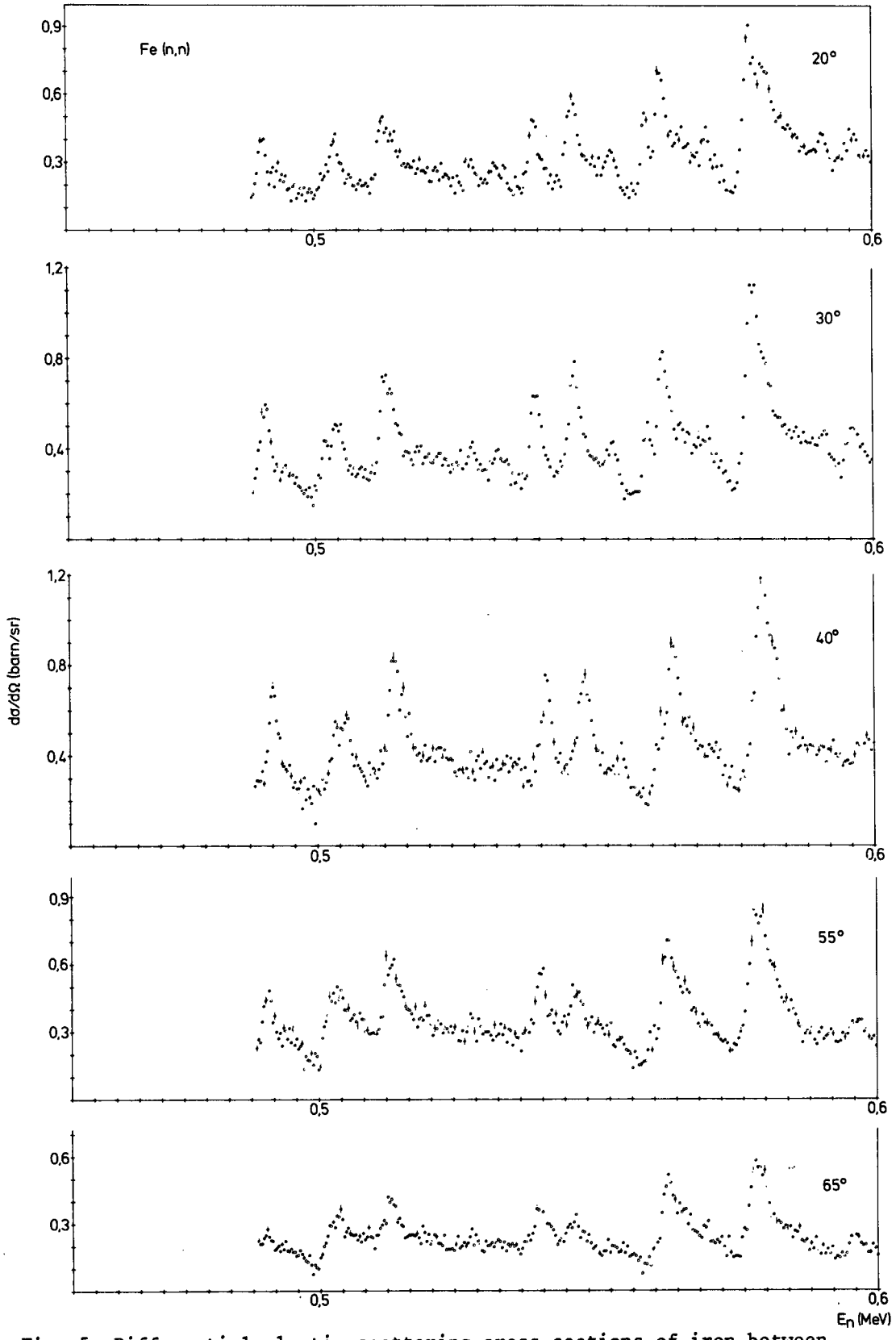

Fig. 5 Differential elastic scattering cross sections of iron between 0.4 and 0.6 MeV.

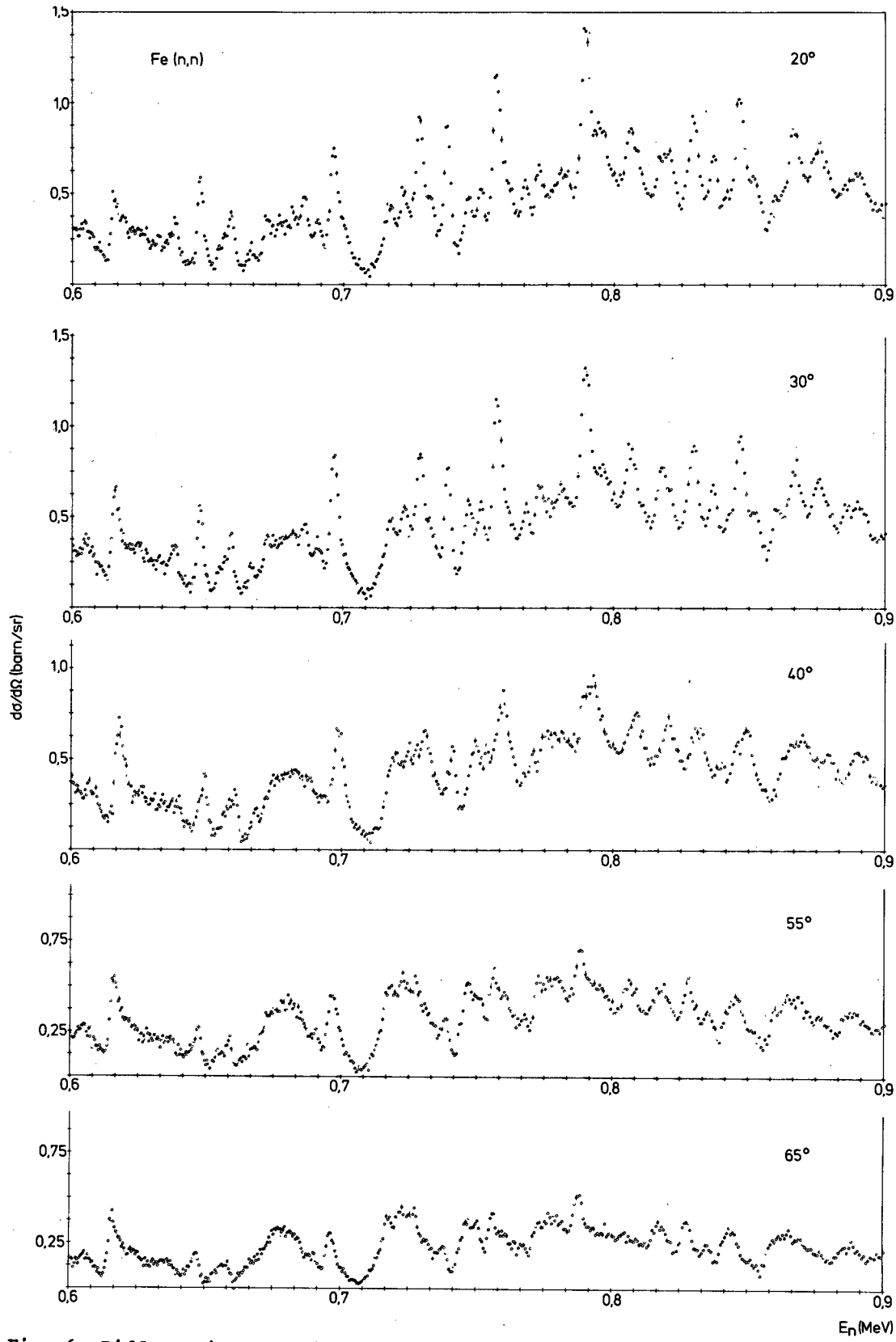

Fig. 6 Differential elastic scattering cross sections of iron between 0.6 and 0.9 MeV.

Table III. Neutron resonance parameters of $^{56}Fe+n$

E_R (MeV)	Γ_n (keV)	ℓ	J	E_R (MeV)	Γ_n(keV)	ℓ	J
450.87±.09	.05	1	(3/2)	613.38±.20	2.47	0	1/2
456.73±.09	<.05	-	-	614.36±.15	.22	1	1/2
457.62±.09	.07	1	3/2	628.28±.15	.10	(1)	(1/2)
463.96±.09	.10	(1)	(3/2)	626.16±.15	.10	(1)	(1/2)
469.46±.15	1.76	0	1/2	630.54±.15	.25	1	1/2
480.70±.10	.27	1	1/2	632.91±.15	.15	1	1/2
486.75±.10	<.06	(1)	(1/2)	634.47±.15	<.08	-	-
489.50±.10	.39	1	1/2	635.87±.15	<.08	-	-
490.00±.10	.53	1	3/2	636.83±.15	.50	1	1/2
493.34±.10	<.06	(1)	(3/2)	640.94±.15	.10	(1)	(1/2)
498.99±.10	.11	1	1/2	643.56±.15	.10	(1)	(1/2)
499.96±.15	1.12	0	1/2	645.97±.15	1.3	2	3/2
502.84±.10	.60	1	3/2	647.89±.15	<.08	-	-
507.78±.10	<.06	-	(3/2)	652.89±.15	.47	1	1/2
511.24±.10	.42	1	3/2	655.04±.15	.30	1	3/2
512.72±.10	.26	1	1/2	657.31±.15	.62	2	3/2
514.16±.10	<.06	-	-	657.79±.15	.30	1	1/2
526.99±.11	.15	1	1/2	662.70±.16	.08	-	-
531.45±.11	.16	1	3/2	665.02±.16	.20	1	1/2
533.17±.11	.06	2	3/2	665.36±.25	24.3	0	1/2
535.52±.20	.18	0	1/2	670.58±.16	.21	1	1/2
538.28±.11	.46	2	3/2	672.24±.16	.08	-	-
544.02±.20	.19	1	1/2	679.92±.17	.08	(1)	(1/2)
545.27±.12	.46	2	3/2	680.92±.17	<.08	-	-
552.06±.20	.20	1	1/2	683.08±.17	<.08	-	-
556.20±.12	<.06	-	-	684.45±.17	.42	1	3/2
558.41±.12	.47	2	3/2	688.95±.17	.46	1	1/2
560.51±.15	1.96	0	1/2	690.35±.17	.42	1	1/2
561.01±.12	.20	1	3/2	692.84±.17	1.94	0	1/2
565.02±.13	.12	1	1/2	694.90±.17	.78	2	3/2
568.94±.13	.15	2	3/2	695.42±.17	.41	1	1/2
571.35±.13	<.06	-	-	701.71±.17	<.09	-	-
574.98±.13	.26	1	1/2	713.67±.17	.17	1	(1/2)
575.50±.13	.55	0	1/2	715.10±.17	.17	1	1/2
576.79±.13	.70	2	3/2	716.40±.40	27.8	0	1/2
577.37±.13	.20	1	1/2	716.43±.17	<.09	-	-
579.12±.13	.34	1	1/2	720.66±.17	.21	1	1/2
587.94±.13	<.07	-	-	721.21±.17	.15	1	3/2
589.93±.14	.20	1	1/2	727.03±.18	1.19	2	3/2
590.95±.14	<.07	-	-	731.08±.18	.21	1	1/2
594.72±.15	.15	1	1/2	737.11±.18	.74	1	3/2
595.40±.15	.13	0	1/2	738.70±.18	.09	-	-
598.74±.14	<.07	-	-	741.62±.18	8.9	0	1/2
602.87±.14	.15	0	1/2	744.94±.18	.36	1	1/2
609.55±.14	.10	(0)	(1/2)	749.52±.18	1.01	1	3/2

Table III. (continued)

Table III. (continued)

E_R (MeV)	Γ_n(keV)	ℓ	J	E_R (MeV)	Γ_n(keV)	ℓ	J
752.61 ±.19	9.6	0	1/2	827.69±.22	1.01	2	3/2
755.49 ±.19	1.28	2	3/2	832.95±.22	.18	1	1/2
758.51 ±.19	.10	1	(1/2)	834.86±.22	1.05	1	3/2
764.20 ±.19	.15	1	1/2	837.46±.22	.15	(1)	(1/2)
766.07 ±.19	.85	1	3/2	839.86±.22	1.90	0	1/2
769.30 ±.19	6.66	0	1/2	844.42±.22	1.35	2	3/2
770.35 ±.20	.15	2	(5/2)	849.47±.23	.15	1	1/2
771.45 ±.20	.10	(1)	(1/2)	851.10±.23	.53	1	1/2
777.19 ±.20	.21	(1)	(1/2)	855.66±.23	3.54	0	1/2
779.62 ±.20	.42	1	1/2	857.98±.23	<.10	-	-
782.02 ±.20	.35	1	1/2	861.41±.23	.31	1	1/2
784.59 ±.20	1.42	0	1/2	862.22±.23	<.10	-	-
788.13 ±.20	1.37	2	5/2	863.05±.23	2.1	0	1/2
793.22 ±.20	.20	1	1/2	864.36±.23	1.1	2	3/2
794.89 ±.21	.21	1	(1/2)	866.08±.23	<.10	-	-
800.79 ±.21	<.09	-	-	867.93±.24	.12	1	(1/2)
803.65 ±.21	.34	1	1/2	872.00±.24	1.9	1	1/2
805.89 ±.21	.49	1	1/2	874.11±.24	.32	(1)	(3/2)
813.75 ±.21	.39	1	1/2	876.95±.24	.18	(1)	(1/2)
815.92 ±.21	1.29	1	1/2	881.64±.24	.64	0	1/2
818.15 ±.21	.90	0	1/2	887.17±.24	.58	1	1/2
819.25 ±.21	.53	1	1/2	889.58±.24	.63	1	1/2
824.77 ±.22	.35	0	1/2	895.94±.24	.65	1	1/2
825.15 ±.22	72	1	1/2	898.73±.25	.72	(0)	1/2

Table IV. Resonance parameters of T=3/2 resonances of ^{16}O+n (preliminary)

E_R(keV)	Γ_N/Γ	Γ(keV)	Γ_N(keV)	Γ_N^o(eV)	J^π
7371.6 ± 0.7	0.95	4.6 ± 0.4	4.4 ± 0.4	1.8	$1/2^-$
8845.4 ± 0.8	0.60	7.9 ± 0.8	4.8 ± 0.5	1.9	$3/2^-$
9411.7 ± 1.0	0.19	2.2 ± 0.2	0.33 ± 0.05	0.6	$5/2^-$
10729.0 ± 1.2	0.15	21.2 ± 2.1	3.18 ± 0.3	3.8	$7/2^-$
10794.0 ± 1.2	0.1	30 ± 10	-	-	$3/2^-$

1.6 Isobaric Analog Impurities from Total and Differential Neutron Scattering Cross Sections of Silicon

S. Cierjacks, S.K. Gupta, I. Schouky

Resonance parameters of neutron resonances in ^{28}Si+n have been obtained by analyzing simultaneously the measured differential neutron scattering cross sections and total neutron cross sections in the neutron energy range of 1 to 1.4 MeV. In the analyses R-matrix single channel multilevel theory was applied. The resonance at 1254 keV in ^{28}Si+n has be identified as the J = 1/2$^+$ analog of the T = 3/2 first excited state in ^{29}Al. The identification also took into account experimental radiative neutron capture data and shell model calculations for the radiative width. An estimate of the average reduced neutron widths of T = 1/2 s-wave resonances in the range of 0 to 1.9 MeV showed that the T = 3/2 s-wave resonance width was smaller by about a factor of 5, indicating an isospin impurity of 18 %. The results of this study have been published in Physical Review C [13].

1.7 Investigation of Low Lying T = 3/2 States in ^{16}O+n

S. Cierjacks, D. Erbe, G. Schmalz, B. Leugers,
F. Hinterberger$^+$, P. v. Rossen$^+$

The formation and the decay of T = 3/2 resonances in neutron scattering on light T_z = 1/2 nuclei is isospin-forbidden. Thus both processes can proceed only through isospin impurities in either the initial or the final states. Therefore, measurement of such states provides an important method to determine isospin mixing matrix elements which measure the deviation of isospin symmetry of nuclear forces. Moreover, Ikossi et al. [14] have observed an intriguing periodic behaviour with a period of eight masses in the proton reduced width of analog states excited in proton isospin-forbidden elastic scattering from self-conjugate even-even nuclei. As a further step it is also interesting to see whether a similar effect is also present in the isospin-forbidden neutron scattering on the same targets. In continuation of our previous study of T = 3/2 states in ^{29}Si an additional study was carried out for the ^{16}O+n system. In the ultra-high resolution transmission measurements performed for this nucleus with the Karlsruhe isochronous cyclotron, five of the six lowest T = 3/2 resonances

---

$^+$Institut für Strahlen- und Kernphysik, Universität Bonn

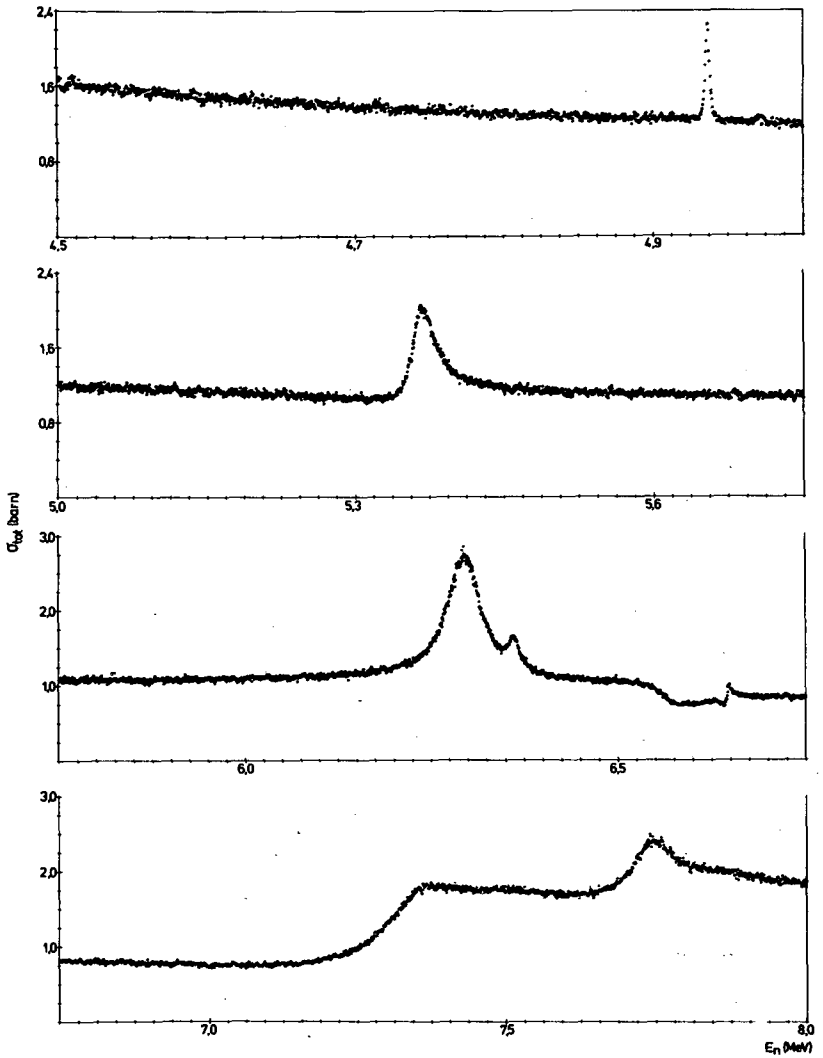

Fig. 7 Total neutron cross section of carbon between 4.5 and 8 MeV measured with a spectrometer resolution of 0.0048 ns/m.

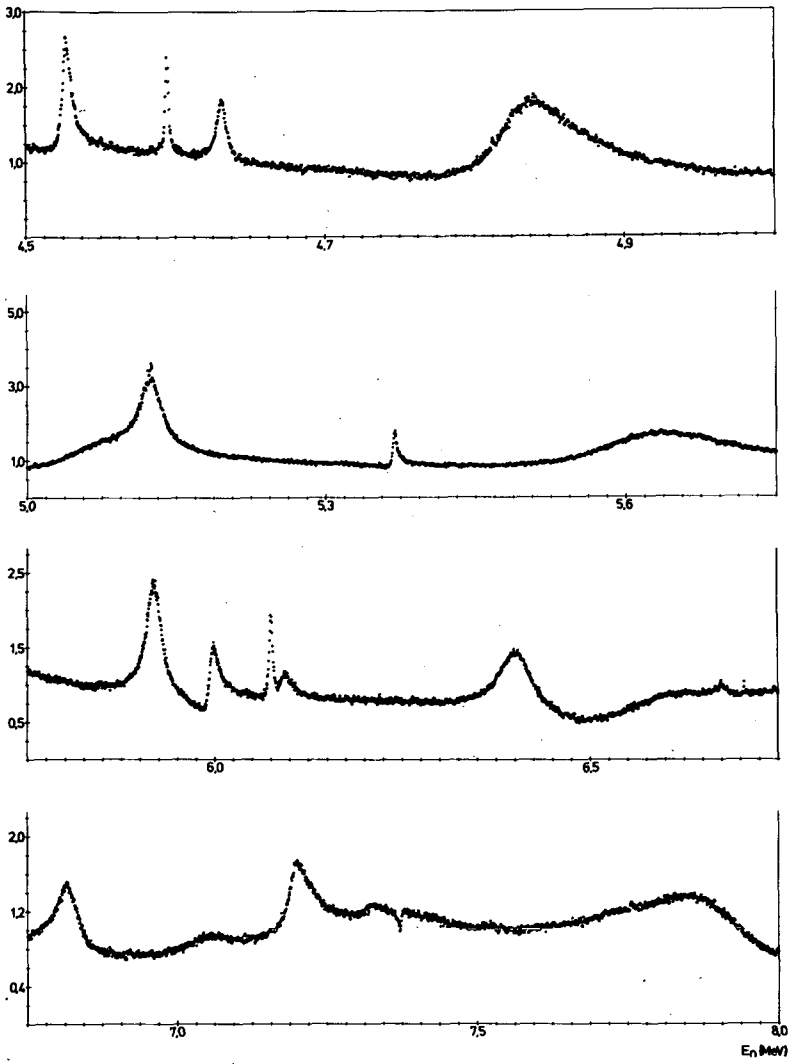

Fig. 8 Total neutron cross section of oxygen between 4.5 and 8 MeV measured with a spectrometer resolution of 0.0048 ns/m.

were observed.

The resonance parameters for these states obtained from a preliminary R-matrix analysis are given in Table IV. The only missing resonance at E_n = 9360.7 keV for which a total width of 8 keV was measured in the ^{13}C (α,n)-reaction[15] should have been observed with the achieved resolution. This indicates that the ratio Γ_n/Γ is very small, so that the resonance excursion does not exceed significantly the statistical fluctuations, which were of the order of 1-2 %. A comparison of the average widths of p- and f-wave T = 1/2 resonances with the widths of the corresponding T=3/2 resonances showed that the latter widths are between 30 and 100 times smaller than their T=1/2 counterparts. The corresponding isospin impurities of 1-3 % are comparable to the value of 2% obtained for T=3/2 d-wave resonances determined by Weigmann et al. [16] in neutron scattering on ^{24}Mg.

1.8 Ultra High-Resolution Total Neutron Cross Sections of Carbon and Oxygen

S. Cierjacks, G. Schmalz, D. Erbe, B. Leugers, F. Hinterberger[+], P. von Rossen[+]

Ultra high-resolution total neutron cross sections of carbon and oxygen were measured at the 190 m flight path of the Karlsruhe fast neutron time-of-flight facility. In the experiments a spectrometer resolution of 0.0048 ns/m was achieved. The experimental results derived between 3 and 30 MeV were obtained by using a high purity graphite sample of 1.0189 at/b and a liquid oxygen sample of 1.2006 at/b. Typical results for part of the measured energy region are shown in Figs. 7 and 8. The complete numerical values of the new highly resolved total cross sections can be requested from the NEA Data Bank, Gif-sur-Yvette, France.

References

[1] G. Schmalz, D. Erbe, G. Haushahn, K. Heidenreich, F. Schulz, A time-of-flight device for ultra-high resolution transmission measurements, contr. paper, Neutron Interlab Seminar, Karlsruhe, Sept. 1977

[2] G.D. James, Neutron energy standards, Symposium Neutron Standards and Applications, Gaithersburg USA, March 1977, NBS Special Publication 493, p. 319

[+] Institut für Strahlen- und Kernphysik, Universität Bonn

[3] I. Szabo, J.L. Leroy, J.P. Marquette, Absolute measurement of fission cross sections of ^{235}U, ^{239}Pu and ^{241}Pu in the energy range from 15 keV to 2.6 MeV; II. All Union Conf. on Neutron Physics, Kiev, 1973, Vol. 3, p. 27

[4] I. Szabo, J.P. Marquette, Measurement of the neutron induced fission cross sections of ^{235}U and ^{239}Pu in the MeV energy range, NEANDC/NEACRP Specialists Meeting on Fast Neutron Fission Cross Sections, Argonne, USA, June 1976, p. 218

[5] B. Adams, R. Batchelor, T.S. Green, The energy dependence of the fission cross sections of ^{238}U, ^{235}U and ^{239}Pu for neutrons in the energy range 12.6 - 20 MeV, J. Nucl. Energy 14 (1961) 85

[6] G. Grenier, Private communication to S. Cierjacks, Sept. 1977

[7] P.H. White, G.P. Warner, The fission cross sections of $^{233,234,236,238}U$, ^{237}Np, $^{239,240,241}Pu$ relative to that of ^{235}U for neutrons in the energy range 1-14 MeV, J. Nucl. Energy 21 (1967) 671

[8] R.K. Smith, Neutron induced fission cross sections for $^{233,235,238}U$ and ^{239}Pu from 2-10 MeV, Bull. Am. Phys. Soc. 2 (1957) 196

[9] R.L. Henkel, Summary of neutron induced fission cross sections, Los Alamos Scientific Laboratory Report, LA-2114 (1957)

[10] V.G. Nesterov, G.N. Smirenkov, Cross section of ^{240}Pu fission with neutrons of energies 0.04 - 4 MeV, Atomnaya Energ. 9 (1960) 16

[11] K. Kari. Ph.D. Thesis, Universität Karlsruhe, to be submitted

[12] I. Schouky, S. Cierjacks, Measurement of elastic scattering cross sections on iron and determination of neutron resonance parameters, NEANDC/NEACRP Specialists Meeting on Neutron Data of Structural Materials for Fast Reactors, Geel, Belgium, December 1977

[13] S. Cierjacks, S.K. Gupta, I. Schouky, Isobaric analog impurity from total and differential neutron scattering cross sections of silicon, Phys. Rev. C17 (1978) 12

[14] P.G. Ikossi, T.B. Clegg, W.W. Jacobs, E.J. Ludwig, W.J. Thompson, Isospin-forbidden T = 3/2 resonances in ^{25}Al, ^{29}P and ^{33}Cl and the systematics of isospin mixing, Nucl. Phys. A 274 (1976) 1

[15] A.B. McDonald, T.K. Alexander, O. Häusser, Isospin-forbidden particle decay in light nuclei, Nucl. Phys. A 273 (1976) 464

[16] H. Weigmann, R.L. Macklin, J.A. Harvey, Isobaric analog impurities for neutron capture and transmission by magnesium, Phys. Rev. C14 (1976) 1328

2. 3 MV Van-de-Graaff-Accelerator

2.1 Structural Materials

2.1.1 A Measurement of the Neutron Capture Cross Section of ^{58}Fe

Ly Di Hong, H. Beer, F. Käppeler

(Relevant to request numbers: 691104, 762179)

The neutron capture cross section of ^{58}Fe is of particular interest for the astrophysical nucleosynthesis. For mass numbers $56 < A \lesssim 75$ the solar system abundances of the chemical elements are determined by two different synthesizing processes: an equilibrium process (e-process) at very high temperature and density forming preferably isotopes with high binding energy per nucleon up to $A \sim 65$, and a slow neutron capture process (s-process) which builds up the isotopes with $A > 56$, starting from the most abundant nuclide ^{56}Fe as a seed [1].

As the ^{58}Fe abundance cannot be produced in the e-process like the abundances of the neighbouring nuclei due to its low neutron separation energy, the neutron capture cross section of ^{58}Fe plays a key role for the calculations of s-process abundances in the mass range A = 56 to 65. For this reason, the previously unknown cross section for the capture of keV neutrons in ^{58}Fe has been measured at the Karlsruhe 3 MV pulsed Van-de-Graaff-accelerator. Neutrons were produced from the ^{7}Li (p,n) reaction with a pulsed proton beam (repetition rate 500 kHz, pulse width $\lesssim 1$ nsec) providing an average beam current of 0.4 μA. Neutron energies were determined by the time-of-flight technique covering the energy interval between 10 and 200 keV. Capture γ-rays were detected by an 800 ℓ liquid scintillator tank and the events were stored in a matrix of 16 pulse height channels versus 1024 time-of-flight channels. More details about the experimental technique are described in ref. [2].

The capture yield data were analysed to determine total radiation widths using the Monte Carlo code TACASI [3]. The computations include a correction for multiple scattering and self shielding. The calculated total radiation widths together with recently measured neutron widths [4] are summarized in Tables I and II. For astrophysical s-process calculations the capture cross section was averaged over a Maxwellian distribution corresponding to a thermal energy of kT = 30 keV. The value obtained was

24 ± 6 mb which was considerably greater than the theoretical estimate of 4.5 mb from Allen et al. [5]. With this new value a calculation of the s-process abundances near the iron seed was carried out. Good agreement with natural abundances was obtained taking into account the calculated e-process abundances of Woosley et al. [6].

2.2 Main Fissile and Fertile Isotopes

2.2.1 A Measurement of the ^{235}U Capture-to-Fission-Ratio in the Energy Range from 10 to 500 keV

H. Beer, F. Käppeler

(Relevant to request numbers: 621249, 692373, 714008)

The capture-to-fission cross section ratio σ_c/σ_f of ^{235}U has been measured in the neutron energy range between 10 and 500 keV at the Karlsruhe pulsed 3 MV Van-de-Graaff-accelerator [7]. An 800 ℓ liquid scintillator tank served to detect capture and fission events by means of their gamma rays. A fission neutron counter in coincidence with the scintillator tank was used to discriminate between capture and fission events. The whole energy range of the measurement was covered in five different runs with overlapping energy regions.

The uncertainty of the present measurement is composed of a statistical uncertainty of typically 6 % and a systematic uncertainty of about 4 %, which results from the calculation of the respective spectrum fractions for capture and fission events. In Fig. 1 the present results are plotted in the energy range between 10 keV and 1 MeV together with the values from other authors. Excellent agreement was obtained between the present results and the data of de Saussure et al. [8]. Most of the data in Fig. 1 are consistent within the quoted error bars except the results of Bandl et al. [9] in the energy range between 20 and 30 keV and the results of Weston et al. [10] in the energy range from 200 to 400 keV.

Table I. The s-wave resonance parameters of ^{58}Fe

Resonance energies E_o (keV)	Neutron widths Γ_n (eV)	Radiation widths Γ_γ (eV)	Correction for multiple scattering and resonance self shielding (%)
10.339 ± 0.047	416 ± 32	1.60 ± 0.50	56.7
43.55 ± 0.25	6370 ± 210	2.17 ± 0.50	36.4
67.18 ± 0.44	997 ± 49	1.00 ± 0.28	6.5
93.9 ± 0.69	12230 ± 780	7.74 ± 1.78	20.3
121.67 ± 0.97	2670 ± 210	2.26 ± 0.65	7.0
179.5 ± 1.7	2390 ± 250		
241.2 ± 2.6	10800 ± 1400		
266.0 ± 2.9	9200 ± 1300		
309.9 ± 3.7	3100 ± 470		
321.0 ± 3.9	1030 ± 160		

Maxwellian averaged capture cross section $\langle\sigma\rangle$ at kT = 30 keV:

$$\langle\sigma\rangle = (24.6 \pm 6.5)\ \text{mb}$$

Table II. The $\ell > 0$ wave resonance parameters of ^{58}Fe

Resonance energies E_o (keV)	Neutron widths $g\Gamma_n$ (eV)	Radiation widths $\frac{g\Gamma_n\Gamma_\gamma}{\Gamma}$ (eV)	Radiation widths $g\Gamma_\gamma$ (eV)
18.74 ± 0.08		0.23 ± 0.18	
19.346± 0.095	∿2.6	0.30 ± 0.21	∿0.34
26.1 ± 0.13	∿6.8	0.34 ± 0.17	∿0.36
31.50 ± 0.16		0.48 ± 0.22	
34.67 ± 0.19	∿7.9	0.95 ± 0.27	∿1.08
37.66 ± 0.21	27 ± 8	0.78 ± 0.23	0.80 ± 0.23
41.98 ± 0.25		1.27 ± 0.32	
45.94 ± 0.29		0.84 ± 0.27	
54.72 ± 0.33	57 ± 10		
62.04 ± 0.39	53 ± 14		
68.40 ± 0.53		1.52 ± 0.45	
73.44 ± 0.59		1.41 ± 0.41	
88.30 ± 0.77		1.59 ± 0.49	
91.73 ± 0.82		1.02 ± 0.43	
103.15 ± 0.97		0.68 ± 0.51	
112.0 ± 1.1		1.78 ± 0.70	
119.6 ± 1.1		0.69 ± 0.51	
131.3 ± 1.1	200 ± 22	1.79 ± 0.82	1.81 ± 0.84
136.5 ± 1.5		2.99 ± 1.0	
144.2 ± 1.6		2.60 ± 1.06	
152.7 ± 1.4	285 ± 31	2.68 ± 1.14	2.71 ± 1.16

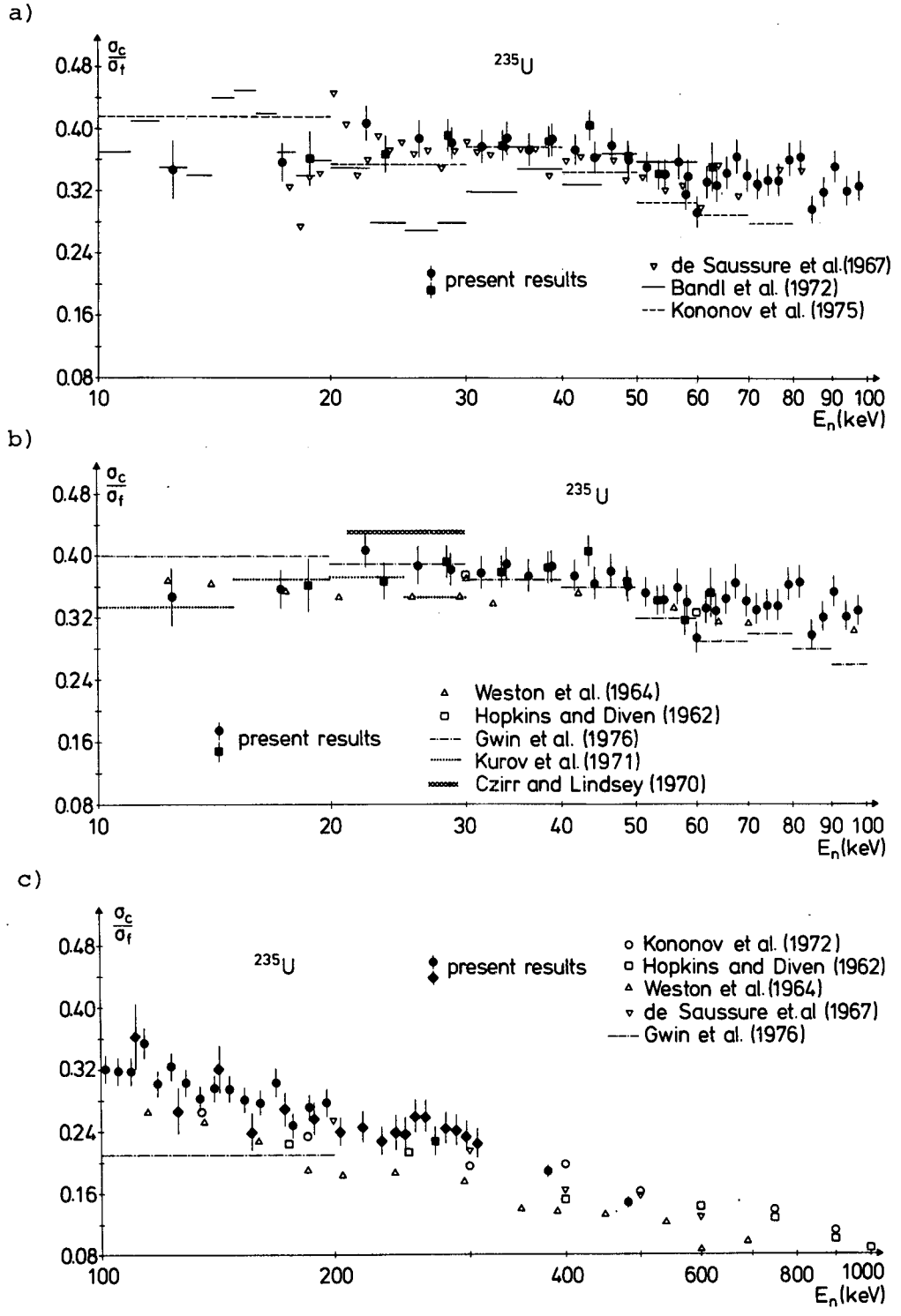

Fig. 1 The capture-to-fission cross section ratio σ_c/σ_f of ^{235}U a), b) in the energy region 10 to 100 keV, c) between 100 to 1000 keV, compared with previous measurements [8-15]. Black dots and squares represent results from different runs of the present experiment.

2.3 Actinide Cross Sections

2.3.1 Neutron Capture Cross Section Measurements on ^{240}Pu and ^{242}Pu in the Energy Range from 50 to 250 keV

K. Wisshak, F. Käppeler

(Relevant to request numbers: 682071, 691389, 692451, 692452, 692453, 714032, 721137, 754006, 762214, 712102, 721098, 721142, 742010, 754014, 762223, 722043, 732128)

To improve the information on neutron capture cross sections of Pu-isotopes for fast reactor calculations, it was desirable to extend the energy range of our first measurement [16,17] to higher energies. This was possible by using the T(p,n) reaction for the production of kinematically collimated neutrons. With this reaction and a slightly modified experimental set-up, a maximum neutron energy of about 250 keV was achieved. Two measurements have been performed at a flight path of 66 mm, using ^{197}Au as a reference sample. The target consisted of tritium-loaded titanium (0.8 Curie/cm^2) on a tungsten backing. To minimize contamination, the target was coated with a thin aluminium layer. The overall statistical and systematic uncertainty of the measurements is 7-10 % for ^{240}Pu and 10-15 % for ^{242}Pu. Fig. 2 shows the cross section of ^{240}Pu determined from the experimental ratios of both measurements using the evaluated cross section of ^{197}Au from ENDF/B-IV. For comparison the data of Weston et al. [18] and of our previous experiments are given, together with the evaluated cross sections from ENDF/B-IV and KEDAK-3.

2.3.2 Measurement of the Neutron Capture Cross Section of ^{241}Am in the Energy Range from 10 to 250 keV

K. Wisshak, F. Käppeler

(Relevant to request numbers: 712108, 712109, 712110, 721099, 742108, 752033, 741127, 762153, 702081)

For the capture cross section measurement of ^{241}Am the same experimental method was applied as used recently for the plutonium isotopes 240 and 242. The high activity of ^{241}Am, however, called for a more careful sample preparation. A sintered pellet of 3.6 g AmO_2, 17.7 mm in diameter and 2.2 mm in thickness, has been prepared, which was welded in a 0.15 mm thick stainless steel canning. Experiments using the $^{7}Li(p,n)$- as well as the T(p,n)-reaction for neutron production have been completed and the

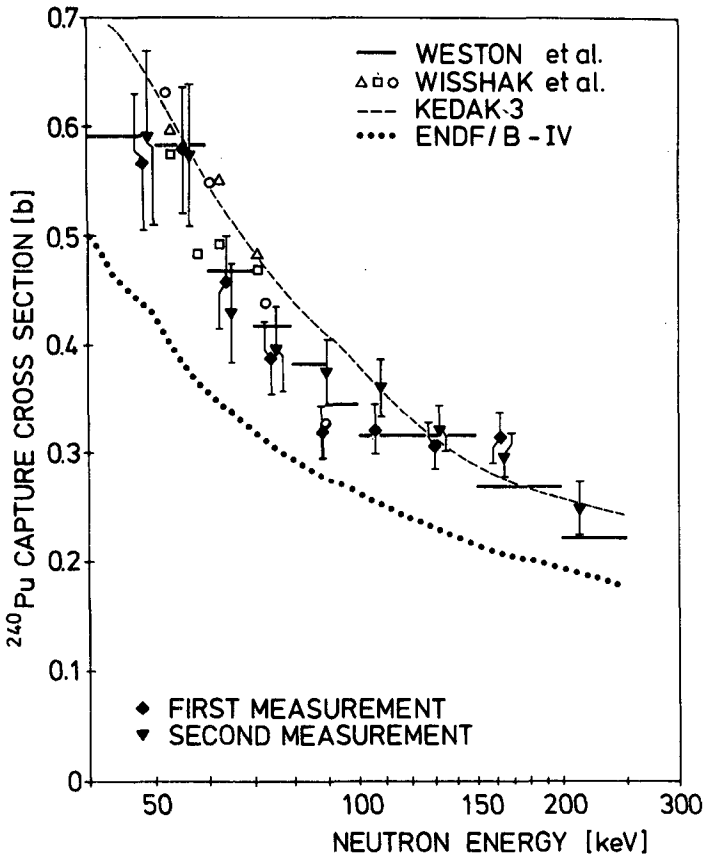

Fig. 2 The neutron capture cross section of ^{240}Pu. The black triangles and squares give the data from the present measurements.

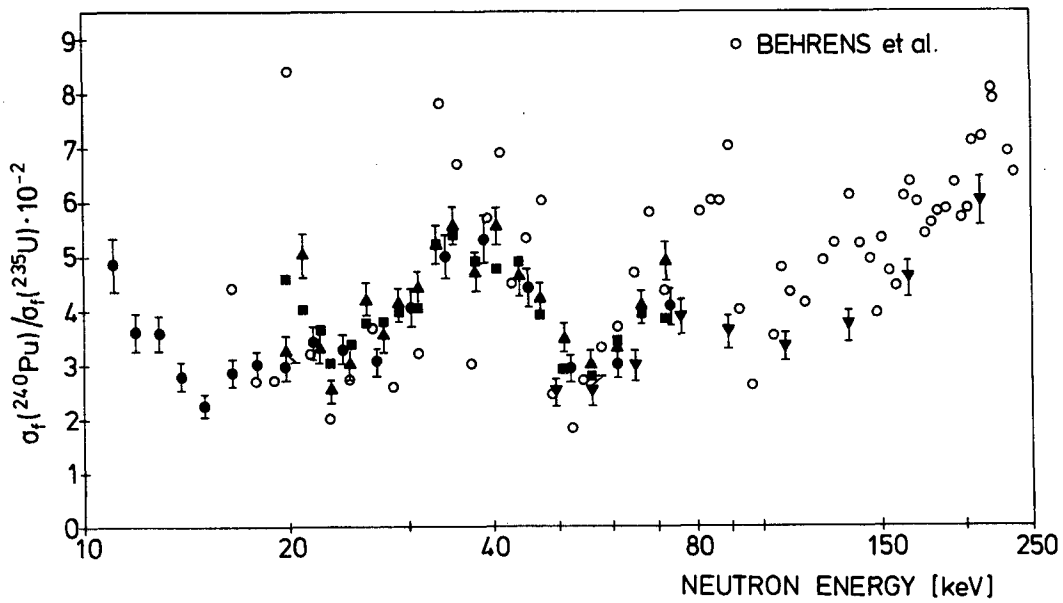

Fig. 3 The fission cross section of ^{240}Pu relative to ^{235}U (the different symbols identify the respective runs of the capture cross section measurement).

evaluation is in progress. During the data acquisition it turned out that the effect-to-background ratio achieved was nearly the same as in the previous measurements on plutonium samples. The data evaluation is facilitated by the fact that the correction for fission events is very small and that no isotopic impurities had to be taken into account. Therefore, the systematic uncertainties are expected to be smaller than in the previous experiments.

2.3.3 The Subthreshold Fission Cross Section of ^{240}Pu Between 10 and 250 keV

F. Käppeler, K. Wisshak

(Relevant to request numbers: 671130, 714030, 721089, 721090, 721091, 742022, 742105, 754003, 762213)

Each measurement of neutron capture cross sections of fissile isotopes with a gamma detector has to be corrected for the simultaneously observed fission gamma rays. In our experiments with Pu isotopes (see contribution 2.3.1),a fission neutron detector and a ^{235}U reference sample were used to determine this correction. On the other hand, this technique offers also the possibility to measure the fission cross section of the respective Pu isotope relative to ^{235}U. Unfortunately, this holds only for the ^{240}Pu sample where the contamination with ^{239,241}Pu is small enough (0.74 % and 0.68 %, respectively). In this case about 70 % of the fission events observed are due to the subthreshold fission in ^{240}Pu, whereas in the case of ^{242}Pu the fission rate is completely dominated by the isotopic impurities in the sample.

The experimental set-up and the data analysis are described in references [16,17]. The correction for fission events in ^{239}Pu and ^{241}Pu was calculated from evaluated cross sections taken from KEDAK 3. The spectrum from the reference sample was used for normalization. The $\bar{\nu}$ values were taken from ref. [19].

In Fig. 3 the experimental values for the fission cross section ratio of ^{240}Pu relative to ^{235}U are shown. The statistical uncertainty of the individual points is 1-3 %,the systematic uncertainty 7-9 %. For comparison, recent data of Behrens et al. [20] are also shown in the figure. The statistical uncertainty of those values amounts to 10-30 %, whereas the systematic uncertainties in the energy range given are not discussed in detail in the preliminary publication of ref. [20].

2.3.4 Measurement of the Neutron Fission Cross Section of ^{241}Am via Fragment and Neutron Detection

W. Hage[+], H. Hettinger[+], S. Kumpf[+], F. Käppeler, K. Wisshak

(Relevant to request numbers: 712103, 732115, 742018, 742107, 762225, 702080)

A systematic study of the ^{241}Am fission cross section between 20 and 1500 keV was started with a measurement of the cross section shape below 1 MeV. In view of the very small subthreshold cross section and the severe background problems caused by the high α-activity, fission events were recorded detecting fission neutrons instead of fission fragments. Doing so, the sensitivity was improved considerably so that very distinct peaks for fission events could be observed in the time-of-flight spectra even below the fission threshold of ^{241}Am. However, since the experimental information about the fission neutron spectrum of ^{241}Am is rather poor, the absolute accuracy of the fission cross sections obtained is limited. Very accurate information, however, was obtained on the energy dependence of the cross section relative to ^{235}U, which was used as a standard. In order to minimize the influence of possible (but unknown) fragment angular anisotropies in ^{241}Am, the neutron detector was located at an angle of 135° with respect to the neutron beam. Fig. 4 shows preliminary results for part of the energy range. The new results are plotted as black points. In all cases, the statistical uncertainty is less than the size of the dots; it is about 6 % at 130 keV and 1 % at 900 keV. For the evaluation, the energy dependence of $\bar{\nu}$ and the fission neutron spectrum of ^{241}Am has been assumed to be the same as that for ^{235}U. Due to this assumption a systematic uncertainty of at least 10 % has to be attributed to the fission cross section values derived in this way. Nevertheless, good agreement was found with the recent results of Behrens and Browne [21].

From the fission cross section of Fig. 4, the penetrability of the fission barrier of ^{241}Am was calculated assuming a 1/v-dependence for the compound formation and normalizing to 1.0 at a neutron energy of 1.4 MeV. A fit to this penetrability curve was carried out with the code of Wong and Bang [22]. In this way, improved parameters, given in Table III for the double-humped fission barrier could be determined as compared to the literature [23].

[+] JRC EURATOM, Ispra, Italy

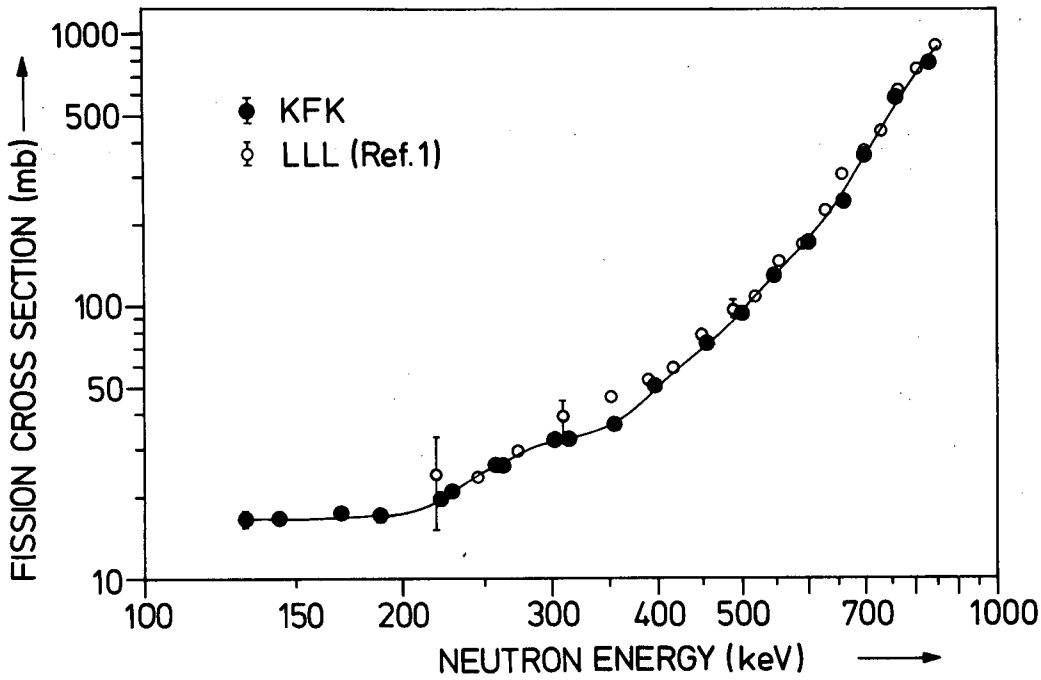

Fig. 4 Preliminary results from the ^{241}Am fission cross section measurement (black points). The values of ref. (21) are shown for comparison (open points).

Table III. Parameters for the inner fission barrier of ^{241}Am

	Barrier height E_A (MeV)	Barrier curvature $\hbar\omega_A$ (MeV)
This work	6.44	0.80 ± 0.07
Back et al. (23)	6.35	0.60 ± 0.15

A second measurement using fragment detection was carried out at energies around 1 MeV with a gas scintillation chamber to determine absolute cross section ratios of ^{241}Am and ^{235}U for normalization. The analysis of this experiment is presently under way.

2.3.5 Development of a Fast Spherical Avalanche Fission Detector with Intrinsic α-Discrimination for the Measurement of the Fission Cross Section of ^{244}Cm

M.A. Kazerouni, F. Käppeler

(Relevant to request numbers: 732108, 752048)

For the measurement of fission cross sections of highly α-active transuranium isotopes, such as ^{244}Cm, a detector with good α-discrimination, very fast timing and long lifetime is required. A spherical avalanche detector was developed for this purpose which combines the favourable geometry, first suggested by Dabbs et al. [24] with the advantage of an excellent time resolution and intrinsic α-suppression. Fig. 5 gives a schematic view of the detector. It is operated in a steady gas flow of a pure quenching gas at a pressure of a few mbar.

First tests of this detector with ^{252}Cf and ^{241}Am sources showed an excellent behaviour with respect to the above requirements. The α-discrimination can be achieved by setting gas pressure and counter voltage such that the weaker ionization of the α particles is quenched completely by the gas and only the fission fragments can be detected. Fig. 6 shows this behaviour for a gas pressure of 21 mbar. The dashed lines give the relation between pulse height for fission fragments and α particles and counter voltage (left scale). Important for the discrimination between the two groups is the pulse height ratio R which is given by the full line (right scale). As the voltage is decreased the α pulses are more efficiently quenched than those caused by fragments. In this way the ratio R can easily be set to 100 or even more. With a ^{241}Am source of 2×10^6 α sec^{-1} a discrimination factor of better than 10^{-10} was measured in a two-days run.

Furthermore, the efficiency and the time resolution were determined with a ^{252}Cf source. The time resolution was measured against the prompt fission γ-rays which were detected by a fast plastic scintillator. A time resolution of $\lesssim$0.5 nsec was found for the avalanche detector. The efficiency

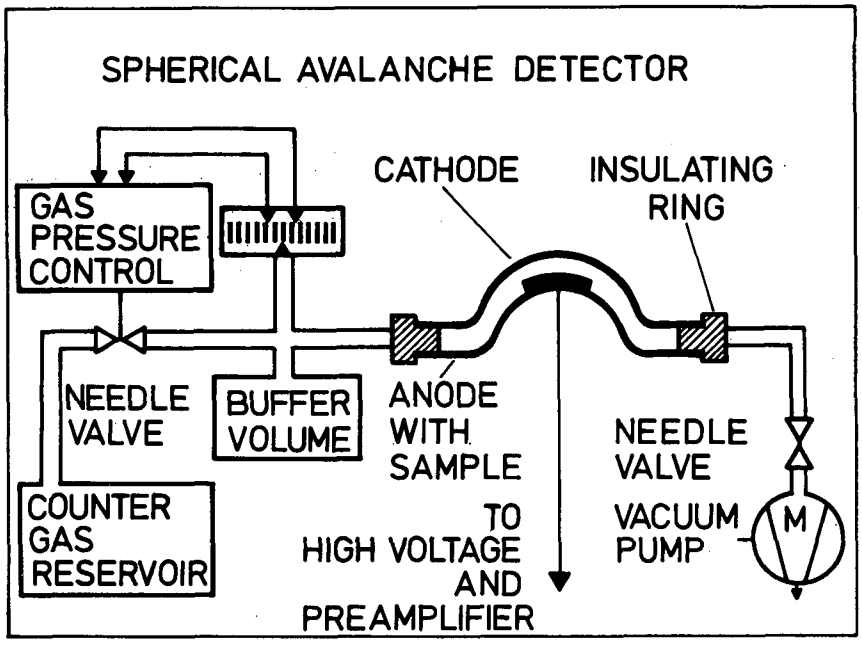

Fig. 5 Schematic diagram of the spherical avalanche detector with the gas pressure stabilization circuit.

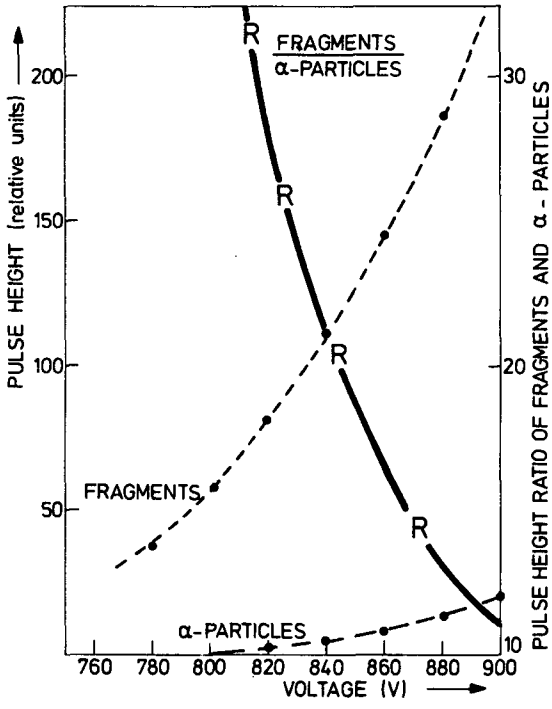

Fig. 6 Relative pulse heights of α particles and fission fragments as a function of the counter voltage (dashed lines). The solid line gives the pulse height ratio (right scale).

was determined with a calibrated ^{252}Cf source to 97.5 ± 2.0 %. This high efficiency makes the detector also suitable for very accurate measurements.

2.4 Fission Products

2.4.1 Capture Cross Sections of the Krypton Isotopes

F. Hensley, F. Käppeler, B. Leugers
(Relevant to request number 742040)

The activities on capture cross section measurements on Kr continue [25]. The neutron capture cross sections of natural Kr and ^{84}Kr were measured. The data are being analysed. Fig. 7 shows time-of-flight spectra obtained from a natural Kr sample and an empty canning, and the net Kr spectrum after subtracting the background. The high rate of background events causes an enhancement of the statistical uncertainty, although cross sections are well obtainable from the shown spectra. For the more expensive isotopes of Kr yet to be measured, due to the less sample mass this uncertainty may become a serious limit to accuracy. For this reason the measuring technique is presently being improved with the goal to achieve less background.

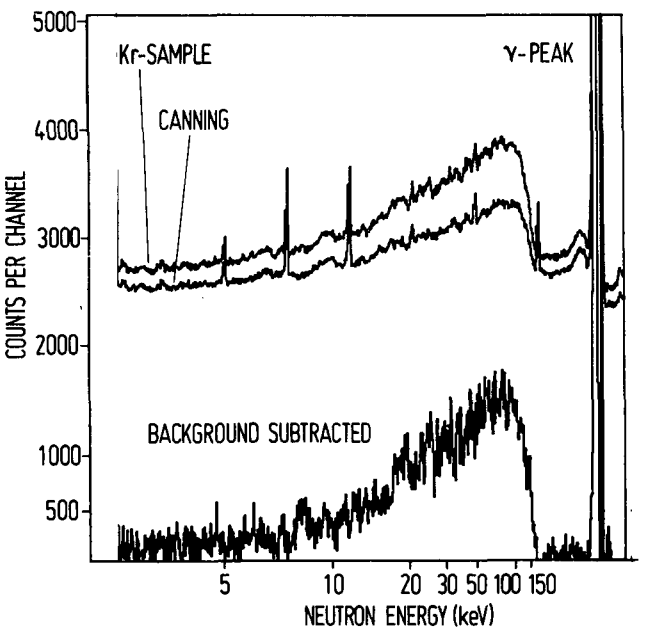

Fig. 7 Time-of-flight spectra from neutron capture cross section measurements on natural Krypton.

References

[1] D.D. Clayton, "Principles of Stellar Evolution and Nucleosynthesis", Mc Graw Hill, New York (1968)

[2] H. Beer, R.R. Spencer, Nucl. Phys. A240 (1975) 29

[3] F.H. Fröhner, General Atomic Report, GA-6906 (1966)

[4] H. Beer, Ly Di Hong, F. Käppeler, Nucl. Sci. Eng., in press

[5] B.J. Allen, J.H. Gibbons, R.L. Macklin, Adv. Nucl. Phys. 4 (1971) 202

[6] S.W. Woosley, W.D. Arndt, D.D. Clayton, The Astrophysical J. Suppl. 261 (1973) 231

[7] H. Beer, F. Käppeler, Report KFK 2223 (1975) p. 22; Report KFK 2379 (1976) p. 12

[8] G. de Saussure, L.W. Weston, R. Gwin, R.W. Ingle, J.H. Todd, A. Lottin, Proc. of the Conf. on Nucl. Data for Reactors, Paris 1966, Vol. II (IAEA, Vienna 1967) p. 233

[9] R.-E. Bandl, H. Miessner, F.H. Fröhner, Nucl. Sci. Eng. 48 (1972) 324

[10] L.W. Weston, G. de Saussure, R. Gwin, Nucl. Sci. Eng. 20 (1964) 80

[11] V.N. Kononov, E.D. Poletaev, B.D. Yurlov, Sov. Atomic Energy, 38 (1975) 105

[12] J.C. Hopkins, B.D. Diven, Nucl. Sci. Eng. 12 (1962) 196

[13] R. Gwin, E.G. Silver, R.W. Ingle, H. Weaver, Nucl. Sci. Eng. 59 (1976) 79

[14] M.A. Kurov, Yu. V. Ryabov, So Tong Hsik, N. Chikov, Sov. Atomic Energy 30 (1971) 315

[15] J.B. Czirr, J.S. Lindsey, Proc. Conf. on Nucl. Data for Reactors, Vol. I, Helsinki(1970), p. 331

[16] K. Wisshak, F. Käppeler, Nucl. Sci. Eng., in press

[17] K. Wisshak, F. Käppeler, NEANDC(E)-182 U Vol. V

[18] L.W. Weston, J.H. Todd, Nucl. Sci. Eng. 63 (1977) 143

[19] F. Manero, V.A. Konshin, Atomic Energy Review 10 (1972) 637

[20] J.W. Behrens, J.C. Browne, G.W. Carlson, Report UCID-17047, Lawrence Livermore Laboratory (1976)

[21] J.W. Behrens, J.C. Browne, Report UCID-17324, Lawrence Livermore Laboratory (1976)

[22] C.Y. Wong, J. Bang, Phys. Lett. 29B (1969) 143

[23] B.B. Back, J.P. Bondorf, G.A. Otroschenko, J. Pedersen, B. Rasmussen, Nucl. Phys. A 165 (1971) 449

[24] J.W.T. Dabbs, Proc. Conf. on Nuclear Cross Sections and Technology, Washington, D.C., March 1975, ed. R.A. Schreck and C.D. Bowman, NBS Spec. Publ. 425 (1975), Vol. 1, p. 81

[25] F. Hensley, NEANDC(E)-182 U, Vol. V

INSTITUT FÜR NEUTRONENPHYSIK UND REAKTORTECHNIK
KERNFORSCHUNGSZENTRUM KARLSRUHE

1. Nuclear Data Evaluation

1.1 Revised Parameters for Low-energy Resonances of ^{238}U+n

B. Goel

(Relevant to request numbers: 692401, 692402, 693066, 741123)

New measurements of the first few resonances of ^{238}U+n [1-3] have shown the radiation widths to be significantly smaller (by 6-12%) than the values available to date in the files KEDAK-3, ENDF/B-IV and in the "barn book" BNL 325. Because of the practical importance of ^{238}U resonance capture the KEDAK parameters of the levels at 6.67, 20.86 and 36.67 eV were reevaluated. A subthreshold level was newly introduced to match the thermal cross sections. Table I shows the revised resonance parameters.

1.2 Evaluation of Transuranium Cross Sections for Burn-up Calculations

B. Goel, F.H. Fröhner, H. Jahn

(Relevant to request numbers: 721098, 721142, 752031, 752029, 752030, 671135, 671136, 681807, 712108, 712110, 721099, 741127, 742014, 742015, 752032, 752033, 762153, 762103, 762225, 671137, 691341, 721100, 732101, 732102, 752036, 762171, 691339, 732100, 752034, 752035, 762226, 721101, 732104, 741128, 752038, 712111, 752037, 752040, 752039, 671139, 732107, 752042, 762154, 762173, 732105, 752041, 671192, 752046, 752047, 762156, 762174, 752043, 732043, 752044, 752045, 762155, 671142, 732109, 752049, 762157, 762228, 752048)

Transuranium cross sections important for burn-up and hazard index calculations are being evaluated. Preliminary results indicate that for instance the data base for the widely used burn-up code ORIGEN is dubious. Some important actinide cross sections are off by a factor of two relative to experimental data and Hauser-Feshbach calculations with width fluctuation corrections.

1.3 Evaluation of Resonance Cross Sections of Cr, Fe, Ni Suitable for Doppler Effect Calculations

F.H. Fröhner

(Relevant to request numbers: 721035, 741031, 753031, 692082, 692083, 692084, 753033, 741033, 741034, 691081, 741035, 753034, 692101, 692102, 692103, 692104, 712024, 721039, 741040, 742033, 741046, 691102, 741049, 721047, 753037, 692128, 692129, 692131, 702009, 741053, 753039, 741056, 741059, 691128, 741062, 682013, 762139, 741065, 682014, 741068)

A new KEDAK evaluation for resonance cross section of Cr, Fe and Ni was completed [4]. Special emphasis was placed on suitability for shielding calculations and for Doppler effect studies via temperature-dependent self-shielding factors. Therefore a hybrid cross section representation was adopted, i.e. Reich-Moore formulae for the s-wave cross sections with their strong level-level interference but negligible Doppler broadening, and single-level Breit-Wigner formulae for p- and d-wave levels with their negligible level-level interference but important Doppler broadening. Unknown resonance spins were fixed by Monte Carlo sampling based on known E_0, $g\Gamma_n$ and $g\Gamma_n\Gamma_\gamma/\Gamma$ values, Bayes' theorem and the Porter-Thomas hypothesis. Point cross sections for the natural elements were calculated up to 300 keV neutron energy, broadened to the KEDAK standard temperatures 300, 900, 1500 and 3100 K. To our knowledge this is the first evaluated cross section set which permits estimation of the contribution of these elements to the Doppler coefficient of a fast reactor with a quality corresponding to present knowledge of the microscopic cross sections.

References

[1] D.K. Olsen et al., Report ORNL-TM-5915 (1977), and D.K. Olsen et al., Nucl. Sci. Eng. 62 (1977) 479

[2] F. Poortmans, private communication (to be published in Nucl. Sci. Eng.)

[3] H. J. Liou, R.E. Chrien, Nucl. Sci. Eng. 62 (1977) 463

[4] F.H. Fröhner, Proc. Specialist Meeting on Neutron Data of Structural Materials for Fast Reactors, Geel, 5-8 Dec. 1977, in press

Table I. Recommended parameters for the first 3 s-wave resonances

Resonance energy (eV)	Γ_n (meV)	Γ_γ (meV)
6.67	1.495	23.7
20.86	9.94	23.67
36.68	33.64	23.64

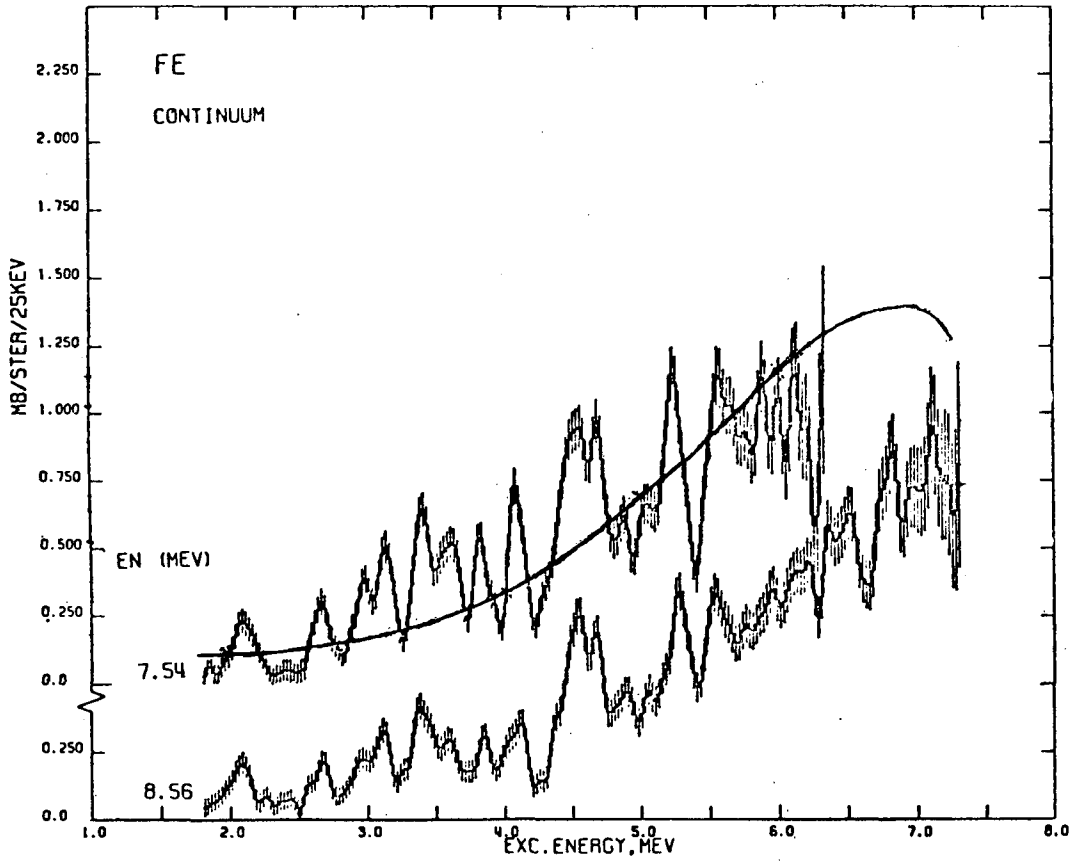

Fig. 1 The angle-averaged continuum differential inelastic-scattering cross sections per 25 keV per atom of natural iron for the two contaminant-free sets of measurements.

2. Prediction of Double-differential Inelastic Neutron Cross Sections Including Precompound Components

C.H.M. Broeders, I. Broeders, H. Jahn

(Relevant to request numbers: 753035, 702007, 712022)

Experimentally determined absolute values of angle-integrated secondary-energy distributions in inelastic neutron scattering compared so far to theoretical calculations [1] were obtained from experiments with 14.6 MeV neutrons [2,3]. Below this energy which is obtained from the d-t reaction there is a gap with no experimental data down to 8.56 MeV. From 8.56 to 4.19 MeV there are measurements from Oak Ridge [4]. It is necessary to fill the gap by model calculations. We could demonstrate [1] that at 14.6 MeV Blann's geometry-dependent hybrid model for precompound processes, with absorption and excitation calculated from the optical model, plus a Hauser-Feshabach term for compound processes works quite well. It should be noted that these calculations yielded absolute values in good agreement with experimental data without any fit parameters apart from those of a standard optical model. We have now tested our method also at lower energies. Fig. 1 shows a comparison for the case of ^{56}Fe for 7.54 MeV incident neutron energy. The model-calculated results are represented by the smooth line through the fluctuating cross section measured at Oak Ridge [4]. The model is seen to yield the average of the measured values with good accuracy. This is an indication that the dependence of the angle-integrated secondary-energy dependent differential inelastic neutron cross section on the incident neutron energy can also be expected to be well reproduced by the geometry-dependent hybrid model plus the Hauser-Feshbach term.

References

[1] H. Jahn, C.M.H. Broeders, I. Broeders, Report NEANDC(E) 182 U, Vol. V (1977) p. 39; Proc. Internl. Conf. on Nucl. Reaction Mechanisms, Varenna, Italy, June 13-17 (1977) p. 185

[2] D. Hermsdorf, A. Meister, S. Sassonoff, K. Seidel, F. Shahin, Report ZKF-277 (1974)

[3] I.F. Hansen, I.D. Andersen, P.S. Brown, R.I. Howerton, I.L. Kammerdiener, C.M.Logan, E.F.Plechaty, C. Wang, Nucl.Sci.Eng. 51 (1973) 278

[4] W.E. Kinney and F.G. Perey, Report ORNL 4515 (1970)

3. Conversion from Wigner-Eisenbud to Kapur-Peierls Resonance Parameters without Matrix Inversion

F. H. Fröhner

Kapur-Peierls resonance parameters have the undesirable features that they are complex and energy-dependent in an ill-specified way. Nevertheless, they are needed whenever Doppler broadening of resonances is to be calculated by means of the well known Voigt profiles as is usual in reactor physics. On the other hand essentially all resonance parameters extracted from experimental data are of the Wigner-Eisenbud or Reich-Moore type, i. e. real and E-independent. Many authors worked on the conversion from one type of representation to the other (cf. e. g. Refs. [1-6]). Available prescriptions are either approximations, at the level of the multi-level Breit-Wigner formulae at best, or they involve brute-force inversion of a high-dimensional level matrix and are thus not very transparent. The fact that in most situations the Wigner-Eisenbud parameters are quite close to the Kapur-Peierls parameters suggests a formally simpler relationship. In fact, if the conversion is restricted to reaction channel c, it is found that

$$\mathcal{E}_\mu = E_\mu - \frac{i\Gamma_{\mu c}/2}{1 - \sum\limits_{\lambda \neq \mu} \frac{i\Gamma_{\lambda c}/2}{E_\lambda - \mathcal{E}_\mu}} , \qquad (1)$$

$$\frac{iG_{\mu c}}{2} = \left(\sum_\lambda \frac{i\Gamma_{\lambda c}/2}{(E_\lambda - \mathcal{E}_\mu)^2} \right)^{-1} , \qquad (2)$$

where $\mathcal{E}_\mu$, $G_{\mu c}$ are the complex Kapur-Peierls parameters that correspond to the real Wigner-Eisenbud or Reich-Moore parameters E_μ, $\Gamma_{\mu c}$ (resonance energy and partial width), and the sums are over levels. Eq. (1) is quite convenient for iteration by resubstitution, even in cases of heavy level overlap. Once $\mathcal{E}_\mu$ is known with sufficient accuracy the partial width $G_{\mu c}$ is readily obtained from eq. (2). This procedure can be successively applied to all pertinent reaction channels.

References

[1] P. Moldauer, Phys. Rev. 135 (1964) B642; Phys. Rev. 136 (1964) B947

[2] D.R. Harris, Report LA 4327 (1970)

[3] F.T. Adler, D.B. Adler, Nuclear Data for Reactors, Vol. II. IAEA Vienna (1970) p. 777

[4] G. de Saussure, R.B. Perez, Nucl. Sci. Eng. 52 (1973) 412

[5] J. Krebs, G. le Coq, J.P. l'Hériteau, P. Ribon, Nuclear Data for Reactors, Vol. II, IAEA Vienna (1970) p. 789

[6] M. Segev, Report TNSD-R/462 (1977)

INSTITUT FÜR CHEMIE (1): NUKLEARCHEMIE
KERNFORSCHUNGSANLAGE JÜLICH

1. Neutron Data

1.1 Investigation of Trinucleon Emission Reactions

S.M. Qaim, G. Stöcklin, R. Wölfle, C.H. Wu

In continuation of earlier radiochemical studies on fast-neutron induced trinucleon emission reactions, (n,t) cross sections were measured for neutrons produced via break-up of 53 MeV deuterons on a Be target (E_n= 11.5-43.5 MeV; I_{max} at 22.5 MeV; FWHM= 15.8 MeV) and the systematics of cross sections were established. Measurements were carried out using both tritium counting and γ-ray spectroscopy of the activation products. The results are shown [1] in Fig. 1 and lead to two conclusions:

(a) The (n,t) cross sections for the lightest elements are exceptionally large, presumably due to occurrence of deuteron- and triton-like structures which facilitates pick-up and knock-out reactions. The data for even-Z and odd-Z elements follow different trends. For elements with Z>20 the emission of a triton is relatively independent of the target element and does not account for more than 0.25% of $\sigma_{n.e.}$

(b) For nuclei with A>40 the emission of three particles (1p2n) is much more favoured than the emission of a bound trinucleon (^3H).

A study of (n,^{3}He) reactions is also underway. In addition to the radiochemical measurements, mass spectrometric technique has also been combined. Cross sections have been measured so far for Al, Ca, Mn, Zn and Nb.

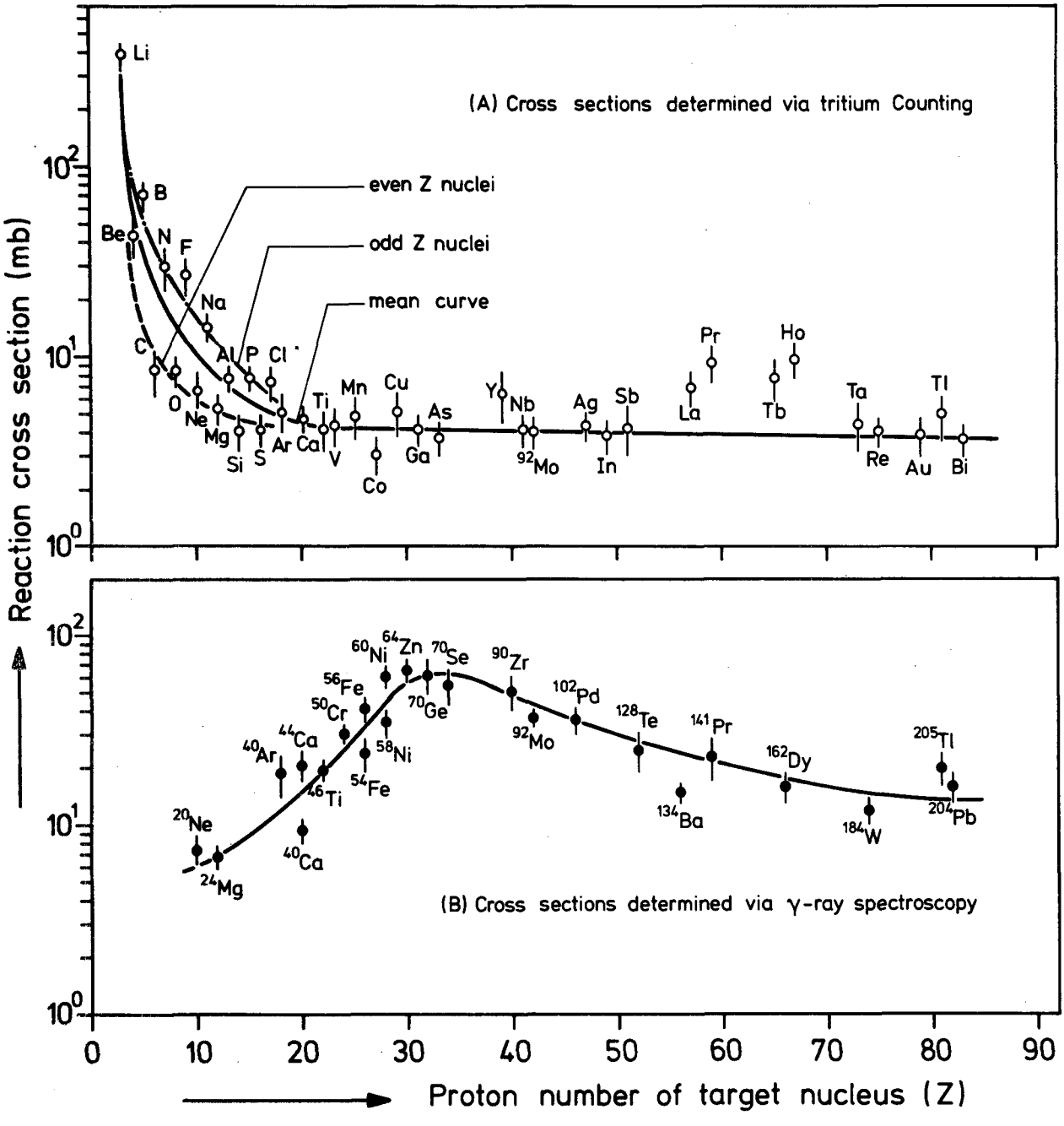

Fig. 1 Cross sections of nuclear reactions induced by fast neutrons plotted as a function of Z of the target element. (A) Data for [(n,t)+(n,xt)] reactions. (B) Data for [(n,t)+(n,n'd)+(n,p2n)] reactions.

1.2 Nuclear Data Measurements on FR-Wall and Structural Materials

S.M. Qaim, G. Stöcklin
(Relevant to request numbers: 741289, 741290, 741291, 741295, 741296, 741297, 741298, 741299, 762106, 762108, 762109, 762240, 762242, 762244)

In connexion with the determination of nuclear data for FRT-related first wall and structural materials, activation cross sections were measured at $E_n = 14.7 \pm 0.3$ MeV for several (n,x) reactions on Fe, Co and Ni. The study of (n,n'p) and (n,n'α) reactions was continued further. The results of those measurements were presented at the Specialist Meeting in Geel [2].

1.3 Precision Measurements of Nuclear Reaction Cross Sections at 14 MeV

S.M. Qaim

Cross sections for (n,α) reactions at 14.7±0.3 MeV on ten stable nuclides of the lanthanides Ce, Nd, Eu, Tb, Tm, Yb and Lu were measured by the activation technique using high-pressure liquid chromatography. An extensive report on (n,p) cross sections was published [3].

1.4 Formation and Emission of ^{37}Ar in Nuclear Reactors

S.M. Qaim, G. Stöcklin, R. Wölfle

As mentioned in last year's report, ^{37}Ar occurs in gaseous effluents from fission reactors. It is formed via the reaction ^{40}Ca(n,α)^{37}Ar, which takes place on the calcium impurity present in the carbon moderator. We have already reported [4] the cross section for this reaction. Studies on the diffusion dependent release of ^{37}Ar, with a view to determine the complete balance of ^{37}Ar, are underway.

1.5 Evaluation, Compilation and Systematics of Fast Neutron Induced Data

S.M. Qaim, R. Wölfle

Statistical model calculations using the Hauser-Feshbach method were carried out for a further four target nuclei (^{29}Si, ^{50}Cr, ^{54}Fe and ^{58}Ni). The conclusions were similar to those given in last year's report.

The systematics of (n,p) cross sections at 14.7 MeV were investigated in detail [3] and preliminary trends in the (n,n'p) and (n,n'α) reaction cross sections were reported [2]. Some systematic trends in tritium formation cross sections for neutrons produced via break-up of 53 MeV deuterons on a Be target (see above) were analysed [1].

A compilation of 14 MeV neutron induced reaction cross sections relevant to activation analysis was completed [5]. A summary of our nuclear data activities was given [6].

2. Charged Particle Data

S.M. Qaim, S.M. Sahakundu, G. Stöcklin, R. Weinreich

With a view to optimizing the conditions of production of medically important radioisotopes, in continuation of our earlier work [7,8] excitation functions of several charged particle induced nuclear reactions were measured. For example, for the production of ^{201}Tl via the process $^{203,205}Tl(p,xn)^{201}Pb \xrightarrow{EC,\beta^+} {}^{201}Tl$ the excitation functions of proton induced nuclear reactions on $^{203,205}Tl$ were determined over the energy range of 10 to 45 MeV. Part of the results are shown in Fig. 2. Through a choice of the energy of the incident protons it is possible to eliminate the contamination from $^{200}Pb(^{200}Tl)$ and to obtain ^{201}Tl in a highly pure form.

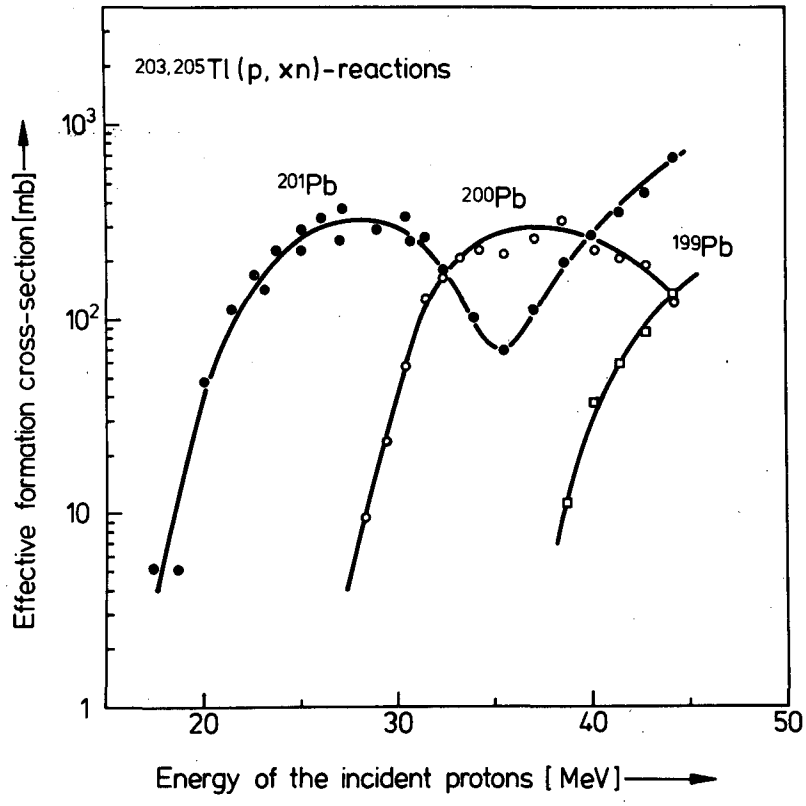

Fig. 2 Excitation functions for the formation of ^{201}Pb, ^{200}Pb and ^{199}Pb in the interactions of protons with natural thallium.

The nuclear data relevant to the production of short-lived ^{30}P were also measured. Following four reactions were investigated. $^{27}Al(\alpha,n)^{30}P$; $^{31}P(p,pn)^{30}P$; $^{31}P(n,2n)^{30}P$ and $^{32}S(n,t)^{30}P$. The excitation function of the (α,n) reaction was measured over E_α = 8 to 28 MeV and that of the (p,pn) reaction over E_p = 16 to 36 MeV. From considerations of product yields, radionuclidic purity, carrier-free form of ^{30}P, and ease in target construction etc., the reaction $^{27}Al(\alpha,n)^{30}P$ appears to be most promising.

An interdisciplinary utilization of accelerators was discussed and the role of accelerators and cyclotrons in the determination of nuclear data for energy research and isotope production was reviewed [9].

References

[1] S.M. Qaim, R. Wölfle, Triton emission in the interactions of fast neutrons with nuclei, Nucl.Phys. A295 (1978) 150

[2] S.M. Qaim, G. Stöcklin, Measurement and systematics of fast neutron induced hydrogen and helium producing reaction cross sections for FRT-related structural materials, Proc. Specialist Meeting on Neutron Data of Structural Materials for Fast Reactors, Geel, Belgium (December 1977), in press

[3] N.I. Molla, S.M. Qaim, A systematic study of (n,p) reactions at 14.7 MeV, Nucl.Phys. A283 (1977) 269

[4] S.M. Qaim, A. Rusheed, G. Stöcklin, R. Wölfle, ^{37}Ar formation from calcium in fission reactors, Int. J.appl.Radiat.Isotopes 28 (1977) 585

[5] S.M. Qaim, 14 MeV neutron activation cross sections, in Handbook of Spectroscopy - Volume III, CRC Press, Inc., Cleveland, Ohio, USA, in press

[6] S.M. Qaim, Contributions to nuclear chemistry and neutron threshold reactions, D.Sc. thesis, University of Birmingham, England (1977)

[7] S.M. Qaim, G. Stöcklin, R. Weinreich, Excitation functions for the formation of neutron deficient isotopes of bromine and krypton via high-energy deuteron induced reactions on bromine: Production of ^{77}Br, ^{76}Br and ^{79}Kr, Int.J.appl. Radiat.Isotopes 28 (1977) 947

[8] R. Weinreich, S.M. Qaim, G. Stöcklin, Cyclotron production of medically useful halogen radioisotopes, Proc. 15th International Annual Meeting of the Society of Nuclear Medicine, Groningen, The Netherlands, (September 1977), in press

[9] G. Stöcklin, Interdisciplinary utilization of accelerators, Proc. Regional Seminar, Buenos Aires, Argentina (December 1977), IAEA-SR-20, in press

INSTITUT FÜR KERNPHYSIK: EXPERIMENTELLE KERNPHYSIK II
KERNFORSCHUNGSANLAGE JÜLICH

1. Studies at the Fission Product Separator JOSEF

T.A. Khan, W.-D. Lauppe, H. Lawin, H.A. Selič, K. Sistemich

The separator JOSEF [1] at the research reactor FRJ-2 "Dido" of the Kernforschungsanlage Jülich is used since 1974 for nuclear spectroscopic investigations on the fission products in the mass regions A ≈ 100, 132 and 150. The ß-decays of ^{96}Sr, ^{96}Y, ^{97}Sr, ^{97}Y, ^{98}Sr, ^{98}Y, ^{99}Y, ^{99}Zr, ^{146}La, ^{147}Ce, ^{147}La and the level schemes of the corresponding daughters were investigated* up to 1976 [2-6]. In 1977 the activities concentrated on the level schemes of ^{100}Zr, ^{132}Sn and ^{133}Sb (Figs. 1 - 3). In $^{100}_{40}$Zr$_{60}$ a 0^+ state at 331 keV excitation energy has been observed [7], which is the lowest lying level of this kind known presently. Its life time [8] suggests the interpretation of ^{100}Zr as an asymmetric rotator. High spin µs-isomers at excitation energies of about 5 MeV have been found in the doubly magic nucleus $^{132}_{50}$Sn$_{82}$ [9] and its immediate neighbour $^{133}_{51}$Sb$_{82}$ [10]. The spin and parity assignments for the levels of ^{132}Sn result from RPA calculations [11] which fit well the experimental findings. The first two excited levels in ^{133}Sb are interpreted as single proton states whereas the levels above 4 MeV seem to be due to particle-core couplings.

References

[1] H. Lawin, J. Eidens, J.W. Borgs, R. Fabbri, J.W. Grüter, G. Joswig, T.A. Khan, W.D. Lauppe, G. Sadler, H.A. Selič, M. Shaanan, K. Sistemich, P. Armbruster, Nucl. Instr. Meth. 137 (1976) 103

[2] G. Sadler, T.A. Khan, K. Sistemich, J.W. Grüter, H. Lawin, W.D. Lauppe, H.A. Selič, M. Shaanan, F. Schussler, J. Blachot, E. Monnand, G. Bailleul, J.P. Bocquet, B. Pfeiffer, H. Schrader, B. Fogelberg, Nucl. Phys. A252 (1975) 365

[3] K. Sistemich, G. Sadler, T.A. Khan, H. Lawin, W.D. Lauppe, H.A. Selič, F. Schussler, J. Blachot, E. Monnand, J.P. Bocquet, B. Pfeiffer, Z. Physik A281 (1977) 169

[4] K. Sistemich, G. Sadler, T.A. Khan, J.W. Grüter, W.D. Lauppe, H. Lawin, H.A. Selič, F. Schussler, J. Blachot, J.P. Bocquet, E. Monnand, B. Pfeiffer, Report CERN 76-13 (1976) 495

---

* in cooperation with scientists working at the separator LOHENGRIN of the Institute Laue-Langevin, Grenoble, France

[5] E. Monnand, J. Blachot, F. Schussler, J.P. Bocquet, B. Pfeiffer, G. Sadler, H.A. Selič, T.A. Khan, W.D. Lauppe, H. Lawin, K. Sistemich, Report CERN 76-13 (1976) 477

[6] E. Monnand, J. Blachot, J.P. Bocquet, B. Pfeiffer, F. Schussler, K. Sistemich, T.A. Khan, W.-D. Lauppe, H. Lawin, G. Sadler, H.A. Selič, Annual Report 1976 of Institut für Kernphysik, KFA Jülich, KFA-IKP 10/77, p. 48, 49

[7] T.A. Khan, W.D. Lauppe, K. Sistemich, H. Lawin, G. Sadler, H.A. Selic, Z. Physik A283 (1977) 105

[8] T.A. Khan, W.-D. Lauppe, K. Sistemich, H. Lawin, H.A. Selič, Z. Physik A284 (1978) 313

[9] W.-D. Lauppe, K. Sistemich, T.A. Khan, H. Lawin, G. Sadler, H.A. Selič, O.W.B. Schult, Proceedings Int. IUPAP Conf. on Nuclear Structure, Tokio/Japan 1977, in press

[10] K. Sistemich, W.-D. Lauppe, T.A. Khan, H. Lawin, H.A. Selič, J.P. Bocquet, E. Monnand, F. Schussler, Z. Physik 285 (1978) 305

[11] J.S. Dehesa, W.-D. Lauppe, K. Sistemich, J. Speth, Physics Letters, in press

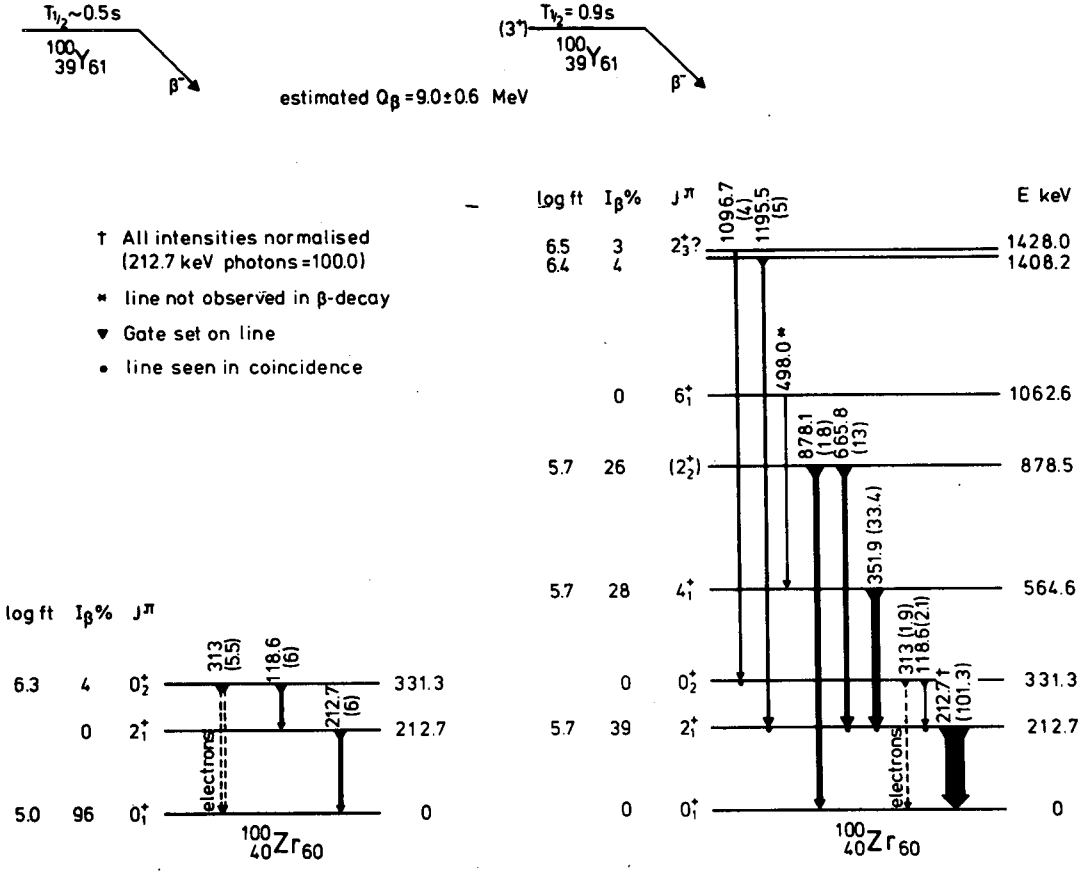

Fig. 1 The level scheme of ^{100}Zr [7]. It is estimated that 30% of the ^{100}Y produced in fission decays through the 0.9 s decay mode.

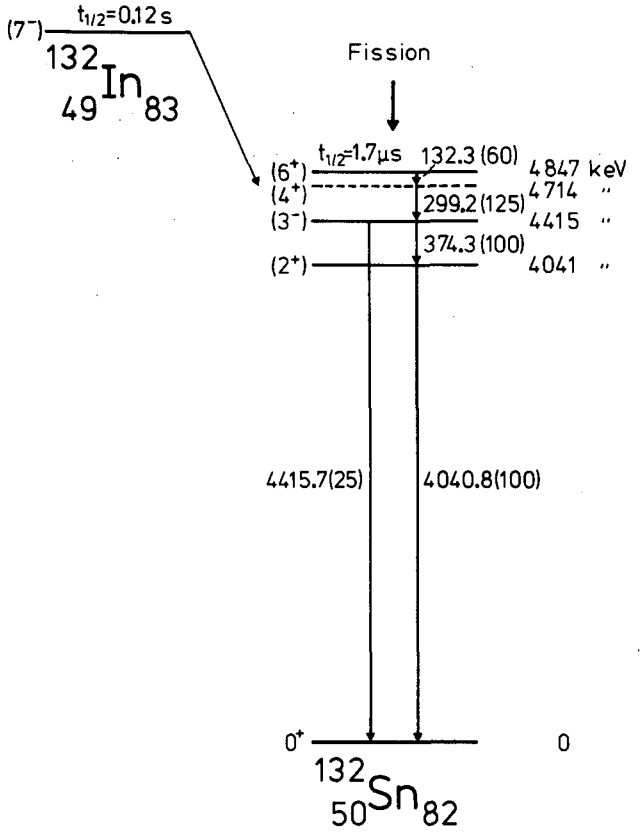

Fig. 2 Level scheme of ^{132}Sn [9].

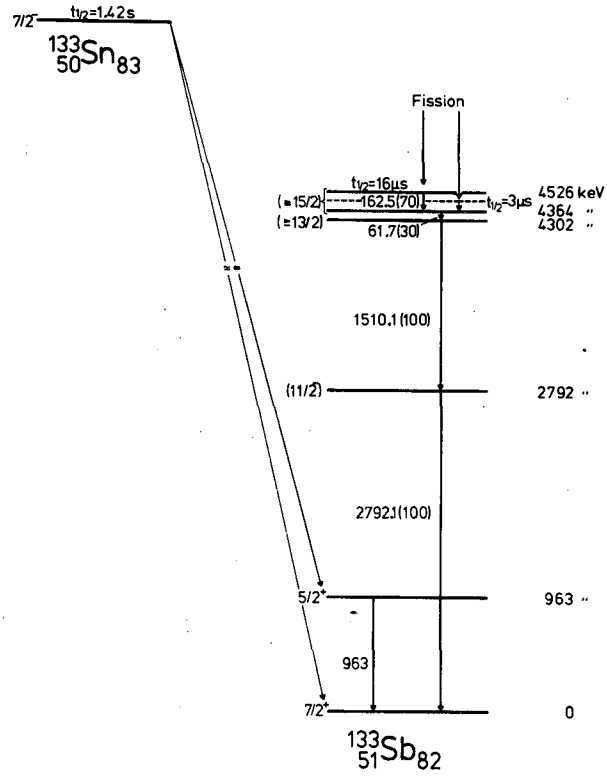

Fig. 3 Proposed scheme of ^{133}Sb [10].

2. Cross Sections for the Formation of ^{48}Cr via α- and ^{3}He-Particle Induced Nuclear Reactions on Natural Titanium

H.J. Probst, R. Weinreich*, S.M. Qaim*

The relatively short-lived ^{48}Cr ($T_{1/2}$: 23 h) should cause less radiation dose than the longer-lived ^{51}Cr ($T_{1/2}$: 27.7 d) and is thus a potentially useful radionuclide for applications in life sciences. In collaboration with the Institut für Chemie (1): Nuklearchemie, KFA Jülich cross sections for the production of ^{48}Cr via α- and ^{3}He particle induced nuclear reactions on natural titanium were measured by the stacked-foil technique. The excitation functions are shown in Fig. 1 and the calculated cumulative yields of ^{48}Cr in Fig. 2.

---

* Institut für Chemie (1): Nuklearchemie, KFA Jülich

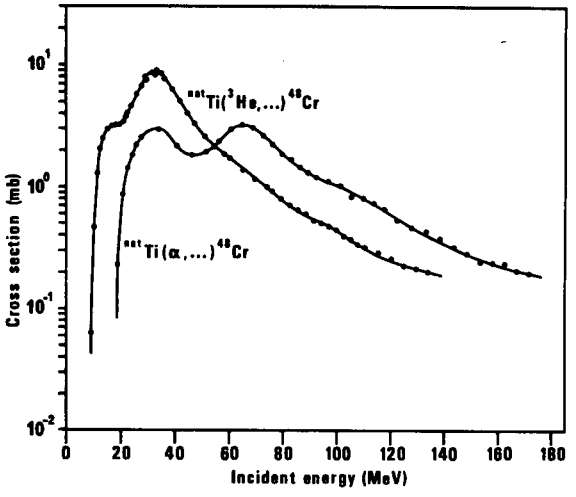

Fig. 1 Excitation functions for the formation of ^{48}Cr in α- and ^{3}He-particle induced nuclear reactions on natural titanium.

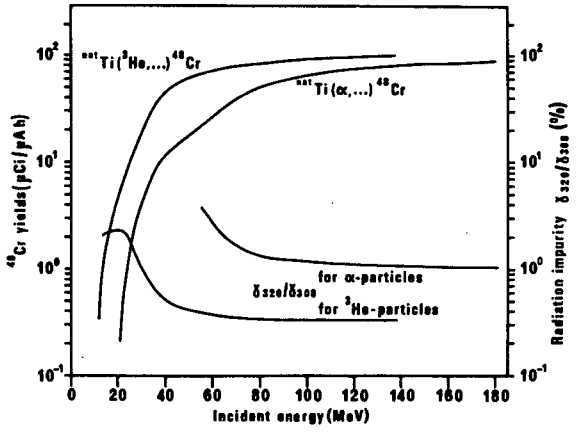

Fig. 2 Cumulative yields of ^{48}Cr in α- and ^{3}He-particle induced nuclear reactions on natural titanium. The radiation impurity due to ^{51}Cr (γ: 320 keV) is given as a percentage of ^{48}Cr (γ: 308 keV).

For incident α-particle energy of 170 MeV the ^{48}Cr yield amounts to 90 μCi/μAh; however, the level of contamination from ^{51}Cr is high. If an upper tolerable limit of ^{51}Cr is placed at < 1%, a ^{48}Cr yield of 55 μCi/μAh can be achieved. As can be seen in Fig. 2, better ^{48}Cr yield values are obtained using ^{3}He-particles. For $E_{^3He}$ = 135 MeV (maximum energy of ^{3}He-particles at the Jülich Isochronous Cyclotron JULIC) the ^{48}Cr yield amounts to 100 μCi/μAh with "effective radiation impurity" due to ^{51}Cr around 0.3%. Even at $E_{^3He}$ = 36 MeV (maximum energy of ^{3}He-particles at the high current Compact Cyclotron CV 28) the ^{48}Cr yield amounts to 35 μCi/μAh with ^{51}Cr radiation impurity of 0.6%, showing thereby good ^{48}Cr production possibilities at the Compact Cyclotron.

3. Production of ^{47}Ca through Deuteron Bombardment of Titanium

H.J. Probst

Studies which are carried out with the use of the radionuclide ^{47}Ca are facilitated considerably if high specific activities or even carrier-free material is available. In view of the successful production of other carrier-free radioisotopes at the high-energy beam of the isochronous cyclotron JULIC, the cross section has been measured for the production of ^{47}Ca through deuteron bombardment of a natural titanium target for deuteron energies up to 90 MeV. A thick target yield of 24 μCi/μAh was obtained. Making use of the full beam intensity one can thus produce more than 0.5 mCi/h of carrier-free ^{47}Ca by bombarding the inexpensive Ti with energetic deuterons.

INSTITUT FÜR EXPERIMENTALPHYSIK
UNIVERSITÄT HAMBURG

1. Charged Particle Induced Neutron Emission

In continuation of our previous work on (n,2n) reactions we have studied (^{3}He,xn) and (α,xn) excitation functions with activation techniques at the Hamburg Isochronous Cyclotron.

1.1 The Reactions ^{9}Be(τ,n)^{11}C and ^{9}Be(α,2n)^{11}C

P. Kofahl, B. Anders, W. Scobel

^{3}He-particles of 6-41 MeV and α-particles of 20-32 MeV have been used to activate foil stacks. The 20.7 ± 0.06 min β^+-activity of ^{11}C was measured with a NaI(Tl) pair spectrometer. The results obtained complete our data [1,2] on the reactions ^{10}B(d,n)^{11}C, ^{11}B(p,n)^{11}C, ^{12}C(n,2n)^{11}C and ^{11}B(d,2n)^{11}C populating the compound systems ^{12}C* and ^{13}C*, respectively. The excitation functions, divided by the optical model cross section $\sigma_c(E^*)$ for absorption of the projectile:

$$\eta(E^*) = \frac{\sigma_{exp}(a,b)}{\sigma_c(E^*)} \qquad (1)$$

are given in Fig. 1. Neglecting the small isospin dependence for light nuclei, $\eta(E^*)$ may be interpreted [3] as a decay probability averaged over the spins I populated in the compound system:

$$\sigma(a,b) = \sum_I \eta_b(E^*,I)\sigma_c(E^*,I) = \langle\eta_b(E^*,I)\rangle_I \Sigma_I \sigma_c(E^*,I) \ . \qquad (2)$$

Independence of compound system decay from its formation should result in a single function $\eta(E^*) = \langle\eta_b(E^*,I)\rangle_I$ for all reactions proceeding via the same compound system as long as the number of I values contributing in eq. (2) is small. This is correct for the p-, n- and d-induced reactions, but not for the τ- and α-induced reactions, because the high angular momenta in the entrance channel cannot be carried away by neutron emission. For these reactions smaller values of $\eta(E^*)$ are expected in agreement with Fig. 1.

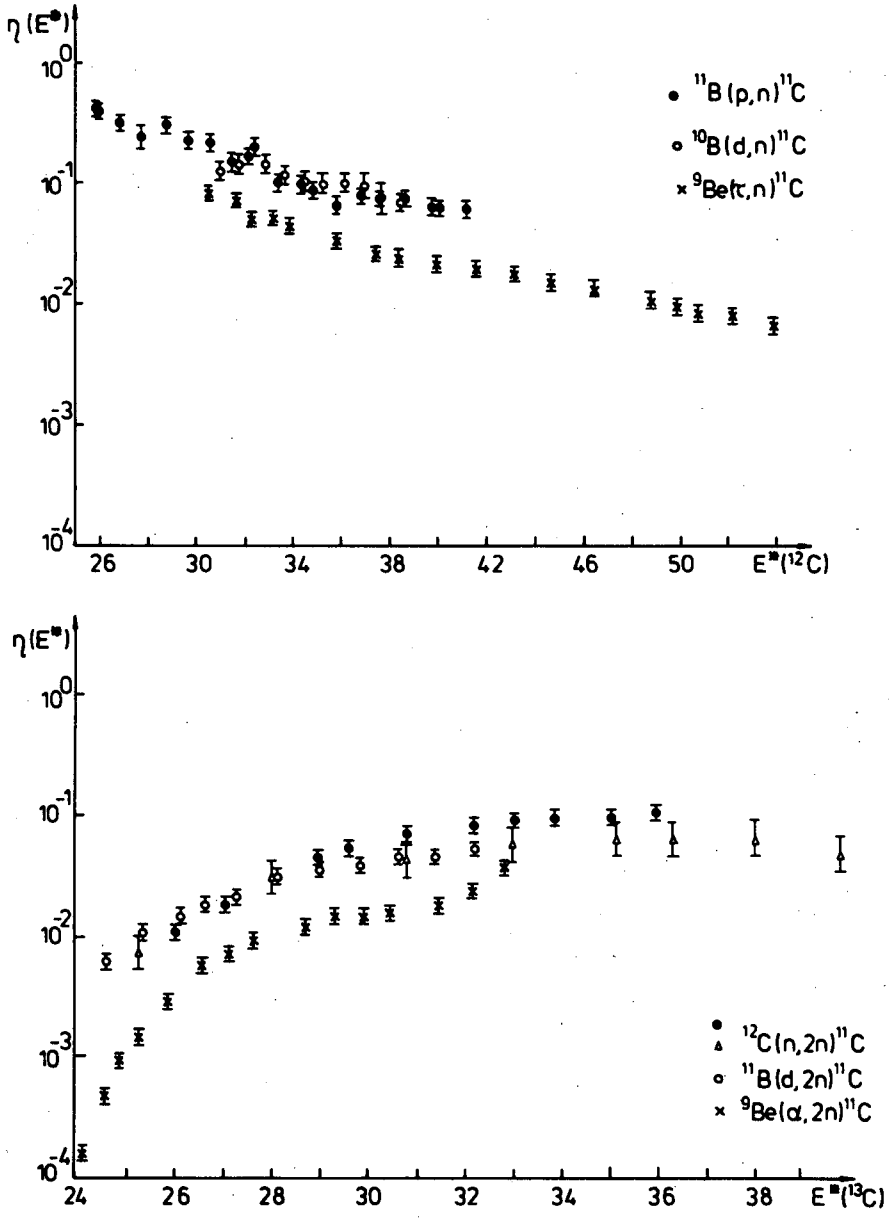

Fig. 1 Reduced excitation functions of reactions proceeding via the compound systems $^{12}C^*$ and $^{13}C^*$, plotted against their excitation energy E^*.

Therefore the calculation of the excitation functions has been performed with a spin dependent statistical model [4]. The results are shown in Fig.2. The remaining disagreement is due to a) problems related to the applicability of the statistical model to such light systems, b) ambiguities in the parameters used and c) contributions resulting from non compound mechanisms, expecially in the (x,n) reactions.

1.2 Excitation Functions of ^{3}He Reactions with ^{63,65}Cu and ^{93}Nb

R. Georgi, H. Bissem, W. Scobel

The ^{3}He induced multiple neutron emission from ^{63,65}Cu and ^{93}Nb has been investigated with projectiles between 11 MeV and 44 MeV. Single foils and foil stacks including aluminium degraders have been irradiated and subsequently analyzed with a Ge(Li) detector. The reactions and the γ-lines followed are listed in Table I. The excitation functions obtained are shown (with one exception) in Figs. 3a-3d together with the results of refs.[5-7].

Comparisons with model calculations show that
(i) the full statistical model [4] cannot explain the high energy tails of the excitation functions (Fig.3e); in the region with dominant compound contribution its prediction is not significantly better than that of the simpler Ewing-Weisskopf model;
(ii) in calculations with a combined compound/precompound model [8] nucleon binding energies should be taken from experimental data whenever possible, and pairing corrections should be implemented in the calculation, especially near closed shells (see e.g. (in Fig.3f) the improvement obtained this way for the reaction ^{93}Nb(τ,4n)^{92}Tc);
(iii) the best description of the experimental data is obtained by combining the Ewing-Weisskopf calculation with the geometry dependent hybrid model (GDH) and an initial configuration of n_o=4 excitons (1.5 neutrons, 2.5 protons, no hole). These values are in good agreement with those obtained [9,10] from the energy spectra of particles emitted in ^{3}He induced reactions.

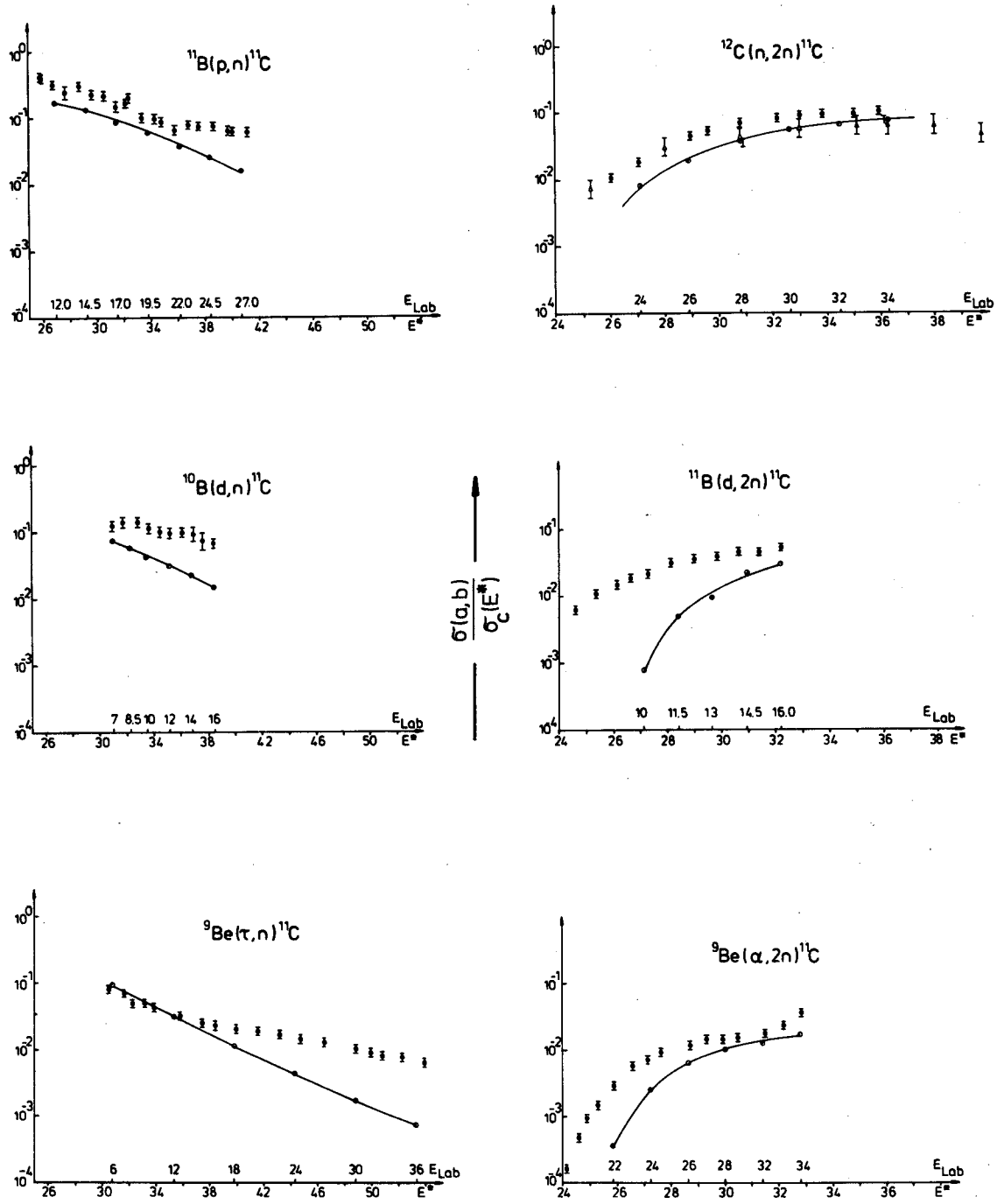

Fig. 2 Experimentally determined quantities $\eta(E^*)$ compared with full statistical model calculations (solid lines).

TABLE I. Reactions and γ-lines used for identification

Reaction	$T_{1/2}$	E (keV) g.s.	Branching ratio	$T_{1/2}$	E (keV) m.s.	Branching ratio
$^{63}Cu(\tau,n)^{65}Ga \rightarrow ^{65}Zn$	15m	115 153	0.55 0.09			
$^{63}Cu(\tau,2n)^{64}Ga \rightarrow ^{64}Zn$	2.6m	808.8 991.6	0.14 0.46			
$^{63}Cu(\tau,3n)^{63}Ga \rightarrow ^{63}Cu$*	38.8m	669.6 961.9	0.112 0.084			
$^{65}Cu(\tau,n)^{67}Ga \rightarrow ^{67}Zn$	78.0h	93.3	0.70			
$^{65}Cu(\tau,2n)^{66}Ga \rightarrow ^{66}Zn$	9.4h	834 1039	0.06 0.37			
$^{65}Cu(\tau,3n)^{65}Ga \rightarrow ^{65}Zn$	15.2m	115 153	0.55 0.09			
$^{65}Cu(\tau,4n)^{64}Ga \rightarrow ^{64}Zn$	2.6m	991.6 1386.9	0.46 0.14			
$^{93}Nb(\tau,n)^{95}Tc \rightarrow ^{95}Mo$	20h	765.8	0.94	61d	203.9	0.64
$^{93}Nb(\tau,2n)^{94}Tc \rightarrow ^{94}Mo$	293m	849.7 702.6	0.977 0.998	52m	871 871	1.00 0.94
$^{93}Nb(\tau,3n)^{93}Tc \rightarrow ^{93}Mo$	2.75h	1363 1521	0.67 0.25	43.0m	390	0.63
$^{93}Nb(\tau,4n)^{92}Tc \rightarrow ^{92}Mo$	4.4m	147.9	0.55			

* $(\tau,3n) + (\tau,2np)$

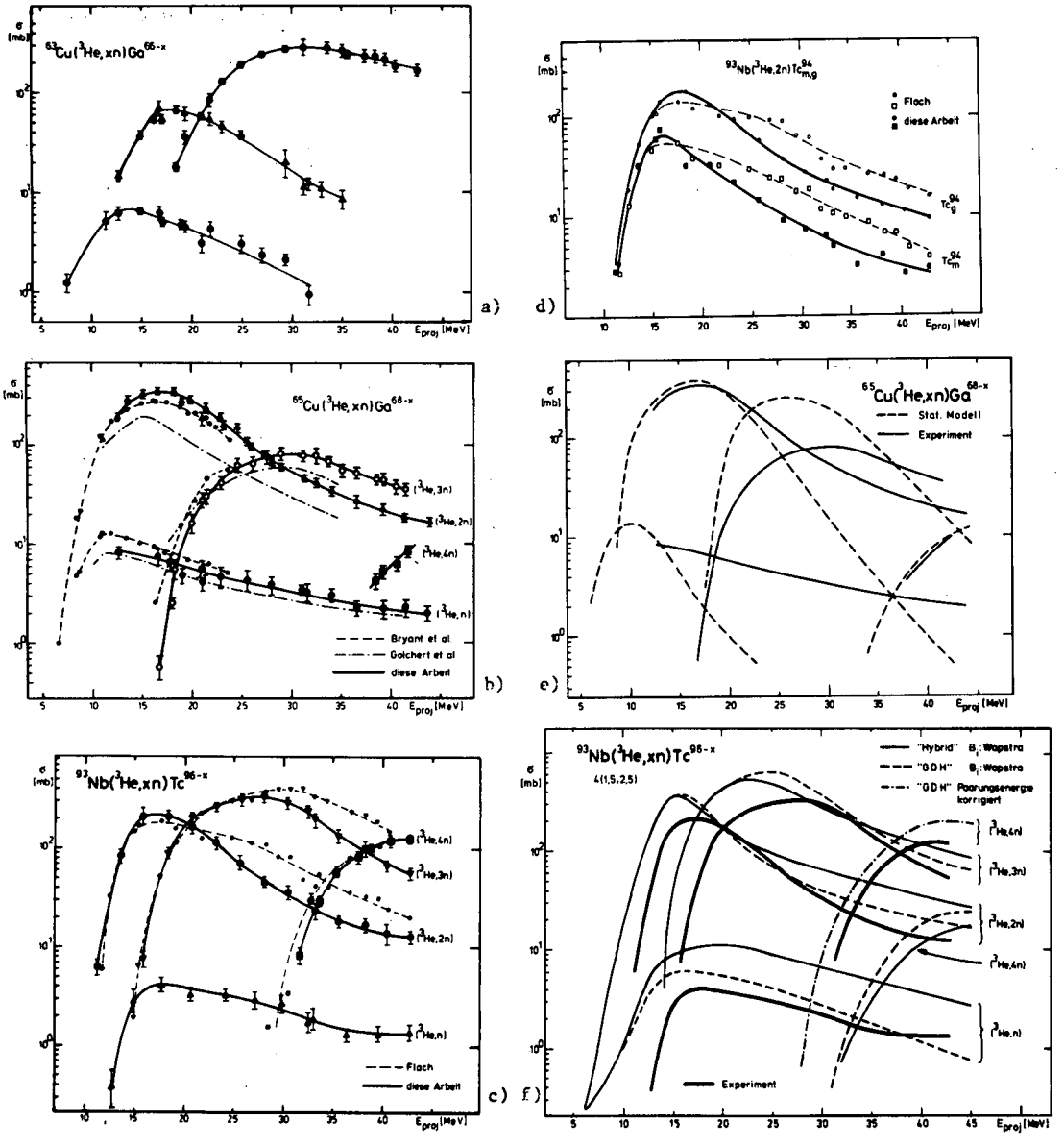

Fig. 3 Experimentally determined excitation functions (Fig. 3a-3d) and comparisons with model calculations (Fig. 3e, 3f). See text for details.

References

[1] B. Anders, M. Bormann, W. Scobel, EANDC(E)157 "U" (1973)

[2] A. Ackermann, B. Anders, M. Bormann, W. Scobel, Proc. Int. Conf. on Nucl. Cross Sections and Technology, Washington, D.C. (March 1975), NBS Special Publication No. 425 (1975) p. 819

[3] J.M. Miller, Proc. Int. Conf. on Statistical Properties of Nuclei (Albany, 1972) p.505

[4] M. Uhl, Nucl.Phys. A184 (1972) 253

[5] S. Flach, Thesis (Karlsruhe,1976), KFK-Report 2279

[6] N.W. Golchert, J. Sedlet, D.G. Gardner, Nucl.Phys. A152 (1970) 419

[7] E.A. Bryant, D.R.F. Cochran, J.P. Knight, Phys.Rev. 130 (1963) 1512

[8] M. Blann, Code 'Overlaid Alice', US-ERDA Report COO-3494-29 (1976)

[9] A. Chevarier et al., Nucl.Phys. A231 (1974) 64

[10] J. Bisplinghoff et al., Nucl.Phys. A269 (1976) 147

INSTITUT FÜR REINE UND ANGEWANDTE KERNPHYSIK
UNIVERSITÄT KIEL, FORSCHUNGSREAKTOR GEESTHACHT

Fast Chopper Time-of-Flight Spectrometer and Crystal Spectrometer

H.G. Priesmeyer, U. Harz, P. Fischer, K. Freitag, P. Podewils

1. Measurements on Cd Isotopes

(relevant to request number: 752002)

A detailed discussion of the measurements on the ^{114}Cd enriched sample has been published [1]. The measurements on enriched ^{108}Cd have been completed. Analysis of resonance parameters is in progress.

2. Investigation of GFP Samples

From the pool of gross fission product samples, which have to be remeasured during their cooling time in order to identify the resonances in the transmission spectrum, the KWO (Kernkraftwerk Obrigheim) sample with a burnup of 18500 MWd/to of UO_2 nuclear fuel, originally enriched to 2.8 % has been measured in the energy region around 2 eV and in the resolved resonance region. Between 2.68 eV and 1.056 eV no other resonances have been detected. An analysis of the high energy region is in progress.

3. Measurements of the Total Neutron Cross Section of ^{99}Tc

(relevant to request number: 741076)

Recently published evaluations of the resonance parameters of ^{99}Tc show considerable discrepancies among the experimental values as well as between some experimental values and the theoretical expectation. Since ^{99}Tc is an important fission product with a high fission yield, it has been measured with optimum energy resolution with the Fast Chopper. From 15 g of material two samples of different thicknesses have been prepared. The investigations concentrated on the two lowest resonances at 5.6 eV and 20.3 eV. They are essentially Doppler-broadened and are being analysed by the SHAPE code of Atta and Harvey. Fig. 1 shows the transmission of two runs on ^{99}Tc.

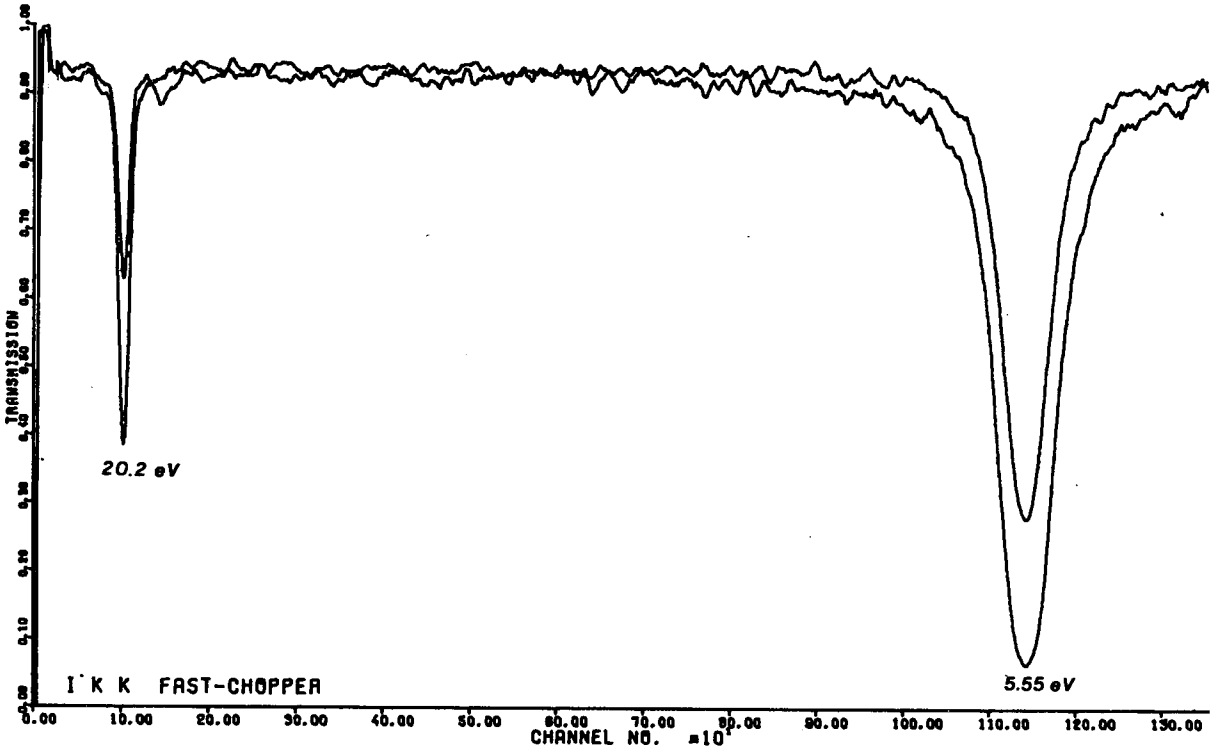

Fig. 1 Neutron transmission of two ^{99}Tc samples of different thicknesses between 24 eV and 4.5 eV.

4. ^{240}Pu Resonance at 1.056 eV

A transmission measurement on plutonium enriched to 8 % in ^{240}Pu is prepared, in order to clarify the significant differences in the resonance parameters of the large resonance at 1.056 eV, as stated by the Advisory Group on TND (cf. Technical Document IAEA - 186, Vol. II p. 30 & 31).

5. Total Cross Section of ZrH at 77K

The measurements with the crystal spectrometer have confirmed Fermi's theory, although they do not show the minima as sharp as predicted. They have been continued by increasing the energy resolution of the spectrometer to about 0.5 % (using a Cu monochromator crystal in 200 direction) and by reducing the overall deadtime to less than 5 µsec by use of a Li-6 glass scintillation detector. The total cross section (cf. Fig. 2) shows structures, which were not seen before and which can be related to structures in the double differential cross section in the energy region of the first minimum (~ 137 meV) measured at Batelle some years ago. More detailed information can be found in [2] and [3].

References

[1] K. Freitag, Der totale Neutronenwirkungsquerschnitt der Cd Isotope 110,111,112,114 und 116 im Resonanzbereich, Diplomarbeit, Kiel (1977)

[2] P. Podewils, H.G. Priesmeyer, in Inelastic Neutron Scattering, IAEA-SM219/4 - Vienna (1977)

[3] P. Podewils, Diplomarbeit i.V. (1978)

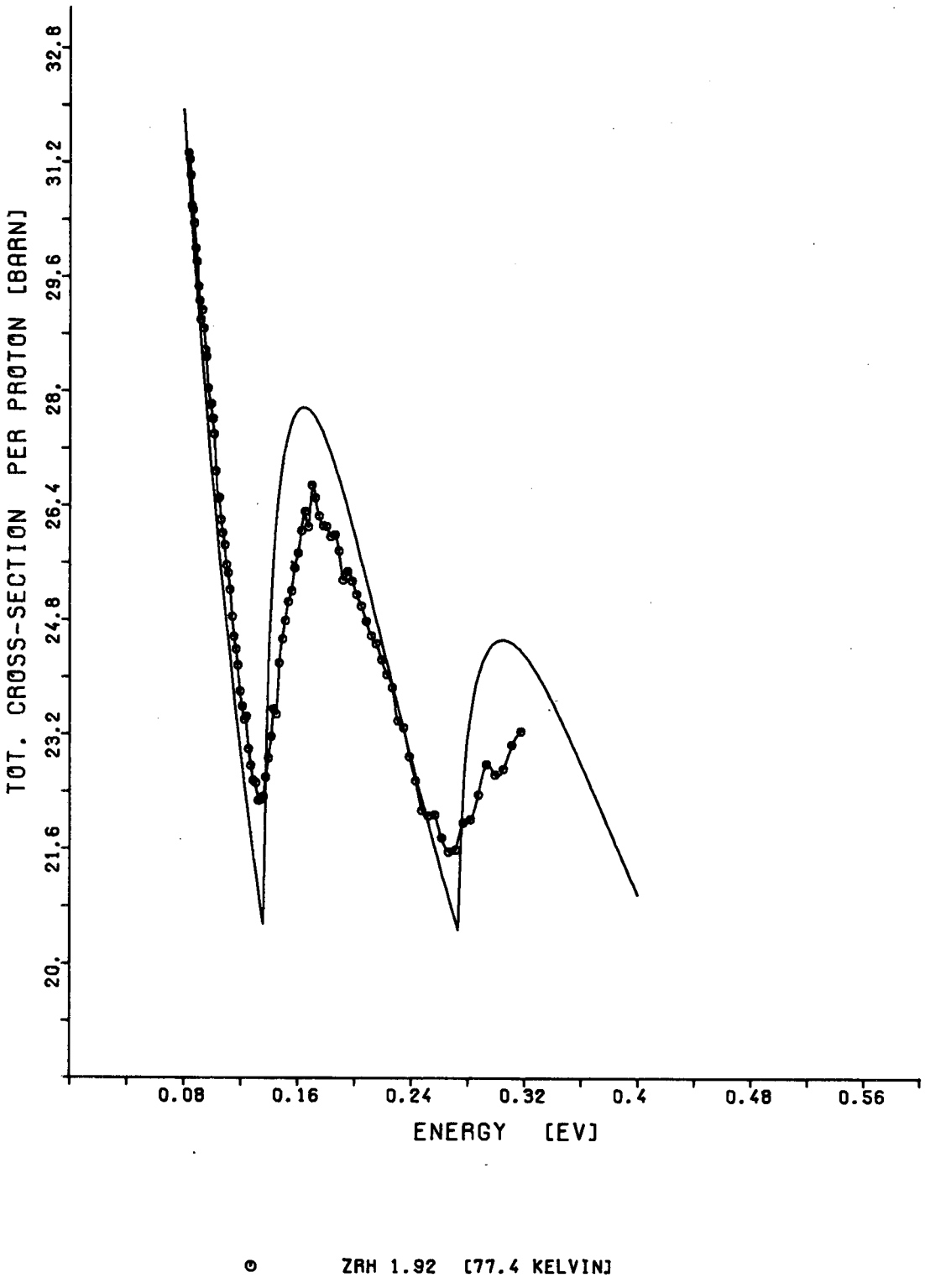

Fig. 2 Total neutron cross section per proton of $ZrH_{1.92}$ at liquid nitrogen temperature.

INSTITUT FÜR KERNCHEMIE
UNIVERSITÄT ZU KÖLN

1. Spontaneous Fission Decay Constant of ^{238}U

K. Thiel, W. Herr

Previous determinations of the spontaneous fission decay constant of ^{238}U (λ_f^{238}) cover a wide range of values from 0.7 to 10.3 x $10^{-17} yr^{-1}$ and employ a variety of radiochemical and physical methods [1]. Recent work on the ^{238}U-spontaneous fission half-life (which is essential for fission track dating) is characterized by a controversial grouping of λ_f^{238}-values around $6.9 \times 10^{-17} yr^{-1}$ [2] and $8.5 \times 10^{-17} yr^{-1}$ [3].

Therefore, by means of a man-made uranium glass of known age, λ_f^{238} was redetermined utilizing the accumulation of latent fission product tracks within the matrix of the glass since the date of glass manufacture (July 1844 $\pm \overset{o}{1}$ yr). The U-content of the glass was determined by neutron induced ^{235}U-fission to be 0.3% using the uranium standard glass NBS SRM 610. All neutron irradiations were performed in the thermal column of the FRJ-1 reactor at the KFA Jülich. The homogeneity of the uranium in the glass was controlled by measuring the ratio ρ_i/D of the density ρ_i of n-induced ^{235}U-fission tracks and the thermal neutron dose D for different irradiated chips of the glass. The variation of this ratio remains within 1.4% which is extremely small.

The ^{238}U spontaneous fission decay constant was then derived from the track density of spontaneous ^{238}U fission tracks counted on polished sections of 28 pieces of the glass using the relation

$$\lambda_f^{238} = \frac{\sigma_f^{238} I_{235/238} \rho_s}{t} S \qquad (1)$$

$$S = \sum_{\nu=1}^{n} (g_\nu D_\nu / \rho_{i\nu}) / \sum_{\nu=1}^{n} g_\nu \qquad (2)$$

where

σ_f^{235} = cross section for thermal n-induced fission of ^{235}U

$I_{235/238}$ = natural isotopic ratio of $^{235}U/^{238}U$

σ_s = spontaneous ^{238}U fission track density

t = age of the uranium glass

n = number of samples (28)

$\rho_{i\nu}$ = induced ^{235}U fission track density of sample ν produced by the neutron fluence D_ν, and

g_ν = weighting factor giving the number of visual fields on sample ν surveyed to count induced tracks.

From the induced track and neutron fluence data a value of $S = 1.1417 \times 10^7$ was determined. The values of the other parameters were taken to be: $\sigma_f^{235} = 580.2 \pm 1.8$ barn [4], $I_{235/238} = (7.259 \pm 0.104) \times 10^{-3}$ [5], $\rho_s = 224.5 \pm 4$ tracks cm^{-2}, and $t = 125.94 \pm 5$ yr. To meet any systematic error arising from the uncertainty of the time interval between cooling of the glass melt and engraving-dating the limits of error of t were chosen to be ±5 yr instead of ±1 yr [1].

A comprehensive study of all the possible sources of error [1,7] shows that there are only negligible interferences due to cosmic ray induced U-fission, natural radioactivity of the glass and thermal track fading. Using eq. (1) a value for the ^{238}U fission decay constant of

$$\lambda_f^{238} = (8.57 \pm 0.42) \times 10^{-17} yr^{-1}$$

is obtained. This result, which yields e.g. fission track ages that are fully consistent with the history of man-made U-glass-ware [6], supports the λ_f^{238}-values grouped around $8.5 \times 10^{-17} yr^{-1}$.

References

[1] K. Thiel, W. Herr, The ^{238}U spontanoeus fission decay constant re-determined by fission tracks, Earth Planet. Sci.Lett. 30 (1976) 50

[2] R.L. Fleischer, P.B. Price, Decay constant for spontaneous fission of ^{238}U, Phys.Rev. 133 (1964) 2975

[3] D. Galliker, E. Hugentobler, B. Hahn, Spontane Kernspaltung von ^{238}U and ^{241}Am, Helv.Phys.Acta 43 (1970) 593

[4] G.C. Hannah, C.H. Westcott, H.D. Lemmel, B.P. Leonard, Jr., J.S. Story, P.M. Attree,Revision of values for the 2200 m/s neutron constants for four fissile nuclides, At.Energy Rev. 7 (1969) 3

[5] W.J. de Wet, J. Turkstra, Determination of $^{235}U/^{238}U$ ratios by activation analysis utilizing high resolution γ-spectrometry, J.Radioanal.Chem. 1 (1968) 379

[6] F. Kirchheimer, Das Uran und seine Geschichte, Schweizerbart'sche Verlagsbuchhandlung, Stuttgart (1963)

[7] K. Thiel, Universität zu Köln, Thesis (1974)

2. Excitation Functions for p-Induced Reactions with Ti, V, Fe, Co, and Ni in the Energy Region from 10 to 45 MeV

R. Michel, G. Brinkmann, H. Weigel, W. Herr

Thin target production cross sections can be regarded as a basis for the interpretation of cosmic ray produced radionuclides in extraterrestrial matter. With regard to the radiation history of meteoritic and lunar material, the bambardment with solar protons of energies below 100 MeV is an important factor. However, there exists a considerable lack of experimental excitation functions for the light and medium-weight elements which are the main targets in this kind of matter.

For this reason, a systematic study of p-induced reactions on cosmochemically relevant target elements (here Ti, Fe and Ni) was started. Furthermore, experimental excitation functions allow to test the actual theories of nuclear reactions. Since for Ti, Fe and Ni an unambiguous assignment of an observed radionuclide to a particular reaction channel is difficult because of their complex natural isotopic composition, we investigated additionally vanadium and cobalt as target elements.

41 individual excitation functions were measured in the energy region from 10 to 45 MeV using the stacked foil technique. The irradiation was performed at the isochronous cyclotron JULIC at the KFA Jülich. The product nuclides observed and the respective reaction types involved are presented in Table I. Details of the experimental procedure are given elsewhere [1].

Table I. Summary of radionuclides for which excitation functions have been determined

TARGET ELEMENT	PRODUCT NUCLIDES OBSERVED — REACTION TYPES				
	(p,Xn)	(p, pXn)	(p, 2pXn)	(p, 3pXn)	(p, 4pXn)
NICKEL	^{61}Cu	^{56}Ni ^{57}Ni	^{55}Co ^{56}Co ^{57}Co $^{58m+g}Co$ $^{60m+g}Co$		$^{52m+g}Mn$
COBALT	^{56}Ni ^{57}Ni	^{56}Co ^{57}Co $^{58m+g}Co$		^{54}Mn ^{56}Mn	
IRON	^{55}Co ^{56}Co ^{57}Co $^{58m+g}Co$	^{52}Fe	$^{52m+g}Mn$ ^{54}Mn	^{51}Cr	^{48}V
VANADIUM	^{48}Cr ^{49}Cr ^{51}Cr	^{48}V		$^{46m+g}Sc$ ^{47}Sc ^{48}Sc	
TITANIUM	^{48}V	(^{44}Ti) *	^{43}Sc ^{44m}Sc ^{44g}Sc $^{46m+g}Sc$ ^{47}Sc ^{48}Sc		^{43}K

cosmochemically important target element — found in lunar or meteoritic samples — decay products found in extraterrestrial material

* Measurements on the formation of ^{44}Ti from Ti have not yet been finished.

The experimental data were compared with theoretical excitation functions calculated by means of the computer code OVERLAID ALICE [2] which combines the Weisskopf-Ewing evaporation theory [3] with the preequilibrium hybrid model of Blann [4].

In general, the theory reproduces the experimental values quite well. A typical example is demonstrated in Fig. 1, giving (p,xn) reactions on natural iron. However, some difficulties, e.g. with respect to the preequilibrium emission of complex particles, have still to be considered [5]. In Fig. 2 a comparison between experimental and theoretical excitation functions for the (p,2pxn) reactions on Ni is shown. For the product radionuclides ^{56}Co, ^{57}Co, and also to some extent with minor restrictions for $^{60m+g}$Co, the agreement is satisfactory. The production of $^{58m+g}$Co at energies below 22 MeV via the ^{61}Ni(p,α)- and ^{62}Ni(p,αn)-reactions is underestimated by the theory. Similar discrepancies were observed with respect to the emission of α-particles in p-induced reactions on Ti [1]. In the case of the ^{55}Co-production from Ni at ~30 MeV the theory predicts values which are lower by more than one order of magnitude. This deviation is probably due to preequilibrium emission of α-particles not considered in the hybrid model.

References

[1] R. Michel, G. Brinkmann, H. Weigel, W. Herr, Proton induced reactions on titanium with energies between 13 and 45 MeV, submitted to J.Inorg.Nucl.Chem.

[2] M. Blann, Rep. COO-3493-32 (1977)

[3] V.F. Weisskopf, D.H. Ewing, On the yield of nuclear reactions with heavy elements, Phys.Rev. 57 (1940) 472

[4] M. Blann, Hybrid model for preequilibrium decay in nuclear reactions, Phys.Rev.Letters 27 (1971) 337

[5] R. Michel, H. Weigel, W. Herr, Proton induced reactions on nickel with energies between 12 and 45 MeV, submitted to Z.Physik.

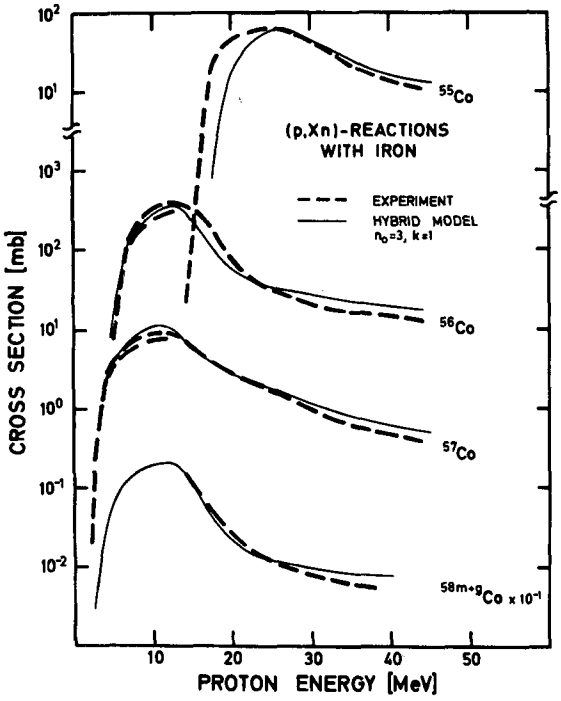

Fig. 1 Experimental excitation functions for (p,xn)-reactions on natural iron and theoretical predictions based on the hybrid model.

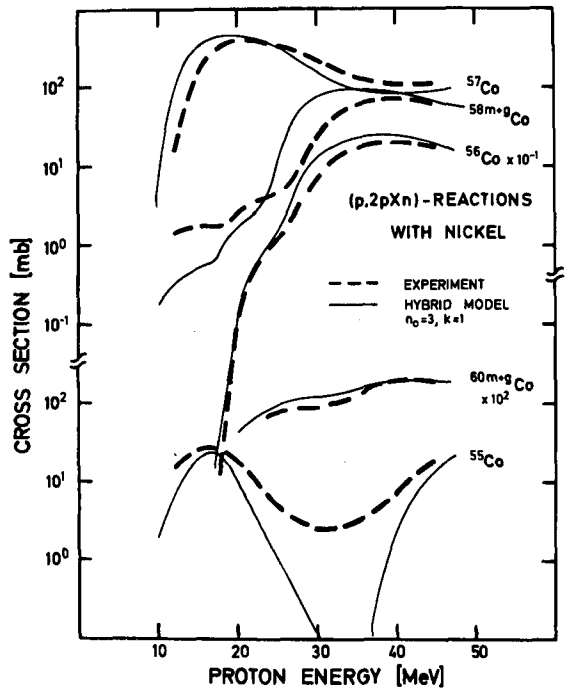

Fig. 2 Experimental excitation functions for (p,2pxn)-reactions on natural nickel and theoretical predictions based on the hybrid model.

3. Activation Cross Section σ_{therm} and Half-life of ^{53}Mn

R. Wölfle[+], W. Herr, U. Herpers

Because of applications in cosmochemistry the nuclear data of the longlived radionuclide ^{53}Mn are of growing interest. Even in literature, e.g. in recent data compilations [1,2], the value of the activation cross section of ^{53}Mn is often incorrect. Therefore, in this progress report we refer to our detailed publication [3] dealing with the activation cross section σ_{therm} and with the half-life of ^{53}Mn.

The σ_{53} = 66 ± 7 barn was determined by a 587 days reactor irradiation of meteoritical manganese containing spallogenic ^{53}Mn. The redetermination of the product $T_{53} x \sigma_{53}$ = (260 ± 32)barn x years resulted in a half-life of T_{53} = (3.9 ± 0.6) x 10^6 yr.

References

[1] Nuklidkarte, 4. Auflage, W. Seelmann-Eggebert, G. Pfennig, H. Münzel, Institut für Radiochemie, Gesellschaft für Kernforschung m.b.H., Karlsruhe (1974)

[2] G. Erdtmann, Neutron activation tables, Kernchemie in Einzeldarstellungen, Vol. 6, Verlag Chemie (1976)

[3] R. Wölfle, W. Herr, U. Herpers, Determination of the activation cross section σ_{therm} and of the half-life of ^{53}Mn by a 587 days reactor irradiation, Radiochim.Acta 18 (1972) 207

[+] Institut für Chemie (1): Nuklearchemie, KFA Jülich

FACHBEREICH ANORG. CHEMIE UND
KERNCHEMIE
TECHNISCHE HOCHSCHULE DARMSTADT

(p,t...)-, (d,t...)- and (α,t...)-Cross Sections for Al, V, Nb and Au

M. Merkel, H. Münzel

Thick-target-yields of tritium have been determined by irradiating stacks of Al, V, Nb and Au foils with deuterons and α-particles up to 50 MeV and with protons up to 25 MeV. The tritium activities were measured by heating each foil in a H-atmosphere and then transferring the gas to a proportional counter. The thick-target-yields for the different projectile energies were used to calculate average cross sections for the formation of tritium. The results obtained for the α-reactions are shown in Fig. 1. The bars give the average cross sections for the energy interval indicated by the breadth of the line. A comparison of the data shows that all the investigated excitation functions are very similar to each other, i.e. they do not depend strongly either on the type of the projectile or on the nucleon number of the target nucleus. At 50 MeV the cross sections for the d- and α-reactions are about 30 mb, which corresponds to approx. 3% of the total reaction cross section.

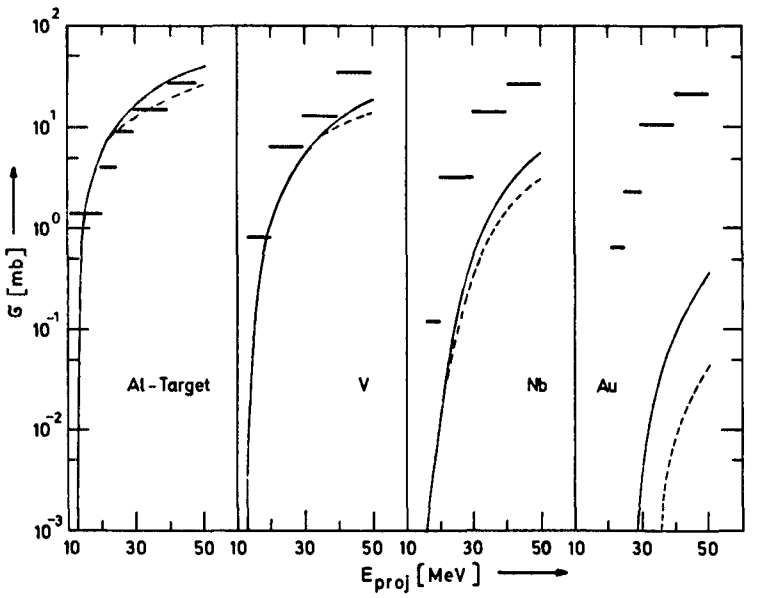

Fig. 1 Average cross sections of (α,t...)-reactions for the target materials Al, V, Nb and Au; for further explanations cf. text.

The excitation functions predicted by the Precompound-Compound-Model are also shown in Fig. 1 by the upper curves. The cross sections due to the formation of the compound nucleus are given as dashed curves. In the case of Al the agreement is reasonable. However, for the heavier target materials large deviations occur. Obviously the model used underestimates seriously the emission of composite particles in the first stages of the reaction.

INSTITUT FÜR KERNCHEMIE
JOHANNES GUTENBERG-UNIVERSITÄT MAINZ

1. Charge Distribution in Thermal Neutron Induced Fission Reactions

H.O. Denschlag, G. Fischbach, M. Weis

Radiochemical measurements of independent and cumulative yields of fission products have been continued [77 NEA 1]. The values obtained are listed in Table I. For the presentation of the data the form introduced by Meek and Rider [77 MEE 2] has been adopted wherever applicable.

General agreement with predictions derived from the systematics [77 MEE 1, 78 WAH 1] is found for elemental yields.

However, the isomeric ratios of ^{97}Nb calculated from the yields given in Table I and, especially, ^{99}Nb measured directly [77 WEI 1], are found to differ substantially from predictions [76 MAD 1] as shown in Table II.

References

76 MAD 1 D.G. Madland, T.R. England, Los Alamos Report LA-6595-MS (1976) and Nucl.Sci.Eng., in press

77 MEE 1 M.E. Meek, B.F. Rider, Compilation of fission product yields, Report NEDO-12154-2 (1977)

77 NEA 1 H.O. Denschlag, G. Fischbach, H. Meixler, G. Paffrath, W. Rudolph, M. Weis, K. Wolfsberg in NEANDC(E)-182 U Vol. V, INDC (Ger) - 19/L + Special (1977) p. 65

77 WEI 1 M. Weis, H.O. Denschlag in Jahresbericht 1976, Institut für Kernchemie, Universität Mainz (1977) p. 89

Table I. Fission yields

Measured nuclide	Fission reaction	Meas. type	Value	Error (1σ)	Norm. nuclide	Norm. fission reaction a)	Norm. value	Ref.
^{96}Nb	U235T	IN	$6.9 \cdot 10^{-4}$	$1.3 \cdot 10^{-4}$	^{97}Nb		0.012	78WEI 1
$^{97m+g}$Nb	U235T	FI	0.20	0.02	^{97}Zr		99.8	"
^{97m}Nb	U235T	FI	<0.009	-	^{97}Zr		99.8	"
^{97g}Nb	U235T	FI	>0.19	-	^{97}Zr		99.8	"
^{98g}Nb	U235T	IN	0.062	0.008	^{97}Nb		0.012	"
^{99m}Nb	U235T	CU	2.24 c)	0.13	^{97}Nb		0.012	"
^{141}Ba	U235T	FI	13.2	2.0	^{141}Ba		100 b)	78FIS 1
^{143}Ba	U235T	FC	96.3	2.7	^{143}La		100 b)	"
^{144}Ba	U235T	FC	84.0	6.7	^{144}La		100 b)	"
^{145}Ba	U235T	FC	57.9	3.6	^{145}Ce		100 b)	"
^{146}Ba	U235T	FC	32.0	2.0	^{146}Ce		100 b)	"

a) If different from fission reaction studied.

b) The measurement of the nuclide of interest and of the normalizing nuclide had to be carried out in two separate experiments with different separation times. These two experiments were correlated to each other via a measurement of ^{142}Ba (chains 143 and 144) or of ^{144}Ba (short separation times) and of ^{144}La (long separation times) (chains 141,145,146). In the evaluation of the latter measurements a value of the fractional cumulative yield of ^{144}Ba (FC: (82.7±1.9)%) was used.

c) This result may be converted to a fractional yield of 36.6±2.2% and is in excellent agreement with and slightly more accurate than the value of 36.4±4.5 obtained independently and quoted in [77 NEA 1].

Explanation of symbols used in Table I

U235T	Thermal neutron induced fission of U-235
FI	Fractional independent yield (%)
FC	Fractional cumulative yield (%)
IN	Absolute independent yield (%)
CU	Absolute cumulative yield (%)
g	Ground state
m	Metastable state

78 FIS 1 G. Fischbach, H.O. Denschlag, in Jahresbericht 1977, Institut für Kernchemie, Universität Mainz (1978), in press

78 WAH 1 A.C. Wahl, Contribution to the Second Advisory Group Meeting on FPND, Petten (September 1977)

78 WEI 1 M. Weis, H.O. Denschlag, in Jahresbericht 1977, Institut für Kernchemie, Universität Mainz (1978), in press

Table II. Ratios of independent formation of isomeric states

Nuclide	Spin	IN (high spin) / IN (total)		
		Experiment	Reference	Prediction [76 MAD 1]
^{97m}Nb ^{97g}Nb	$1/2^-$ $9/2^+$	≥0.95	78 WEI 1	0.81
^{97m}Nb ^{99g}Nb	$1/2^-$ $9/2^+$	0.077±0.009	77 WEI 1	0.81

2. Investigation of β^--Strength Functions of Nuclei far from the β-Stability Line by Neutron and Gamma-Ray Spectroscopy

K.-L. Kratz, H. Ohm, K. Sümmerer, M. Zendel, S.G. Prussin[1], K.D. Wünsch[2]

The investigation of delayed particles provides an interesting tool for studying nuclear properties in the region 4-10 MeV

1) Department of Nuclear Engineering, University of California, Berkeley
2) II. Phys. Institut, Universität Giessen and Institut Laue-Langevin, Grenoble

excitation energy. On the neutron-rich side of the ß-stability line it has become evident that the strength function (S_β) in β^--decay holds a key position because of its pronounced energy dependence. In this context, high-resolution neutron spectroscopy is especially valuable because the β^--delayed neutrons probe the most interesting top part of the excitation spectrum in a very sensitive way.

In the mass region of the fission products, the main β^--strength should be due to Gamow-Teller (GT) allowed transitions. According to early calculations of Ikeda et al. [1] the GT strength is concentrated in a broad resonance centered near the isobaric analog state, and only the "tail" of this resonance is energetically accessible to β^--decay. Based on the widely used "gross theory" of ß-decay [2], up to now in most publications unrealistic assumptions like S_β = const. or $S_\beta \sim \rho(E^*)$ - with $\rho(E^*)$ being the level density - which do not fulfil any sum rules are used to interpret measured ß-strength distributions [3-8]. Our high-resolution experiments, however, allow the study of fine structures in the low-energy tail of the GT giant resonance for highly unstable nuclei [9]. Those nuclear structures are expected from the known structures of S_β in nuclei near the ß-stability line from the isovector M1 γ-decay of isobaric analog states [10-12] and from shell model calculations [13-15].

As shown in Fig. 1 for the isotope sequence of the odd-mass rubidium precursors 89-97, the shapes of the experimental β^--strength functions exhibit, in contrast to the present theoretical concepts [2,4], pronounced resonances and a systematic behaviour as a function of mass number and Q_β as expected from the explanation given above. Furthermore, in the energy region 4-7 MeV the integral strength is found to be systematically about five times higher than that predicted by the "gross theory". In the light of these results, very recent attempts of a purely statistical description of the β^--delayed neutron decay assuming $S_\beta \sim \rho(E^*)$, which - contrary to the authors' beliefs [8] - do not describe our experimental data, are reduced to rather academic interest.

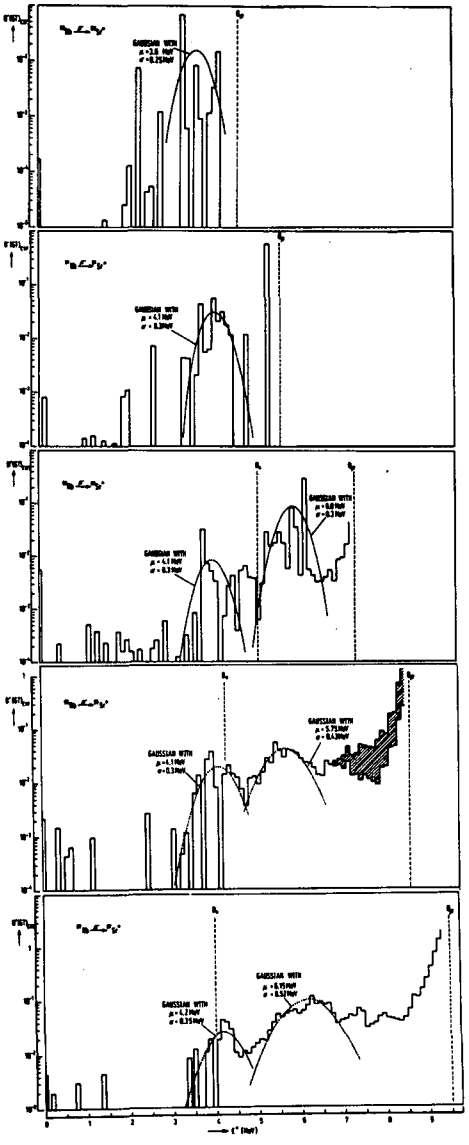

Fig. 1 Experimental β^--strength functions of odd-mass rubidium precursors 89-97.

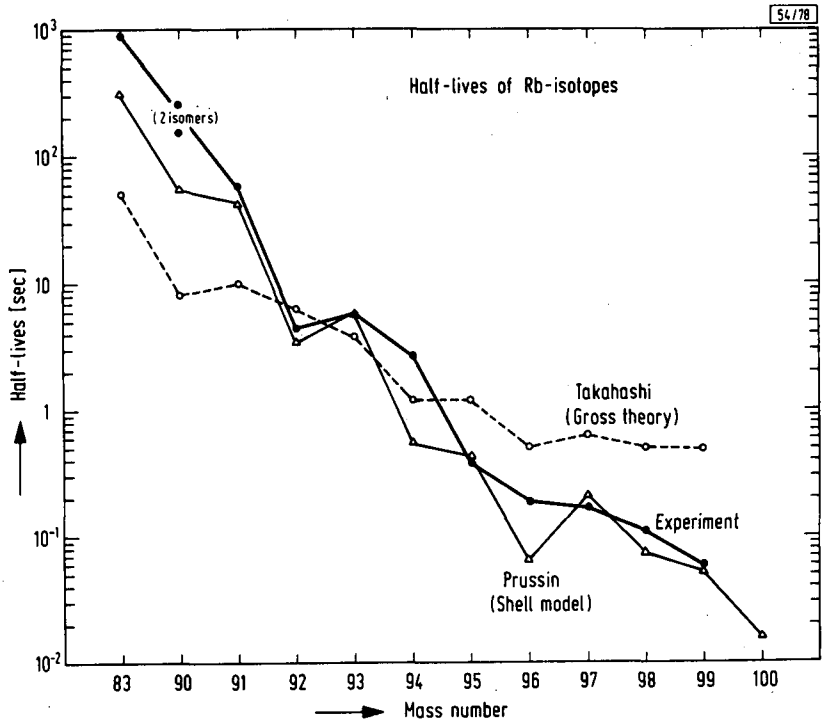

Fig. 2 Beta-decay half-lives of rubidium isotopes; comparison of experimental data with predictions from the "gross theory" [2] and shell model calculations [17].

The particular importance of investigations described in this report lies in the fact that the shape of the ß-strength function is decisive not only in predictions of ß-decay half-lives (see for example Fig. 2), but also for ß-delayed neutron and ß-delayed fission probabilities and in this way for the production rates of heavy nuclides by astrophysical processes like the r- or n-process [10,16].

References

[1] K. Ikeda et al., Phys. Rev. 133B (1964) 549

[2] K. Takahashi, Progr. Theoret. Phys. (Kyoto) 47 (1972) 1500

[3] A.C. Pappas, T. Sverdrup, Nucl. Phys. 188 (1972) 48

[4] P.G. Hansen, Adv. Nucl. Phys. 7 (1973) 159

[5] G. Rudstam, S. Shalev, Nucl. Phys. A235 (1974) 397, and references cited therein

[6] J.C. Hardy, CERN-Report 76-13 (1976) 267

[7] B. Johnson et al., CERN-Report 76-13 (1976) 277

[8] J.C. Hardy et al., paper submitted to Nucl. Phys. (1977)

[9] F.M. Nuh et al., Nucl. Phys. A293 (1977) 410

[10] H.V. Klapdor, Phys. Lett. 65B (1976) 35

[11] C. Gaarde et al., Nucl. Phys. A143 (1970) 497; A184 (1972) 241

[12] H.V. Klapdor et al., Nucl. Phys. A245 (1975) 133; A263 (1976) 477

[13] J. Randrup, Nucl. Phys. A207 (1973) 209

[14] A.A. Shihab-Eldin et al., Phys. Lett. 69B (1977) 143

[15] S.P. Ivanova et al., Yad. Fiz. 24 (1976) 278

[16] C.O. Wene, H.V. Klapdor, Contribution to the Conf. on Nuclear Structure, Tokyo (1977), and to be published

[17] W. Halverson, S.G. Prussin, unpublished results (1977)

REAKTORSTATION GARCHING,
FACHBEREICH PHYSIK,
TECHNISCHE UNIVERSITÄT MÜNCHEN

1. Interactions of Slow Neutrons with the Chromium Isotopes

L. Koester, K. Knopf, W. Waschkowski

Neutron transmission experiments and determinations of coherent scattering lengths were performed on natural chromium and enriched samples of ^{50}Cr, ^{52}Cr, ^{53}Cr and ^{54}Cr. By means of the Christiansenfilter-technique we obtained new values for the scattering lengths of the bound atoms:

$$b(^{nat}Cr) = 3.635 \pm 0.007 \text{ fm},$$
$$b(^{50}Cr) = -4.50 \pm 0.05 \text{ fm},$$
$$b(^{52}Cr) = 4.914 \pm 0.015 \text{ fm},$$
$$b(^{53}Cr) = -4.20 \pm 0.03 \text{ fm},$$

and

$$b(^{54}Cr) = 4.55 \pm 0.10 \text{ fm}.$$

The transmission experiments with neutrons of 510 ueV, 1.26 eV and 5.19 eV energy resulted in data for the absorption cross section

$$\sigma_a(^{nat}Cr) = 3.05 \pm 0.08 \text{ b}$$

and for the free scattering cross section at "zero energy":

$$\sigma_o(^{nat}Cr) = 3.381 \pm 0.010 \text{ b}.$$

Data for incoherent and spin-state scattering and for the potential-scattering radius of the nuclei could be deduced from these results.

2. Scattering of Slow Neutrons by the Isotopes of Sulfur and Silicon: Coherent and Incoherent Cross Sections

L. Koester, K. Knopf, W. Waschkowski

By means of the Christiansenfilter-technique we have determined the coherent scattering lengths b for bound atoms of the following isotopes:

^{28}Si: b = 4.106 ± 0.006 fm
^{29}Si: b = 4.70 ± 0.10 fm
^{30}Si: b = 4.58 ± 0.08 fm
^{32}S : b = 2.804 ± 0.002 fm
^{33}S : b = 4.74 ± 0.19 fm
and ^{34}S : b = 3.48 ± 0.03 fm.

The scattering length of the elements were measured in the same set up. The results are in very good agreement with the known highly exact values. Taking account of the available precision data of the free cross sections for the elements we were able to derive the following values for the free cross sections at "zero energy":

natural Si: incoherent cross section σ_i = 0.007 ± 0.002 b
isotopic incoherent σ_i^{is} = 0.0026 ± 0.0007 b

^{28}Si: σ_o = 1.992 ± 0.006 b
^{29}Si: σ_o = 2.72 ± 0.14 b; σ_i = 0.10 ± 0.05 b
^{30}Si: σ_o = 2.49 ± 0.09 b

natural S: incoherent cross section σ_i = 0.008 ± 0.003 b
isotropic incoherent σ_i^{is} = 0.0057± 0.0007 b

^{32}S: σ_o = 0.9432 ± 0.0021 b
^{33}S: σ_o = 3.0 ± 0.3 b; σ_i = 0.3 ± 0.4 b
^{34}S: σ_o = 1.454 ± 0.025 b

These results are in fairly good agreement with scattering parameters derived from the resonance data.

PHYSIKALISCHES INSTITUT
UNIVERSITÄT TÜBINGEN

1. The $^{10}B(n,\alpha)^{7}Li$ and $^{14}N(n,\alpha)^{11}B$ Reactions at 13.9 MeV

M. Mörike, T. Rohwer, G. Staudt, F. Weng

In continuation of our earlier studies of (n,α) reactions on light nuclei [1-3], differential cross sections of the reactions $^{10}B(n,\alpha)^{7}Li$ and $^{14}N(n,\alpha)^{11}B$ were measured at E_n = 13.9 MeV. The alpha particles were detected with a counter telescope in which two gas proportional counters are followed by a silicon detector [4]. Our data are in fair agreement with the results of other authors at E_n = 14.1 and 14.9 MeV. The values of the integrated cross sections are σ= 18.5 ± 2.5 mb for $^{14}N(n,\alpha_o)^{11}B$, σ = 10.1 ± 2.0 mb for $^{14}N(n,\alpha_1)^{11}B$, and σ = 11.0 ± 2.0 mb for the unresolved transition $^{10}B(n,\alpha_{01})^{7}Li$. The final results shall be published elsewhere [5].

2. (n,α) Cross Sections on Light Nuclei at 14 MeV

M. Mörike, G. Staudt

The integrated cross sections for the (n,α) ground state transitions are sensitively dependent on the mass number of the target nucleus. In Fig. 1 the cross sections for target nuclei with A = 6-40 at about 14 MeV incident energy are shown. Data for nine of the given nuclei are taken from the references given in Table I and for ten nuclei the data were obtained recently in our laboratory at E_n = 13.9 MeV. It can be seen from the figure that the magnitude of the cross sections for α-like target nuclei is comparatively larger than that for non-α-like nuclei except for the data on ^{26}Mg. For the target nucleus ^{20}Ne the experimental results are very inconsistent. Therefore a further $^{20}Ne(n,\alpha)$ experiment is under way in this laboratory. A typical energy spectrum at $\Theta \approx 10^{o}$ is given in Fig. 2. In this figure the carbon and oxygen background caused by the foil of the gas target is not corrected.

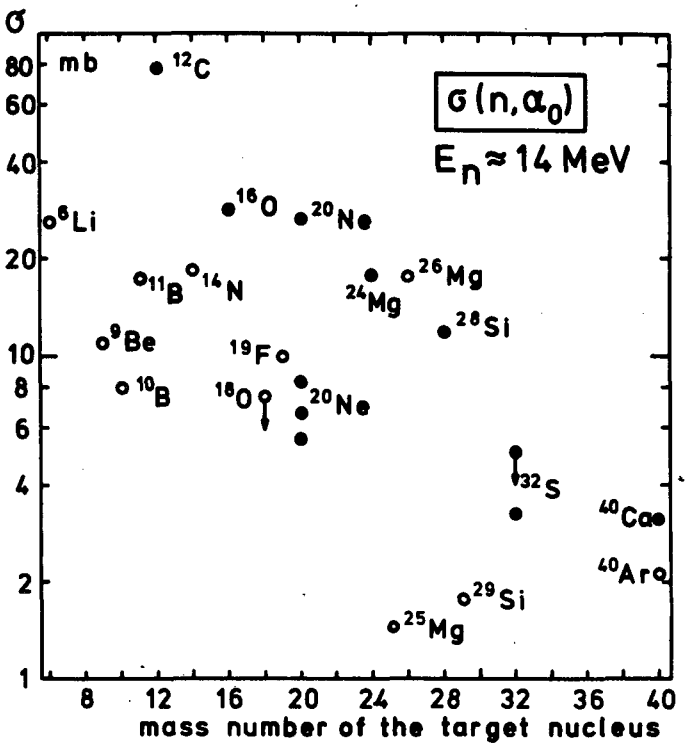

Fig. 1 Integrated cross sections of the (n,α) ground state transitions in the mass region A = 6-40 at a neutron energy of about 14 MeV. For references cf. Table I.

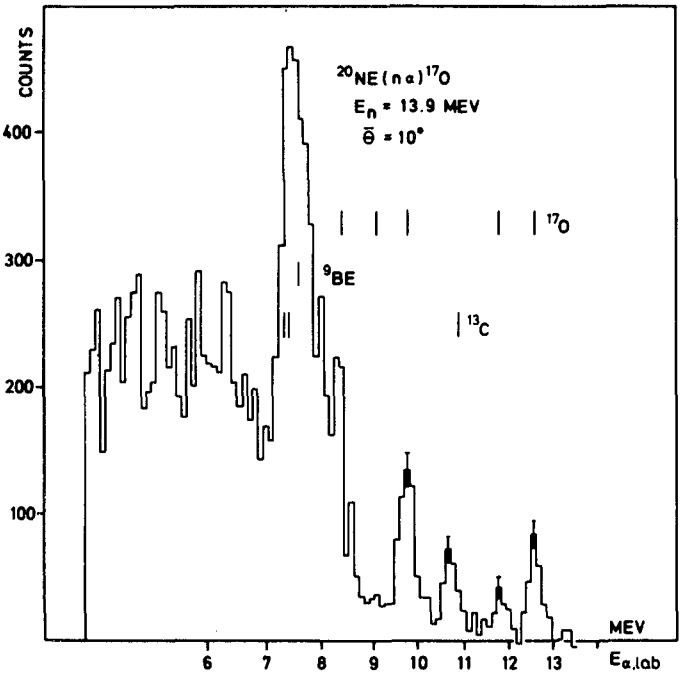

Fig. 2 Energy spectrum of α-particles from the reaction $^{20}Ne(n,\alpha)^{17}O$ at 13.9 MeV.

Table I. The integrated cross sections for the (n,α_o) ground state transitions in the mass region A = 6-40

Target nucleus	E_n MeV	$\sigma(n,\alpha_o)$ mb	Ref.	Target nucleus	E_n MeV	$\sigma(n,\alpha_o)$ mb	Ref.
^{6}Li	14.4	26 ± 3	6	^{20}Ne	14.3	6.6 ±2.4	13
^{9}Be	14.1	~11	7	^{20}Ne	14.1	26.8 ±5.0	14
^{10}B	13.9	~ 8	5	^{24}Mg	13.9	~17	15
^{11}B	14.1	17.7±5	8	^{25}Mg	13.9	1.4 ±0.3	15
^{12}C	13.9	80 ±10	1,9	^{26}Mg	13.9	17.7 ±3.1	15
^{14}N	13.9	18.5± 2.5	5	^{28}Si	14.0	12 ±1	16
^{16}O	13.9	28.5± 3.5	2	^{29}Si	14.0	1.75±0.25	16
^{18}O	14	<7.6± 1.7	10	^{32}S	14.0	<5	17
^{19}F	13.9	10 ± 3	3	^{32}S	13.9	3.2 ±0.7	18
^{20}Ne	14.1	5.5± 0.9	11	^{40}Ar	14.3	2.1	19
^{20}Ne	14.1	8.0± 1.2	12	^{40}Ca	13.9	3.1 ±0.8	18

References

[1] M. Brendle, M. Mörike, G. Staudt, G. Steidle, Z.f.Naturforschung 23a (1968) 1129

[2] H.J. Brede, M. Mörike, B. Schürenberg, G. Staudt, F. Weng, Z.Physik 245 (1971) 1

[3] T. Rohwer, M. Mörike, G. Staudt, Z.Physik A281 (1977) 107

[4] M. Brendle, M. Mörike, G. Staudt, G. Steidle, Nucl.Instr. Meth. 81 (1970) 141

[5] M. Mörike, G. Staudt, F. Weng, Z.Physik, to be published

[6] D. Rendić, Ph.D. thesis, Zagreb (1967)

[7] W. Smolec, S. Burzynski, K. Rusek, I.M. Turkiewicz, J. Turkiewicz, P. Zupranski, Nucl.Phys. A257 (1976) 397

[8] M. Bormann, D. Kaack, V. Schröder, W. Scobel, L. Wilde, Z.Physik 258 (1973) 285

[9] J. Lachkar, F. Cocu, G. Haouat, P. Le Floche, Y. Patin, J. Sigaud, NEANDC (E) 168 "L"

[10] M. Schmidt-Hönow, W. Herr, Radiochim.Acta 17 (1972) 142
[11] W.N. McDicken, W. Jack, Nucl.Phys. 88 (1966) 457
[12] R. Bachinger, M. Uhl, Acta Phys.Aust. 33 (1971) 317
[13] S. Kardonsky, H.L. Finston, E.T. Williams, Phys.Rev. C4 (1971) 846
[14] H. Karge, Ph.D. thesis, Jena (1970)
[15] M. Brendle, R. Enge, G. Steidle, Z.Physik A 285 (1978) 293
[16] A. Rubbino, D. Zubke, Nucl.Phys. 85 (1966) 606
[17] L. Gonzâles, J. Rapaport, Nucl.Phys. 72 (1965) 218
[18] H.J. Brede, Z.Physik 254 (1972) 375
[19] S. Kardonsky, H.L. Finston, E.T. Williams, Phys.Rev. C4 (1971) 840

PHYSIKALISCH-TECHNISCHE BUNDESANSTALT
BRAUNSCHWEIG

1. Radionuclide Data

1.1 Gamma-Ray Emission Probabilities

U. Schötzig, K. Debertin

The fission product nuclide ^{131}I plays an important role in nuclear medicine, in the surveillance of power reactors, and for the calibration of germanium spectrometers. Gamma-ray emission probabilities per decay for eight lines in the energy region from 80 keV to 723 keV were derived from activity and emission-rate measurements. A further radionuclide useful for the efficiency calibration of germanium spectrometers is ^{226}Ra for which relative gamma-ray emission probabilities were determined in the energy region from 186 keV to 2448 keV. In both cases the measurement uncertainties at the 68% confidence level were of the order of ±1%.

1.2 International Intercomparison of Gamma-Ray Emission-Rates of ^{152}Eu Sources

K. Debertin

An intercomparison of gamma-ray emission-rate measurements by means of germanium spectrometers and ^{152}Eu sources was organized by the working group "α-, ß-, γ-Ray Spectrometry" of the International Committee for Radionuclide Metrology (ICRM). 26 laboratories from 15 countries participated in the intercomparison. Details on its performance and on the applied measuring and evaluation techniques and the results for the emission-rates of the ten strongest lines of ^{152}Eu will be presented in the report PTB-Ra-7 (ICRM-S-3). Results and discrepancies are discussed there and a "best" set of gamma-ray emission probabilities for ^{152}Eu with uncertainties of about 0.5% at the 68% confidence level is derived.

2. Neutron Cross Sections

Comparison between Measured and Calculated Average Cross Sections in the Cf-252 Neutron Fission Spectrum

W. Mannhart

The use of activation detectors for obtaining more information about the spectral distribution in unknown neutron fields requires the previous test of such activation detector reactions in well-known so-called "benchmark" neutron fields. An index of the goodness of a reaction is the consistency between the average cross section measured, $<\sigma>_M$, and calculated, $<\sigma>_C = \int\sigma(E)\ \chi(E)dE$, in the benchmark field. $\sigma(E)$ is the energy dependent cross section of the reaction and $\chi(E)$ is the normalized spectral distribution of the benchmark neutron field.

At present, one of the most well-known benchmark neutron fields is that of ^{252}Cf. The spectral distribution function is given by an evaluation based on the analysis of eight spectrum measurements. It consists of a Maxwellian with an energy parameter of 1.42 MeV and of five correction functions in different energy integrals [1]. Average cross sections in the ^{252}Cf neutron fission spectrum measured at PTB [2,3] were compared with calculated values. In this comparison the spectral distribution of ref. 1 was folded with different $\sigma(E)$-data: Cross section data from the 'Evaluated Nuclear Data File' ENDF/B-IV [4], from the ENDF/B-V-file [5,6] being in preparation and from recent experiments [7,8]. The results are given in Table I. The reactions are grouped according to their energy-response ranges in the ^{252}Cf-spectrum. The uncertainty given for the ratios, $<\sigma>_M/<\sigma>_C$, comprises the uncertainty of $<\sigma>_M$ and of $\chi(E)$, and corresponds to the 68% confidence level. The value given in bracket additionally includes the uncertainty of the $\sigma(E)$-data.

Table I. Measured and calculated average cross sections for ^{252}Cf source (cross sections in mb)

Reaction	$\langle\sigma\rangle_M$ Ref.[2,3]	$\langle\sigma\rangle_C$	$\sigma(E)$-data from ref.:	$\langle\sigma\rangle_M / \langle\sigma\rangle_C$
$^{197}Au(n,\gamma)^{198}Au$	76.2 ± 1.8	76.50	[5]	0.996 ± 0.047 (0.069)
$^{115}In(n,\gamma)^{116m}In$	124.1 ± 3.6	130.3	[4]	0.952 ± 0.043 (0.109)
$^{115}In(n,n')^{115m}In$	195 ± 5	189.1	[7]	1.032 ± 0.033 (0.077)
$^{113}In(n,n')^{113m}In$	160 ± 4	142.7	[7]	1.121 ± 0.033 (0.077)
$^{47}Ti(n,p)^{47}Sc$	18.9 ± 0.4	24.06	[6]	0.786 ± 0.032 (0.077)
$^{58}Ni(n,p)^{58}Co$	118 ± 3	115.0	[4]	1.026 ± 0.035 (0.106)
$^{54}Fe(n,p)^{54}Mn$	84.6 ± 2.0	85.58	[8]	0.989 ± 0.033 (0.077)
$^{64}Zn(n,p)^{64}Cu$	39.4 ± 1.0	37.31	[8]	1.056 ± 0.034 (0.078)
$^{46}Ti(n,p)^{46}Sc$	13.8 ± 0.3	13.46	[6]	1.025 ± 0.040 (0.080)
$^{56}Fe(n,p)^{56}Mn$	1.450 ± 0.035	1.476	[4]	0.982 ± 0.057 (0.076)
$^{48}Ti(n,p)^{48}Sc$	0.42 ± 0.01	0.4092	[6]	1.026 ± 0.071 (0.099)
$^{27}Al(n,\alpha)^{24}Na$	1.006 ± 0.022	1.059	[4]	0.950 ± 0.076 (0.091)
$^{197}Au(n,2n)^{196}Au$	5.50 ± 0.14	5.646	[5]	0.974 ± 0.103 (0.144)

References

[1] J. Grundl, C. Eisenhauer, EUR 5667 ef,Part I (1977) 425
[2] W.G. Alberts, E. Günther, M. Matzke, G. Rassl, EUR 5667 ef, Part II (1977) 131
[3] W. Mannhart, NEANDC (E) - 182 U, Vol. V (1977) 84
[4] B.A. Magurno, BNL-NCS-50446 (April 1975)
[5] S.F. Mughabghab, priv. communication (1977)
[6] C. Philis, O. Bersillon, D. Smith, A. Smith, ANL/NDM-27 (January 1977)
[7] D.L. Smith, J.W. Meadows, ANL/NDM-14 (July 1975)
[8] D.L. Smith, J.W. Meadows, ANL/NDM-13 (June 1975)

3. Variable Energy Cyclotron A New High-Precision Fast Neutron Time-of-Flight Facility

H.J. Brede, G. Dietze, R. Jahr, H. Klein, D. Schlegel-Bickmann, H. Schölermann, B. Siebert

A new time-of-flight facility for fast neutron scattering experiments is near completion at the 'Physikalisch-Technische Bundesanstalt' in Braunschweig. Fig. 1 shows the layout. A variable energy cyclotron is mounted on a swivelarm which can be moved around a pivot. Five well collimated flight paths of an overall length of 10 m each make it possible to measure five scattering angles up to 165° at the same time. The detectors are housed in a separate room, which comprises good shielding of background neutrons from the cyclotron and the neutron producing target.

The variable energy cyclotron (delivered by 'The Cyclotron Corporation', Berkeley) produces 2-24 MeV protons and 3-14 MeV deuterons. An internal pulsing system allows to vary the pulse repetition frequency. A pulse-shortening system decreases the pulse width down to about 1 ns.

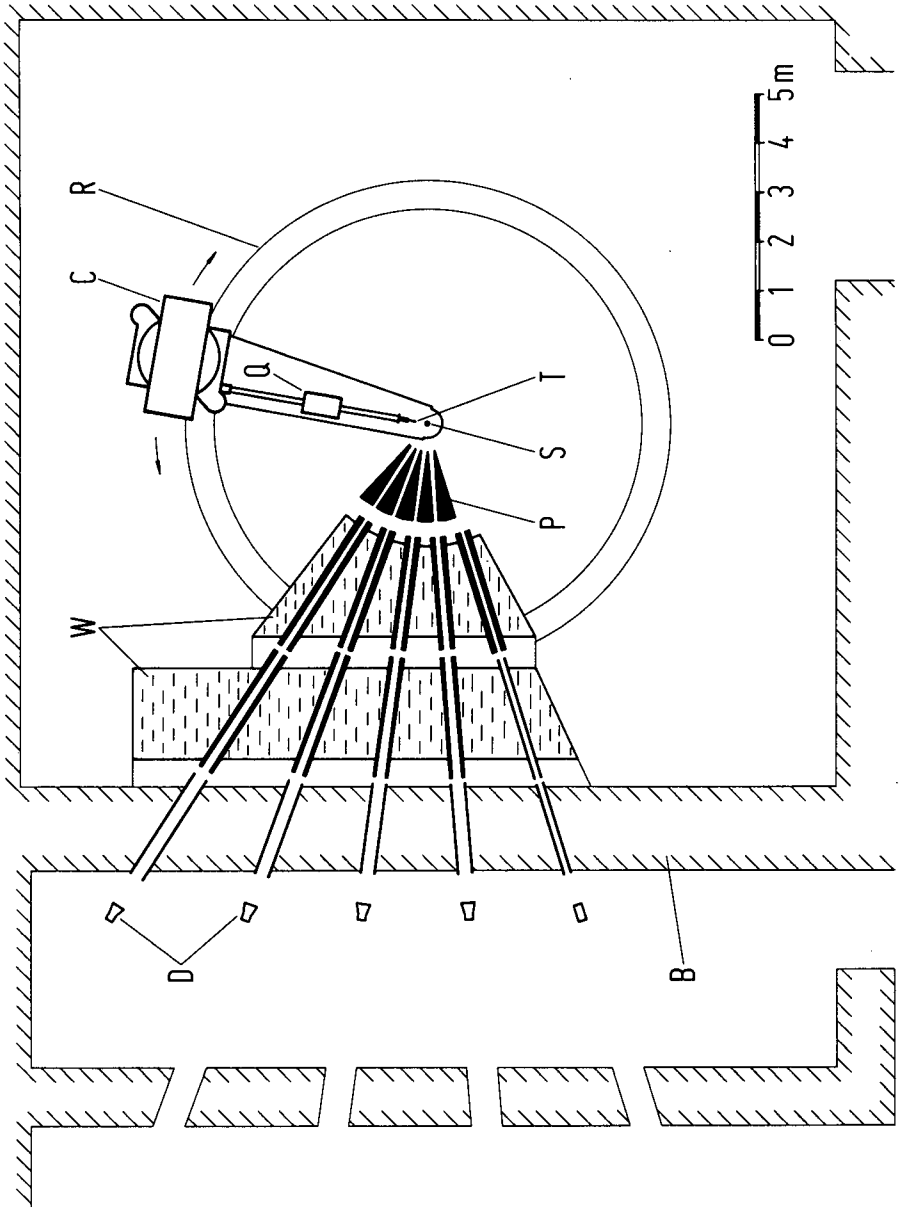

Fig. 1 Layout of the neutron scattering experiment.

C - cyclotron, R - rails, Q - quadrupole magnet,
T - neutron producing target, S - scattering probe,
P - polyethylene shields, W - water tank,
D - neutron detector, B - concrete shield.

Gas targets will be used to produce neutrons by the reactions $^{2}H(d,n)$ and $^{3}H(p,n)$. The entrance of the gas target consists of two helium-cooled nickel-foils of 5 µm thickness. These foils are directly welded on the gas cell in order to avoid scattering material like flanges and O-rings near the neutron source. The scattering sample is a hollow cylinder located about 20 cm away from the neutron producing target. It may have a maximum height of 8 cm and a maximum diameter of 4 cm.

The perturbing effects of time-correlated background neutrons, which are scattered into the detector by the entrance port and the walls of the collimator can be greatly reduced by judicious design. Monte-Carlo calculations were used to determine the best liner material and the optimal design of the channel shape. The bulk shield of the collimator is made up of two waterfilled tanks containing adjustable tubes. Polyethylene turned out to be the best liner material inside the tubes for neutron energies below 14 MeV. The inner cross section of the liner material is machined such as to achieve a good approximation of the transformation from the rectangular shape of the scattering sample to the circular shape of the detector. Near the scattering sample the collimator consists of shadow shields forming asymmetrical, double-truncated channels.

Each detector consists of a liquid scintillation counter (NE 213) of 25 cm diameter and 5 cm thickness which is optically coupled to a XP 2041 multiplier. To achieve good energy resolution and neutron/gamma discrimination properties a computer program was used to design the light guide, which are partially polished and partially coated with TiO_2. The output signals of the detectors (time of flight, pulse height and neutron-gamma) are stored on-line in a PDP 11 computer.

It is expected to start the investigation of neutron scattering on carbon in the energy-range of 8-14 MeV by the end of 1978.

ZENTRALSTELLE FÜR ATOMKERNENERGIE-DOKUMENTATION (ZAED)

An Information System for Physics Data in the Federal Republic of Germany

Status Report

H. Behrens, J.W. Tepel

1. Introduction

Since the publication of the last Progress Report the FACHINFORMATIONSZENTRUM ENERGIE - PHYSIK - MATHEMATIK was founded, with seat on the premises of the Nuclear Research Centre Karlsruhe, of which the ZAED, amongst other institutions, is a part. As activities and tasks are taken over and developed by the FACHINFORMATIONSZENTRUM, the name ZAED will be dropped gradually.

2. Information System for Physics Data in the Federal Republic of Germany

This project has been described in issues NEANDC (E) - 172 U Vol. V and NEANDC (E) - 182 U Vol. V. Therefore, we like to refrain from going into further details.

3. New Data Compilations

The issues in the series Physics Data which were mentioned in NEANDC (E) - 182 U Vol. V as being in preparation, i.e.

1-2 (1977): Survey Index of Pion-Nucleon Scattering Data.
K.H. Augenstein, G. Höhler, E. Pietarinen, H.M. Staudenmaier

3-2 (1977): Datensammlungen in der Physik. Data Compilations in Physics.
H. Behrens, G. Ebel - Supplement to No. 3-1 (1976)

5-2 (1977): Gases and Carbon in Metals (Thermodynamics, Kinetics and Properties).
Part II: Group IIB to VB Metals
(Zn, Cd, Ga, In, Tl, Ge, Si, Sn, Pb, Bi)
E. Fromm, H. Jehn , G. Hörz

5-3 (1978): Gases and Carbon in Metals (Thermodynamics, Kinetics and Properties).
Part III: Group IIIA Metals. Rare Earth Metals
(Sc, Y; La, Ce, Pr, Nd, Sm, Eu, Gd, Tb, Dy, Ho, Er, Tm, Yb, Lu)
E. Fromm, H. Jehn, G. Hörz

7-1 (1977): Compilation of Pion Photoproduction Data.
D. Menze, W. Pfeil, R. Wilcke

8-1 (1977): Optical Properties of Some Insulators in the Vacuum Ultraviolet Region.
R.P. Haelbich, M. Ivan, E.E. Koch

9-1 (1977): Bibliography of Microwave Spectroscopy 1945 - 1975.
B. Starck, R. Mutter, Ch. Spreter, K. Kettmann, A. Boggs, M. Botskor, M. Jones

have been published in the meantime.

The following issues are now being planned:

10-1 (1978): Graphs of Neutron Capture Cross Sections of Fission Product Isotopes from FPLIB 65 and ENDF/B-IV.
M. Mattes

3-3 (1978): Datensammlungen in der Physik. Data Compilations in Physics.
H. Behrens, G. Ebel

In addition, data compilations will probably be published in the course of 1978, or early in 1979, on internal conversion coefficients, nucleon-nucleon scattering data, radiative properties of hadronic atoms, neutron cross sections for some standard reactions.
Here, of course, we have only mentioned those titles which are of interest to the nuclear physicists.

4. Bibliography of Existing Data Compilations

As mentioned under 3. there has been a supplement to this worldwide survey of all existing physics data compilations, and another supplement is planned.

5. International Cooperation in Nuclear Structure and Decay Data

As mentioned in the 1977 issue, the ZAED participated on a collaborative basis in the establishment of an Evaluated Nuclear Structure Data File (ENSDF). In this context, ZAED evaluates the nuclear structure data in the mass region A = 81 to A = 100. Early in 1977 a start was made with the evaluation and compilation of nuclear structure data for A = 86. All available data were used in the construction of new adopted level schemes for the nine isotopes ^{86}As, ^{86}Se, ^{86}Br, ^{86}Kr, ^{86}Rb, ^{86}Sr, ^{86}Y, ^{86}Zr and ^{86}Nb. Spin and parity assignments were made on the basis of internationally accepted rules and as recommended by "Nuclear Data Sheets". In addition to the level schemes a total of over 3o decay and reaction data sets were prepared in the computer-readable ENSDF-format. The data sets were analysed for self-consistency and "best values" were deduced for level energies, gamma ray intensities and energies, as well as for other nuclear properties. The results of this evaluation have been submitted to the Nuclear Data Project in Oak Ridge.
The mass chains A = 84 and A = 87 are presently in hand. They will be completed during the first half of 1978. Until the end of 1978 the mass chains A = 85, A = 91 and A = 92 will be evaluated.

During 1977 the nuclear structure data bank ENSDF which was developed in an IBM environment by the Nuclear Data Project, Oak Ridge National Laboratory, was implemented on the local Siemens 7.755 computer. ENSDF contains nuclear structure data in card image format in the form of variable length data sets in a REGIONAL (1) type structure, i.e. it is a sequentially readable ISAM file. The ISAM keys are constructed from the indentification record of each physical data set and are ordered according to mass number A, atomic charge Z and nuclear reaction type.

ENSDF contains primary physical quantities such as nuclear level energies, spins and parities, gamma energies and intensities, ß-decay log ft values etc. in fixed format regions. Secondary quantities such as nuclear moments and electromagnetic transition rates are stored in free-field formats. Retrieval in ENSDF is possible by

(i) direct access,
(ii) sequential mode, or
(iii) by a mixture of direct and sequential access modes.

A set of Pl/I programs START44, FETCH44, and SAVE44 which allow data manipulation according to mode (i) above were received from Oak Ridge National Laboratory and adapted to our Siemens system. Retrieval of data sets according to atomic mass number, chemical element or information contained in the identification record of each set is possible. Retrieval in sequential mode is useful for horizontal compilations. A PL/I program TIMSEL was written at the ZAED which allows the extraction of life-times of nuclear levels over a broad A or Z-range. This program can be adapted to retrieve other primary physical quantities.

A program based on the ORNL program FETCH44 which retrieves data sets by direct access and examines individual card images in sequence ((iii) above) is presently being developed. This is the most useful form of information retrieval but requires a comparatively large programming effort depending on the complexity and logical interconnections of the data items to be retrieved.

6. Other Activities

Other activities, as described in previous Progress Reports, are continued.

APPENDIX

Addresses of Contributing Laboratories

Institut für Angewandte Kernphysik II
Director: Prof.Dr. G. Schatz
Senior reporters: Dr. S.W. Cierjacks
Dr. F. Käppeler
Kernforschungszentrum Karlsruhe
Postfach 3640
7500 Karlsruhe

Institut für Neutronenphysik und Reaktortechnik
Director: Prof.Dr. K. Wirtz
Senior reporter: Dr. F.H. Fröhner
Kernforschungszentrum Karlsruhe
Postfach 3640
7500 Karlsruhe

Institut für Chemie (1): Nuklearchemie
Director: Prof.Dr. G. Stöcklin
Senior reporter: Dr. S.M. Qaim
Kernforschungsanlage Jülich
Postfach 1913
5170 Jülich 1

Institut für Kernphysik:
Experimentelle Kernphysik II
Director: Prof.Dr. O. Schult
Senior reporter: Dr. K. Sistemich
Kernforschungsanlage Jülich
Postfach 1913
5170 Jülich 1

I. Institut für Experimentalphysik
Director: Prof.Dr. H. Neuert
Senior reporter: Prof.Dr. W. Scobel
Universität Hamburg
Luruper Chaussee 149
2000 Hamburg 50

Institut für Reine und Angewandte Kernphysik
Director: Prof.Dr. K.O. Thielheim
Senior reporter: Dr. H.G. Priesmeyer
Universität Kiel, Geesthacht
Reaktorstr. 1
2054 Geesthacht/Tesperhude

Institut für Kernchemie
Director: Prof.Dr. W. Herr
Senior reporter: Dr. U. Herpers
Universität zu Köln
Zülpicher Str. 47
5000 Köln

Fachbereich Anorganische Chemie und
Kernchemie
Senior reporter: Prof.Dr. H. Münzel
Technische Hochschule Darmstadt
Hochschulstr.
6100 Darmstadt

Institut für Kernchemie
Director: Prof.Dr. G. Herrmann
Senior reporters: Prof.Dr. H.O. Denschlag
Dr. K.L. Kratz
Johannes Gutenberg-Universität Mainz
Friedrich von Pfeiffer Weg 14
6500 Mainz

Physik-Department der
Technischen Universität München
Abteilung E14, Forschungsreaktor
Head and senior reporter: Prof.Dr. L. Köster
8046 Garching/München

Physikalisches Institut
Director: Prof.Dr. H. Krüger
Senior reporter: Prof.Dr. G. Staudt
Universität Tübingen
Morgenstelle
7400 Tübingen

Physikalisch Technische Bundesanstalt
Abteilung 6, Atomphysik
Director: Prof.Dr. S. Wagner
Bundesallee 100
3300 Braunschweig

Zentralstelle für Atomkernenergie-
Dokumentation (ZAED)
Director: Dr. W. Rittberger
Senior reporter: Dr. H. Behrens
Kernforschungszentrum
7514 Eggenstein-Leopoldshafen 2

CINDA TYPE INDEX

A Supplement to Progress Report on Nuclear Data Research in the Federal Republic of Germany for the Period April 1, 1977 to March 31, 1978

NEANDC(E)-192 U Vol. V
INDC(Ger)-20/L + Special

ELEMENT S	A	QUANTITY	TYPE	ENERGY MIN	MAX	DOCUMENTATION REF	VOL	PAGE	DATE	LAB	COMMENTS
B	010	N,ALPHA	EXPT-PROG	14+7		NEANDC(E)	192	5	478	TUE	MOERIKE+P.79 DIFF+INT SIG,TBP
C		TOTAL	EXPT-PROG	45+6	80+6	NEANDC(E)	192	5	478	KFK	CIERJACKS+P.16 GRPHS
C		TOTAL	EXPT-PROG	NDG		NEANDC(E)	192	5	478	KFK	CIERJACKS+P.1 TOF TRANS,TBC
C		RESON PARAMS	EXPT-PROG	49+6	66+6	NEANDC(E)	192	5	478	KFK	CIERJACKS+P.3 2 RES,EN,WTOT
N	014	N,ALPHA	EXPT-PROG	14+7		NEANDC(E)	192	5	478	TUE	MOERIKE+P.79 DIFF+INT SIG,TBP
O		TOTAL	EXPT-PROG	NDG		NEANDC(E)	192	5	478	KFK	CIERJACKS+P.1 TOF TRANS,TBC
O		TOTAL	EXPT-PROG	45+6	80+6	NEANDC(E)	192	5	478	KFK	CIERJACKS+P.16 GRPHS
O	016	RESON PARAMS	EXPT-PROG	74+6	11+7	NEANDC(E)	192	5	478	KFK	CIERJACKS+P.14 T=3/2RES,PRELIM
O		RESON PARAMS	EXPT-PROG	32+6	11+7	NEANDC(E)	192	5	478	KFK	CIERJACKS+P.3 10 RES,EN,WTOT
AL	027	N,ALPHA	EXPT-PROG	FISS		NEANDC(E)	192	5	478	PTB	MANNHART.P.84 AVG SIG CFD CALC
SI	028	RESON PARAMS	EXPT-PROG	10+6	14+6	NEANDC(E)	192	5	478	KFK	CIERJACKS+P.14 ABST
SI	028	THERMAL SCAT	EXPT-PROG	51-6	52+0	NEANDC(E)	192	5	478	MUN	KOESTER+P.78 COH SCAT LENGTH
SI	029	THERMAL SCAT	EXPT-PROG	51-6	52+0	NEANDC(E)	192	5	478	MUN	KOESTER+P.78 COH SCAT LENGTH
SI	030	THERMAL SCAT	EXPT-PROG	51-6	52+0	NEANDC(E)	192	5	478	MUN	KOESTER+P.78 COH SCAT LENGTH
S	032	THERMAL SCAT	EXPT-PROG	51-6	52+0	NEANDC(E)	192	5	478	MUN	KOESTER+P.78 COH SCAT LENGTH
S	033	THERMAL SCAT	EXPT-PROG	51-6	52+0	NEANDC(E)	192	5	478	MUN	KOESTER+P.78 COH SCAT LENGTH
S	034	THERMAL SCAT	EXPT-PROG	51-6	52+0	NEANDC(E)	192	5	478	MUN	KOESTER+P.78 COH SCAT LENGTH
CA	040	N,ALPHA	EXPT-PROG	NDG		NEANDC(E)	192	5	478	JUL	QAIM.P.41 NDG,ABST
TI	046	N,PROTON	EXPT-PROG	FISS		NEANDC(E)	192	5	478	PTB	MANNHART.P.84 AVG SIG CFD CALC
TI	047	N,PROTON	EXPT-PROG	FISS		NEANDC(E)	192	5	478	PTB	MANNHART.P.84 AVG SIG CFD CALC
TI	048	N,PROTON	EXPT-PROG	FISS		NEANDC(E)	192	5	478	PTB	MANNHART.P.84 AVG SIG CFD CALC
CR		EVALUATION	EVAL-PROG	NDG		NEANDC(E)	192	5	478	KFK	FROEHNER.P.34 KEDAK EVL, NDG
CR		THERMAL SCAT	EXPT-PROG	51-6	52+0	NEANDC(E)	192	5	478	MUN	KOESTER+P.77 COH SCAT LENGTH
CR	050	INELASTIC G	EXPT-PROG	NDG		NEANDC(E)	192	5	478	KFK	VOSS+P.6 781KEV GAM, NDG
CR	050	THERMAL SCAT	EXPT-PROG	51-6	52+0	NEANDC(E)	192	5	478	MUN	KOESTER+P.77 COH SCAT LENGTH
CR	052	INELASTIC G	EXPT-PROG	TR	30+6	NEANDC(E)	192	5	478	KFK	VOSS+P.6 1434KEV GAM,SIG,GRPH
CR	052	THERMAL SCAT	EXPT-PROG	51-6	52+0	NEANDC(E)	192	5	478	MUN	KOESTER+P.77 COH SCAT LENGTH
CR	053	THERMAL SCAT	EXPT-PROG	51-6	52+0	NEANDC(E)	192	5	478	MUN	KOESTER+P.77 COH SCAT LENGTH
CR	054	THERMAL SCAT	EXPT-PROG	51-6	52+0	NEANDC(E)	192	5	478	MUN	KOESTER+P.77 COH SCAT LENGTH
MN	052	N,GAMMA	EXPT-PROG	PILE		NEANDC(E)	192	5	478	KLN	WOELFLE+P.67 T1/2 OF MN53
FE		EVALUATION	EVAL-PROG	NDG		NEANDC(E)	192	5	478	KFK	FROEHNER.P.34 KEDAK EVL, NDG
FE		N,N PROTON	EXPT-PROG	15+7		NEANDC(E)	192	5	478	JUL	QAIM+P.41 ACT SIG,NDG,ABST
FE	054	N,PROTON	EXPT-PROG	FISS		NEANDC(E)	192	5	478	PTB	MANNHART.P.84 AVG SIG CFD CALC
FE	056	DIFF ELASTIC	EXPT-PROG	45+5	30+6	NEANDC(E)	192	5	478	KFK	CIERJACKS+P.9 SIG,GRPHS
FE	056	DIFF INELAST	EXPT-PROG	75+6	86+6	NEANDC(E)	192	5	478	KFK	BROEDERS+P.36 GRPH,TBC
FE	056	RESON PARAMS	EXPT-PROG	45+5	83+5	NEANDC(E)	192	5	478	KFK	CIERJACKS+P.959 RESON,TBL
FE	056	N,PROTON	EXPT-PROG	FISS		NEANDC(E)	192	5	478	PTB	MANNHART.P.84 AVG SIG CFD CALC
FE	058	N,FISSION	EXPT-PROG	30+4		NEANDC(E)	192	5	478	KFK	LYDIHONG+P.18 MAXW AVG SIG
FE	058	RESON PARAMS	EXPT-PROG	10+4	32+5	NEANDC(E)	192	5	478	KFK	LYDIHONG+P.18 WN,WG,TBL

ELEMENT S A	QUANTITY	TYPE	ENERGY MIN	MAX	DOCUMENTATION REF VOL PAGE DATE	LAB	COMMENTS
CO	N,N PROTON	EXPT-PROG	15+7		NEANDC(E) 192 5 478 JUL	QAIM	+P.41 ACT SIG,NDG,ABST
NI	EVALUATION	EVAL-PROG	NDG		NEANDC(E) 192 5 478	KFK	PROEHNER.P.34 KEDAK EVL, NDG
NI	N,N PROTON	EXPT-PROG	15+7		NEANDC(E) 192 5 478 JUL	QAIM	+P.41 ACT SIG,NDG,ABST
NI 058	INELASTIC G	EXPT-PROG	NDG		NEANDC(E) 192 5 478	KFK	VOSS+P.6 2 GAM-LINES,NDG
NI 058	N,PROTON	EXPT-PROG	FISS		NEANDC(E) 192 5 478	PTB	MANNHART.P.84 AVG SIG CFD CALC
NI 060	INELASTIC G	EXPT-PROG	NDG		NEANDC(E) 192 5 478	KFK	VOSS+P.6 4 GAM-LINES,NDG
ZN 064	N,PROTON	EXPT-PROG	FISS		NEANDC(E) 192 5 478	PTB	MANNHART.P.84 AVG SIG CFD CALC
KR	N,GAMMA	EXPT-PROG	10+3	+5	NEANDC(E) 192 5 478	KFK	HENSLEY+P.30 TOF SPEC,GRPH,TBC
KR 084	N,GAMMA	EXPT-PROG	NDG		NEANDC(E) 192 5 478	KFK	HENSLEY+P.30 NDG,TBC
ZR HYD	TOTAL	EXPT-PROG	80-2	40-1	NEANDC(E) 192 5 478 JUL		PRIESMEYER+P.59 GRAPH
TC 099	TOTAL	EXPT-PROG	45+0	24+1	NEANDC(E) 192 5 478 JUL		PRIESMEYER+P.57 TRANS,GRPH
CD 108	RESON PARAMS	EXPT-PROG	NDG		NEANDC(E) 192 5 478 JUL		PRIESMEYER+P.57 NDG,TBC
IN 113	TOTAL	EXPT-PROG	FISS		NEANDC(E) 192 5 478	PTB	MANNHART.P.84 AVG SIG CFD CALC
IN 115	N,GAMMA	EXPT-PROG	FISS		NEANDC(E) 192 5 478	PTB	MANNHART.P.84 AVG SIG CFD CALC
IN 115	TOTAL	EXPT-PROG	FISS		NEANDC(E) 192 5 478	PTB	MANNHART.P.84 AVG SIG CFD CALC
CE	N,ALPHA	EXPT-PROG	14+7		NEANDC(E) 192 5 478 JUL	QAIM	+P.41 NDG,ABST
ND	N,ALPHA	EXPT-PROG	14+7		NEANDC(E) 192 5 478 JUL	QAIM	.P.41 NDG,ABST
EU	N,ALPHA	EXPT-PROG	14+7		NEANDC(E) 192 5 478 JUL	QAIM	.P.41 NDG,ABST
TB	N,ALPHA	EXPT-PROG	14+7		NEANDC(E) 192 5 478 JUL	QAIM	.P.41 NDG,ABST
TM	N,ALPHA	EXPT-PROG	14+7		NEANDC(E) 192 5 478 JUL	QAIM	.P.41 NDG,ABST
YB	N,ALPHA	EXPT-PROG	14+7		NEANDC(E) 192 5 478 JUL	QAIM	.P.41 NDG,ABST
LU	N,ALPHA	EXPT-PROG	14+7		NEANDC(E) 192 5 478 JUL	QAIM	.P.41 NDG,ABST
AU 197	N,GAMMA	EXPT-PROG	FISS		NEANDC(E) 192 5 478	PTB	MANNHART.P.84 AVG SIG CFD CALC
AU 197	N,2N	EXPT-PROG	FISS		NEANDC(E) 192 5 478	PTB	MANNHART.P.84 AVG SIG CFD CALC
U 235	N,FISSION	EXPT-PROG	10+6	20+7	NEANDC(E) 192 5 478	KFK	KARI+ P.6 ABSOL,NDG
U 235	ALPHA	EXPT-PROG	10+4	50+5	NEANDC(E) 192 5 478	KFK	BEER+P.19 GRPHS,CFD OTHERS
U 235	FISS YIELD	EXPT-PROG	PILE		NEANDC(E) 192 5 478	MNZ	DENSCHLAG+P.70 NB+BA NUCLIDES
U 235	FISS PROD G	EXPT-PROG	NDG		NEANDC(E) 192 5 478	PTB	SCHOETZIG+P.83 I131,EMISS-PROB
U 238	N,FISSION	EXPT-PROG	SPON		NEANDC(E) 192 5 478	KLN	THIEL+P.61 DECAY-CONST DET
U 238	RESON PARAMS	EVAL-PROG	67+0	37+1	NEANDC(E) 192 5 478	KFK	GOEL.P.33 WN,WG,3 LEVELS
PU 239	N,FISSION	EXPT-PROG	10+6	20+7	NEANDC(E) 192 5 478	KFK	KARI+ P.6 ABSOL,CURV,CFD OTHERS
PU 240	N,FISSION	EXPT-PROG	10+4	25+5	NEANDC(E) 192 5 478	KFK	KAEPPELER+P.25 REL U235,GRPH
PU 240	N,FISSION	EXPT-PROG	10+6	20+7	NEANDC(E) 192 5 478	KFK	KARI+ P.6 ABSOL,CURV,CFD OTHERS
PU 240	RESON PARAMS	EXPT-PROG	11+0		NEANDC(E) 192 5 478 JUL		PRIESMEYER+P.59 TRANS,TBD
PU 240	N,GAMMA	EXPT-PROG	50+4	25+5	NEANDC(E) 192 5 478	KFK	WISSHAK+P.23 GRPH,CFD OTHERS
PU 242	N,GAMMA	EXPT-PROG	50+4	25+5	NEANDC(E) 192 5 478	KFK	WISSHAK+P.23 NDG
AM 241	N,FISSION	EXPT-PROG	13+4	90+5	NEANDC(E) 192 5 478	KFK	HAGE+P.26 GRPH,FISS-BARR CALC
AM 241	N,GAMMA	EXPT-PROG	10+4	25+5	NEANDC(E) 192 5 478	KFK	WISSHAK+P.23 TBC,NDG
CM 244	N,FISSION	EXPT-PROG	NDG		NEANDC(E) 192 5 478	KFK	KAZEROUNI+P.28 DETECT TEST,TBC

ELEMENT S	A	QUANTITY	TYPE	ENERGY MIN	MAX	DOCUMENTATION REF	VOL	PAGE	DATE	LAB	COMMENTS
MA	NY	EVALUATION	EVAL-PROG	NDG		NEANDC(E)	192	5	478	KFK	GOEL.P.33 TRANS-U SIG,NDG,TBC
MA	NY	RESON PARAMS	THEO-PROG	NDG		NEANDC(E)	192	5	478	KFK	FROEHNER.P.37 CONVERSION-CALC
MA	NY	N,PROTON	EVAL-PROG	15+7		NEANDC(E)	192	5	478	JUL	QAIM.P.42 SYSTEMATICS INV,NDG
MA	NY	N,ALPHA	EXPT-PROG	14+7		NEANDC(E)	192	5	478	TUE	MOERIKE+P.79 INTEGSIG A=6-40
MA	NY	N,TRITON	EXPT-PROG	12+7	44+7	NEANDC(E)	192	5	478	JUL	QAIM+P.39 NT+NND+NNP SIG,GRPHS
MA	NY	N,N PROTON	EVAL-PROG	15+7		NEANDC(E)	192	5	478	JUL	QAIM.P.42 SYSTEMATICS INV,NDG
MA	NY	N,N ALPHA	EVAL-PROG	15+7		NEANDC(E)	192	5	478	JUL	QAIM.P.42 SYSTEMATICS INV,NDG